10-5-2017

Investigating The Effects Of Environmental Solutes On The Reaction Environment In Ice And At Ice Surfaces

Philip Malley
Syracuse University

Abstract:

The reaction environments present in water, ice, and at ice surfaces are physically distinct from one another and studies have shown that photolytic reactions can take place at different rates in the different media. Kinetics of reactions in frozen media are measured in snow and ice prepared from deionized water. This reduces experimental artifacts, but is not relevant to snow in the environment, which contains solutes. We have monitored the effect of nonchromophoric (will not absorb sunlight) organic matter on the photolytic fate of the polycyclic aromatic hydrocarbons (PAHs) phenanthrene, pyrene, and anthracene in ice and at ice surfaces. Nonchromophoric organic matter reduced photolysis rates to below our detection limit in bulk ice, and reduced rates at ice surfaces to a lesser extent due to the PAHs partially partitioning to the organics present.

In addition, we have monitored the effect of chromophoric (will absorb sunlight) dissolved organic matter (cDOM) on the fate of anthracene in water, ice, and ice surfaces. cDOM reduced rates in all three media. Suppression in liquid water was due to physical interactions between anthracene and the cDOM, rather than to competitive photon absorbance. More suppression was observed in ice cubes and ice granules than in liquid water due to a freeze concentrating effect.

Sodium Chloride (NaCl) is another ubiquitous environmental solute that can influence reaction kinetics in water, ice, and at ice surfaces. Using Raman microscopy, we have mapped the surface of ice of frozen NaCl solutions at 0.02M and 0.6M, as well as the surface of frozen samples of Sargasso Sea Water. At temperatures above and below the eutectic temperature (-21.1°C). Above the eutectic, regions of ice and liquid water were observed in all samples. Liquid regions generally took the form of channels. Channel widths and fractional liquid surface

coverage increased with NaCl concentration and temperature. Volume maps of the three samples at temperatures above the eutectic point, showed that liquid channels were distributed throughout the ice sample. Liquid fractions were similar at ice surfaces and in the bulk at depths of at least 80 μm.

INVESTIGATING THE EFFECTS OF ENVIRONMENTAL SOLUTES ON THE REACTION ENVIRONMENT IN ICE AND AT ICE SURFACES

by

Philip Patrick Anthony Malley

B.S., University of Scranton, 2012

Dissertation
Submitted in partial fulfillment of the requirements for the degree of
Doctor of Philosophy in Chemistry.

Syracuse University
June 2017

Acknowledgment:

There are several people that I would like to thank. First and foremost, I would like express my gratitude and thanks to my advisor Tara Kahan who made sure that I always crossed every "t" and dotted every "i". Thank you for pushing me past my limits and molding me into the scientist that I am today.

I would like to thank my friends and family for their unconditional love and support during tough times, especially my fiancée Kelly-Ann Gesuelli for always believing in me and encouraging me every step of the way. Words can't express how much joy you have brought to my life. I would also like to thank my friend Robert Terrence Brown for keeping me sane with our daily conversations and banter.

Additionally, I would like to give a big thanks to the members of the Kahan lab, both past and present. Whether we were posing for our annual Christmas photo or discussing which herbivore would make the tastiest steak, I will always have fond memories of working in this group.

I would also like to thank Dr. Mathew Maye and Dr. Ivan Korendovych for allowing me and my lab mates to use their equipment when our lab was still getting its feet wet. Additionally, I want to extend my gratitude to D. J. Donaldson and C. Anastasio for providing insight into research questions that arose during the course of my studies.

To my club soccer team Balls to the Walls, I will always remember sharing beers after our Wednesday night games. They made victory taste sweeter and defeat easier to swallow. I also want to recognize the Syracuse University Boxing Club, especially the club coach Phil Benedict, who became a great mentor and friend. Nothing felt better after an unsuccessful day in

lab than going to practice, working a heavy bag, and perfecting my technique on the hand targets.

Finally, I would like to thank Syracuse University, the Syracuse University Department of Chemistry, the Syracuse University Graduate Student Organization, and the NSF for funding my research, providing teaching and research assistantships, and travel grants to attend national conferences across the United States.

Table of Contents

List of Tables

List of Figures

Chapter One:

Introduction

1.1 Importance of the Cryosphere

The cryosphere is the part of Earth's surface where water is present in solid form. This definition includes the polar ice caps, sea ice, glaciers, lake ice, snow, and permafrost. It is present at high altitudes and also includes many urban areas for at least some fraction of the year. The cryosphere plays a vital role in the energy balance on earth via heat transport and albedo, and makes up 75% of the world's freshwater supply.[1-2] Furthermore, the cryosphere plays a prominent role in many atmospherically relevant reactions by providing a source for reactive species, increasing the measured local photon fluxes via light scattering, and by acting as a reaction substrate.[3-9]

1.2 History of Snow Chemistry

Numerous fields of science have investigated the reaction environments present in snow, ice, and frozen solutions. In the 1960s, food chemists found that – in contrast to expectations – some reactions occurred more quickly once a dilute solution was frozen.[10] This was determined to be a result of enhanced local concentrations due to freeze exclusion; this effect will be discussed in Section 1.6.2. Astrochemists have performed numerous studies investigating ice as a reaction medium, looking at interstellar ice and chemical exchanges between gases and dust occurring in icy mantles.[11-12] The first investigations of snow and ice as reaction media relevant to Earth were conducted in the context of catalytic stratospheric ozone loss, which is initiated by reactions at the surface of ice clouds. Reactions at the surface of polar stratospheric clouds (PSCs) were found to convert inert chloride (Cl^-) to active chlorine ($\cdot Cl$), which catalytically destroyed stratospheric ozone.[13-14] While some of the lessons learned from these areas of research inform our understanding of reactions in snow and ice at Earth's surface, there are some

important differences that make the cryosphere a unique reaction environment. For example, the low temperatures and high energy photons present in space create reaction environments that are very different from those on earth, and PSCs consist primarily of frozen nitric acid hydrates rather than the frozen water that makes up ice at Earth's surface. Chemistry in the cryosphere is a growing area of research with implications ranging from albedo above snowpacks to air and water quality in remote regions and urban centers.

Until fairly recently, the cryosphere was thought to act as a physical sink for atmospheric species, but was not believed to influence chemistry. In the 1980s, researchers discovered that ozone in the atmospheric boundary layer (the lowest part of the atmosphere whose behavior is directly influenced by contact with earth's surface) above remote polar regions was being destroyed rapidly and inexplicably during polar spring.[15] Further investigations into this phenomenon found that ozone was being broken down because of halogen activation occurring in the snowpack and on the surfaces of aerosols.[16-20] This chemistry, which is discussed in greater detail in Section 1.3.1, has some similarities to the catalytic chemistry at the surface of polar stratospheric clouds that leads to ozone hole formation. Gas-phase chemistry continued to be used to predict the concentration of atmospheric species in remote polar regions until field studies conducted in 2000 in the high Arctic (Alert, Canada (82°30'N 62°19'W)) determined that the concentrations of several atmospheric compounds such as formaldehyde, acetaldehyde, NO_x (nitrogen oxides present as NO and NO_2), nitrous acid (HONO), hydroxyl radical ($\cdot OH$), and peroxyl radical ($HO_2\cdot$) were found in concentrations ranging from two to 25 times greater than were predicted by gas-phase chemistry.[21-22] Furthermore, the concentrations of O_3 and Hg^0 were measured to be 4.5 and 8 times lower respectively than predicted.[21-23] In the early 2000s, scientists also discovered that chemistry in or on snow and sea ice was responsible for oxidizing

gaseous elemental Hg.[24-25] These studies demonstrated that chemistry in the snowpack was playing a more prominent role in the fate of atmospheric species than initially believed.

Field, laboratory, and modeling studies over the past two decades have largely focused on several key types of chemistry in the snowpack: Halide activation, which leads to catalytic ozone and mercury loss; photochemical OH production; fate of aromatic pollutants; and composition and chemistry of dissolved organic matter (DOM). More recently, snowpacks near hydraulic fracturing operations have been determined to induce chemistry that is distinct from that in polar snowpacks. Specifically, very high boundary layer ozone concentrations near hydraulic fracturing operations in Vernal, Utah, have been ascribed to unique chemistry in the snowpack.[9, 26]

1.3 Major Research Topics in Polar Photochemistry

1.3.1 Halide Activation

Halide activation occurs when inert halides are converted into reactive gaseous halogen atoms. This is extremely important because atomic halogens can have significant effects on atmospheric chemistry and compositions.[27] During the 1980s, scientists in Barrow, Alaska and Alert, Nunavut observed depletion of tropospheric ozone during polar spring.[28-29] Further investigations identified concurrent high atmospheric bromine concentrations that could not be explained by long range transport.[30] Research conducted at Alert in 1986 found that ozone and bromine concentrations were inversely correlated.[15]

Continuous atmospheric mercury concentrations were first recorded in 1995 at Alert, Canada. It was observed that between March and June, low concentrations of gaseous elemental Hg were observed. This was significant because it had been previously reported that there was

very little variation in Hg levels.[15, 31] After several years of observations, it was determined that these atmospheric mercury depletion events were a real phenomenon.[32-33] It was also determined that ozone depletion events and mercury depletion events are closely correlated.[32] As in the case of ozone, gas-phase mercury was being depleted by bromine in the polar boundary layer. The oxidized mercury then deposits on the snow, increasing snowpack mercury concentrations.[25, 32, 34-37] This increase in condensed-phase mercury has adverse effects on both animal and human populations of Arctic ecosystems.[24-25, 32, 38-39]

Numerous field studies have been conducted in the Arctic and Antarctic to understand the role of halogens in ozone and mercury depletion events.[8] Local chemical events referred to as "bromine explosions" have been identified as being responsible for this chemistry.[8] Bromine explosions refer to the formation of reactive gas-phase bromine in the form of Br_2 and HOBr through oxidation of bromine in the atmosphere in polar regions. Bromide ions (Br^-) at ice surfaces are converted to either Br_2 or HOBr, which are released to the gas phase where they photolyze to form reactive Br atoms. Br^- can be "activated" through reactions with NO_x, OH, and O_3.[40-47] Br_2 and HOBr are released to the gas phase, where they photolyze to form Br atoms. This sets up a catalytic cycle (described in Reactions 1.1 – 1.6) in which Br atoms react with O_3 to form BrO and O_2; HOBr is regenerated via Reaction 1.4, resulting in catalytic ozone destruction.[3, 8]

1.1 $HOBr + Br^- + H^+ \rightarrow H_2O + Br_2$ (multiphase reaction)

1.2 $Br_2 + h\nu \rightarrow 2Br$

1.3 $Br + O_3 \rightarrow BrO + O_2$

1.4 $BrO + HO_2 \rightarrow HOBr + O_2$

1.5 $BrO + BrO \rightarrow 2Br + O_2$

1.6 $HOBr + h\nu \rightarrow Br + OH$

Bromide in coastal snows is sourced from seawater, and in inland snows it is primarily sourced from transported sea spray aerosols.[15, 48] Recently, modeling studies and satellite observations have demonstrated that halogen activation may be initiated by snow blowing events and aerosol chemistry. Wind is capable of lifting salt-containing snow into the atmosphere where bromine can be released into aerosols, or reactions can occur on the saline blowing snow.[49-50] Sea-salt aerosols and seawater on the ice pack will be partially liquid even at temperatures well below the freezing point of water and the concentration of chloride and bromide will increase in the liquid fraction as the temperature decreases.[51]

1.3.2 Photochemical Hydroxyl Radical Formation

Hydroxyl radicals are important compounds in atmospheric chemistry because their concentration in the troposphere is a determining factor in its oxidizing capacity.[52] OH radicals are typically formed in the atmosphere via the photolysis of ozone:

1.7) $O_3 + h\nu \rightarrow O(^1D) + O_2$ ($\lambda < 320$ nm)

1.8) $O(^1D) + H_2O \rightarrow OH + OH$

High solar zenith angles and low water partial pressures in the winter and at high latitudes reduces the rates of these reactions significantly. It was assumed that OH concentrations would be very low at high altitudes such as Alert, Canada. However, as mentioned previously, mixing ratios of boundary layer OH above polar snowpacks were found to be 10 times greater than predicted by gas phase chemistry.[21, 23, 53] It was therefore determined that chemistry within the snowpack must be contributing to OH mixing ratios.

Polar field studies and laboratory investigations have shown that OH can be produced in snowpacks by nitrate photolysis, which also forms NO_x and NO_2^-, which reacts with water

molecules to form HONO.[54-62] HONO emissions have been observed in Greenland and HONO itself can be photolyzed and form gas-phase OH.[55, 63] HONO mixing ratios 20 times greater than predicted by gas-phase chemistry alone have been reported in the atmospheric boundary layer in Alert, Canada and Summit, Greenland.[21, 23] These observations suggest that nitrate photolysis can at least partially explain the higher-than-expected OH concentrations. Many field, lab, and modelling studies have been conducted in order to quantify OH production from nitrate photolysis in ice.[57, 59, 64-66] In addition to nitrate, nitrite and hydrogen peroxide have been investigated as potential OH sources in polar snowpacks.[67-69] Although hydrogen peroxide has a low molar absorptivity at 300 nm compared to nitrate and nitrite, the hydrogen peroxide concentration and quantum yield in the snowpack are large enough to make its photolysis significant.[64-65, 67-71]

1.3.3 Photolysis of Aromatic Pollutants

The snow in remote polar regions is extremely clean with low solute concentrations, making it an ideal medium to analyze reaction kinetics in the field. Numerous types of organic pollutants have been found in remote polar locations in low concentrations due to long range transport.[6] Several studies have investigated photolysis kinetics of aromatic pollutants in snow and ice. Some report different reaction kinetics or mechanisms in ice compared to in liquid water,[4, 6, 72-84] while others report similar kinetics in ice and liquid water.[85] These discrepancies have been ascribed to different reactivities within bulk ice and at ice surfaces.[81-84] Despite the studies listed above, the role of the cryosphere in the chemical processing of aromatic pollutants remains poorly understood. The work presented in this thesis concentrates on the photolysis of PAHs in snow and ice and on understanding ice as a photochemical reaction medium.

1.4 Photolysis of PAHs in the Environment:

1.4.1 Overview

Polycyclic aromatic hydrocarbons (PAHs) consist of two or more fused benzene rings. They are formed from the incomplete combustion of fossil fuels, and can be released into the atmosphere from a variety of sources such as car exhaust and power plants. Upon entering the atmosphere, PAHs can transport and deposit in locations either nearby or far from the emission source.

The Clean Water Act of 1977 listed 16 PAHs as priority pollutants by the EPA.[86] PAHs are carcinogenic and mutagenic: they are capable of reacting with sunlight, and the products formed during photolysis are often more toxic than the parent compound.[87] PAHs can have a variety of adverse health effects depending on the amount of exposure. In the short term, they can cause skin and eye irritation, nausea and vomiting, and inflammation, while prolonged exposure can lead to skin, lung, bladder, and gastrointestinal cancers, damage to DNA, cataracts, kidneys, and livers, and gene mutation cell damaging and cardiopulmonary mortality.[88] Upon photolysis, PAHs form a variety of products, including aromatic alcohols, quinones, ketones, and ethers.[89-91]

1.4.2 Direct Photolysis:

Sunlight at wavelengths longer than 290 nm can reach Earth's surface; shorter wavelengths are filtered by stratospheric ozone.[92-93] Photolysis is a major fate of PAHs in the environment with reactions generally occurring more rapidly in condensed phases compared to gas phase.[92, 94-95]

PAHs can undergo direct photolysis by absorbing UV photons and undergoing electronic excitation, where a bound electron is transferred to a more energetic, but still bound state.

Products can be formed in several ways. PAHs undergo photoionization when they absorb shorter wavelengths of light (λ<290) but this is not relevant to Earth's surface.[96] Direct ionization has been reported not to be an important photolysis pathway for most PAHs exposed to sunlight at Earth's surface.[97-98] PAH photodegradation reactions can proceed via a singlet state or triplet state mechanism.[98] It is important to note that not all PAHs will react via the same mechanism. While some PAHs react predominantly via the triplet state, for example, anthracene, 9-methylanthracene, acenaphthalene, and perylene, other PAHs like pyrene and benzo[a]pyrene react through the singlet state.[99] Molecular oxygen is thought to be important to PAH photolysis, but its role in the mechanism(s) remains poorly understood.[97-99] Scheme 1 illustrates potential PAH photodegradation pathways in aqueous environments.

Scheme 1:

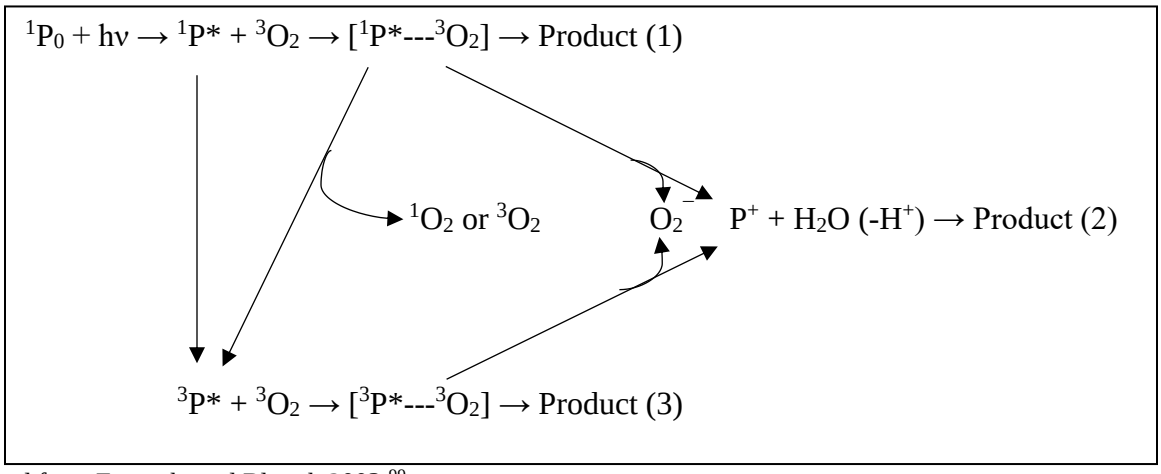

Adapted from Fasnacht and Blough 2003.[99]

PAHs form photolysis products such as aldehydes, quinones, nitrated products (e.g. naphthalene will form 1- and 2-nitronaphthalene when nitrate radicals are present), and other compounds that are more toxic than the parent molecule.[94-95, 100-103] Accurate PAH photolysis kinetics in environmental media are therefore necessary in order to predict the health effects of

PAHs. PAH photolysis kinetics can vary greatly between different media. As mentioned above, photolysis is generally much faster in condensed phases than in the gas phase. Reactivity can also vary between different condensed phases. For example, PAH photolysis rate constants spanned more than two orders of magnitude in different types of fly ash.[104] Factors such as polarity can greatly influence reactivity: PAH photolysis rate constants have been reported to be 2 to 10 times faster in water than in organic solvents.[105-107] In addition, environmental solutes can influence kinetics. For example, halide salts are shown to have varying effects on aromatic pollutant photolysis, suppressing rates in some, enhancing others, and sometimes showing no effect at all.[83, 108-112]

1.4.3 Indirect Photolysis

PAHs can be broken down in the environment through indirect photolysis, where a molecule reacts with light to form a radical, and this radical goes on to react with another compound. Another type of indirect photolysis is photosensitization where a molecule absorbs light and transfers its energy or an electron to the desired reactant. Indirect photolytic reactions in the environment are caused by species such as ·OH, singlet oxygen, and excited triplet state dissolved organic matter.[113-122] As mentioned previously, nitrate, nitrite, and hydrogen peroxide can contribute to indirect photolysis reactions in the snowpack by photolyzing to produce OH.

1.5 Physical Properties of Snow and Ice:

Reactions in snow and ice take place primarily in two locations: veins and pockets within the ice bulk that contain liquid water,[123] and at the ice surface, which has physical and chemical properties that are distinct from both bulk ice and liquid water.[4, 123-126] Reactions have been shown to occur at different rates between these two regions of ice.[83-84] Since ice surfaces are in

contact with the atmosphere, much effort has been put toward understanding their role in physical and chemical processes in the environment.

1.5.1 Ice Surface:

Ice surfaces contain a layer of disordered water molecules that is often referred to as a quasi-liquid or liquid like layer. This layer is similar to premelting layers observed at the surfaces of metals and other crystals near their melting points, but is much thicker (perhaps over 100 nm), and extends to very low temperatures (experimental studies and molecular dynamic simulations indicate that this disordered region can exist up to 60°C below water's freezing point.)[127-128] Researchers have studied the physical properties of this disordered region for several decades using a variety of techniques, investigating exchange processes that occur at the air-ice interface and the ice surface's role in promoting chemical reactions.[4, 123-126, 129-141] A major question is whether the surface can be described as analogous to the liquid phase and if the processes taking place can be accurately described using parameters (such as rate constants and partitioning coefficients) measured in liquid water.

The thickness of the disordered region at the ice surface has been estimated based on experimental studies, molecular dynamics simulations, and thermodynamic calculations. These studies have reported thicknesses near the melting point ranging from 0.3 nm, about the diameter of a water molecule, to almost 100 nm, due to varying initial assumptions. Figure 1.1 summarizes numerous experimental and molecular simulation studies that have probed the depth of the disordered region.[4] Despite the variety of probing techniques and data acquired via modeling, the predicted thickness of this disordered interface is far from conclusive. For example, molecular dynamics simulations consistently predict thicknesses far smaller than those measured experimentally, and different atomic force microscopy (AFM) studies report

thicknesses that vary by two orders of magnitude at the same temperature.[128, 142-146] This figure highlights the fact that the physical properties of the quasi-liquid layer are poorly understood, and that more research is needed to better characterize it.

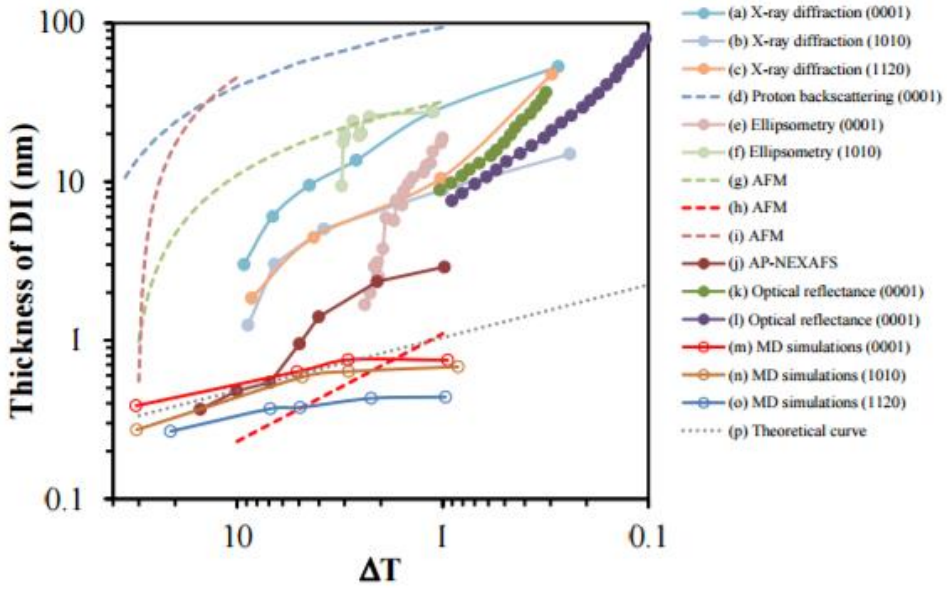

Figure 1.1. Comparison of different methods to derive the thickness of the disordered interface (DI) at the free ice surface versus 1T = Tm − T obtained using different methods. Solid circles are measured data, while dashed lines are results from reported equations fit to experimental data. Molecular dynamics (MD) simulations are represented by open circles. Glancing-angle X-ray diffraction (Dosch et al., 1995) on (a) basal and (b, c) prismatic crystal surfaces, (d) proton backscattering (Golecki and Jaccard, 1978) on basal ice, ellipsometry (Furukawa and Nada, 1997) on (e) basal and (f) prismatic crystal surfaces, (g) atomic force microscopy (AFM) (Döppenschmidt and Butt, 2000) on a 100 ml frozen droplet and vapour deposited on mica, (h) AFM (Pittenger et al., 2001) for vapour-deposited ice on metal, (i) AFM (Goertz et al., 2009) for ice frozen on a metal substrate, (j) ambient pressure near-edge X-ray absorption fine structure (Bluhm et al., 2002) for vapourdeposited ice on metal, HeNe laser optical reflectance (Elbaum et al., 1993) on basal crystals in the presence of (k) water vapour and (l) 30 Torr air, TIP4P/Ice MD simulations (Conde et al., 2008) for (m) basal and (n, o) prismatic crystals, (p) general thermodynamic solution (Dash et al., 2006) Reproduced with permission from Bartels-Rausch et al. 2014.[4]

1.5.2 Impurities at Ice Surfaces:

Molecular dynamics simulations and experimental studies of ice growth from salt solutions have shown that as the temperature drops, ions and other species present in the solution do not freeze with the water molecules.[139-140, 147-150] The same effect has been observed with the inclusion of small organics, as well as acids such as HCl and HNO_3.[7, 151-153] This occurs because

impurities affect the hydrogen bonding network of water frozen as ice, with more disorder observed in the immediate vicinity of the impurity. As water freezes, solutes become excluded and form brines which are present in liquid regions within the ice bulk or at the ice surface.[3, 10, 137, 154-157] This "salting out" effect can increase local solute concentrations like halide salts and organic matter by orders of magnitude compared to the initial concentrations in the liquid solution.[3, 154, 158-159]

1.6 PAH Photolysis in Snow and Ice

1.6.1 PAHs in the Cryosphere

Ice core samples taken from Greenland have shown an increase in PAH concentration over the past 100 years, with PAH concentrations reaching as high as 230 pg/g ice, 50 times more abundant than it was before the 18th century.[160] The dramatic increase in concentration correlates with the increased use of petroleum during that time, with more PAHs being found deposited during the winter months compared to the spring and summer, indicating that this is a relatively recent phenomenon since the world became industrialized.[161-162]

PAHs are found in snow in both urban centers and remote polar regions. In urban areas, PAHs are found in concentrations ranging from 100 ng/L of snow to several µg/L.[163-166] In sparsely populated low latitude regions, PAH concentrations ranging from 35 ng/L to 3.28 µg/L have been reported.[166-168] In remote polar regions, PAHs concentrations are found anywhere from a few ng/L to almost 100 ng/L.[163, 169-170] The relatively high concentrations in remote snowpacks are due to long range transport, since PAHs are emitted primarily in populated regions. Pollutants can travel by ocean transport, but this method can take anywhere from years to decades to occur.[171-172] Most transport is atmospheric, via a process referred to as the global

distillation effect.[173-175] During this process, semi-volatile compounds in warm areas evaporate and condense in colder climates, such as remote polar regions, leading to elevated concentrations of chemicals in regions far from their area of origin.[173-174] Air pollutants can be transported to distances over 100 km from their source via this mechanism.[176-178] The cold temperatures at higher latitudes capture organic pollutants, an effect called cold trapping.[179]

Snow is formed from water vapor condensing on an ice-forming nucleus or water droplets are supercooled onto ice crystals, a process known as riming.[180] Contaminants (including PAHs) are included into snowflakes as part of the ice-forming nucleus, by being scavenged during the riming process, or by the snowflake as it falls through the atmosphere.[181] Furthermore, contaminants can adsorb directly to the snow surface.[182] Due to the large surface area of snowflakes the cold temperature of the snow surface enhancing gas partitioning to the snow surface, snow is an important sink for gas phase organic pollutants.[183-184]

After deposition to earth's surface, the concentration of contaminants depends on both the initial concentration of the contaminant in the falling snow and on the amount of snow that falls.[185] The freezing and thawing process can cause pollutants to redistribute themselves among the snowpack.[186] Furthermore, changes in temperature can affect the equilibria of adsorption onto snow crystals, gas-particle distribution influencing uptake coefficients, and the amount of snow precipitation.[187-188]

1.6.2 Photolysis of PAHs in Snow and Ice

As discussed in Section 1.5, PAH photolysis can proceed very differently at ice surfaces than in liquid water. This may be due to different physical interactions between PAHs and water molecules at liquid and frozen aqueous surfaces. Surface-sensitive emission spectra and molecular dynamics simulations suggest that many aromatic compounds self-associate at the ice

surface, even at submonolayer surface coverages.[81-83, 189] This self-association can lead to a red-shift in the absorption spectra of some aromatic pollutants.[81-82, 189] For other aromatic species, however, including PAHs such as anthracene, red-shifts in the absorbance spectrum cannot explain faster photolysis kinetics at ice surfaces; the reason for enhanced reactivity there remains unknown.[81, 83]

Most studies investigating reactions in snow and ice use deionized water to perform experiments. This reduces the potential for experimental artifacts, but does not reflect the complex composition of snow and ice in the environment. Solutes may greatly affect photochemical kinetics in snow and ice. In fact, their effects may be even greater than in liquid water due to freeze exclusion (or "salting out"). It has been suggested that many reactions in snow will take place in particulate matter contained in snow.[190-191]

Organic matter (OM) is a ubiquitous solute in snow and ice. One type of OM is chromophoric, meaning it absorbs sunlight. A prime example of this is chromophoric dissolved organic matter (CDOM). Studies have shown that the majority of light absorbing faction in snowpack is not from inorganic compounds, but from an unknown organic fraction. This unknown faction is thought to be CDOM.[192] CDOM is formed from decaying plants and microorganisms and is found primarily in two forms: fulvic acid (FA) and humic acid (HA).[193] These compounds are large, with their size ranging to several thousand daltons.[193] Because CDOM absorbs sunlight, it can competitively absorb photons, and thus lower reaction rates. However, it photolyzes to produce several reactive species including singlet oxygen, hydroxyl radicals, peroxy radicals, and excited state DOM, which have been shown to enhance photolysis rates of aromatic pollutants in aqueous solution.[113, 194-197] Only one study has reported the effects of CDOM on pollutant photolysis in snow and ice; CDOM was recently shown to enhance

photolysis kinetics of the insecticide aldrin in snow and ice.[198] Organic matter that does not absorb sunlight may also affect PAH photolysis kinetics in snow and ice. Molecular dynamics simulations have shown that naphthalene adsorbed to ice surfaces coated with an organic monolayer partitioned preferentially to the ice-organic interface, where they likely experience a very different reaction environment than at an air-ice interface.[199]

1.7 Goal of Research

Much remains to be determined about the fate of PAHs in snow and ice. Most studies look at reaction rates in pristine ice, which can help understand the kinetics taking place, but are not necessarily relevant to well populated areas. In urban areas within the cryosphere, the snow and ice is often in contact with many environmental solutes, such as organic matter and salts. The second chapter of this work investigates the effect of nonchromophoric organic matter on the photolytic fate of the PAHs phenanthrene, pyrene, and anthracene in bulk ice and the ice surface.

Chapter three investigates the influence of CDOM on the photolysis kinetics of anthracene in water, bulk ice, and ice surfaces. Possible effects such as competitive photon absorbance, photosensitization, and production of reactive species were investigated.

Chapter four reports investigation into the physical characteristics of the surfaces of frozen saltwater solutions. Samples of frozen sodium chloride solutions and Sargasso Sea Water were analyzed using Raman microscopy to determine the location of halides at frozen surfaces above and below the eutectic temperature of $NaCl\text{-}H_2O$ solutions.

1.8 References

1. IPCC: Climate Change 2007: Synthesis Report – Contribution of Working Groups I, II and III to the Fourth Assessment Report of the Intergovernmental Panel on Climate Change. 2007; p 104.
2. Grannas, A. M.; Bogdal, C.; Hageman, K. J.; Halsall, C.; Harner, T.; Hung, H.; Kallenborn, R.; Klan, P.; Klanova, J.; Macdonald, R. W.; Meyer, T.; Wania, F., The Role of the Global Cryosphere in the Fate of Organic Contaminants. *Atmos. Chem. Phys.* **2013,** *13* (6), 3271-3305.
3. Abbatt, J. P. D.; Thomas, J. L.; Abrahamsson, K.; Boxe, C.; Granfors, A.; Jones, A. E.; King, M. D.; Saiz-Lopez, A.; Shepson, P. B.; Sodeau, J.; Toohey, D. W.; Toubin, C.; von Glasow, R.; Wren, S. N.; Yang, X., Halogen Activation Via Interactions with Environmental Ice and Snow in the Polar Lower Troposphere and Other Regions. *Atmos. Chem. Phys.* **2012,** *12* (14), 6237-6271.
4. Bartels-Rausch, T.; Jacobi, H. W.; Kahan, T. F.; Thomas, J. L.; Thomson, E. S.; Abbatt, J. P. D.; Ammann, M.; Blackford, J. R.; Bluhm, H.; Boxe, C.; Domine, F.; Frey, M. M.; Gladich, I.; Guzman, M. I.; Heger, D.; Huthwelker, T.; Klan, P.; Kuhs, W. F.; Kuo, M. H.; Maus, S.; Moussa, S. G.; McNeill, V. F.; Newberg, J. T.; Pettersson, J. B. C.; Roeselova, M.; Sodeau, J. R., A Review of Air-Ice Chemical and Physical Interactions (AICI): Liquids, Quasi-Liquids, and Solids in Snow. *Atmos. Chem. Phys.* **2014,** *14* (3), 1587-1633.
5. Domine, F.; Albert, M.; Huthwelker, T.; Jacobi, H. W.; Kokhanovsky, A. A.; Lehning, M.; Picard, G.; Simpson, W. R., Snow Physics as Relevant to Snow Photochemistry. *Atmos. Chem. Phys.* **2008,** *8* (2), 171-208.
6. Grannas, A. M.; Jones, A. E.; Dibb, J.; Ammann, M.; Anastasio, C.; Beine, H. J.; Bergin, M.; Bottenheim, J.; Boxe, C. S.; Carver, G.; Chen, G.; Crawford, J. H.; Domine, F.; Frey, M. M.; Guzman, M. I.; Heard, D. E.; Helmig, D.; Hoffmann, M. R.; Honrath, R. E.; Huey, L. G.; Hutterli, M.; Jacobi, H. W.; Klan, P.; Lefer, B.; McConnell, J.; Plane, J.; Sander, R.; Savarino, J.; Shepson, P. B.; Simpson, W. R.; Sodeau, J. R.; von Glasow, R.; Weller, R.; Wolff, E. W.; Zhu, T., An Overview of Snow Photochemistry: Evidence, Mechanisms and Impacts. *Atmos. Chem. Phys.* **2007,** *7* (16), 4329-4373.
7. McNeill, V. F.; Grannas, A. M.; Abbatt, J. P. D.; Ammann, M.; Ariya, P.; Bartels-Rausch, T.; Domine, F.; Donaldson, D. J.; Guzman, M. I.; Heger, D.; Kahan, T. F.; Klan, P.; Masclin, S.; Toubin, C.; Voisin, D., Organics in Environmental Ices: Sources, Chemistry, and Impacts. *Atmos. Chem. Phys.* **2012,** *12* (20), 9653-9678.
8. Simpson, W. R.; von Glasow, R.; Riedel, K.; Anderson, P.; Ariya, P.; Bottenheim, J.; Burrows, J.; Carpenter, L. J.; Friess, U.; Goodsite, M. E.; Heard, D.; Hutterli, M.; Jacobi, H. W.; Kaleschke, L.; Neff, B.; Plane, J.; Platt, U.; Richter, A.; Roscoe, H.; Sander, R.; Shepson, P.; Sodeau, J.; Steffen, A.; Wagner, T.; Wolff, E., Halogens and Their Role in Polar Boundary-Layer Ozone Depletion. *Atmos. Chem. Phys.* **2007,** *7* (16), 4375-4418.
9. Edwards, P. M.; Brown, S. S.; Roberts, J. M.; Ahmadov, R.; Banta, R. M.; deGouw, J. A.; Dube, W. P.; Field, R. A.; Flynn, J. H.; Gilman, J. B.; Graus, M.; Helmig, D.; Koss, A.; Langford, A. O.; Lefer, B. L.; Lerner, B. M.; Li, R.; Li, S. M.; McKeen, S. A.; Murphy, S. M.; Parrish, D. D.; Senff, C. J.; Soltis, J.; Stutz, J.; Sweeney, C.; Thompson, C. R.; Trainer, M. K.; Tsai, C.; Veres, P. R.; Washenfelder, R. A.; Warneke, C.; Wild, R. J.; Young, C. J.; Yuan, B.; Zamora, R., High Winter Ozone Pollution from Carbonyl Photolysis in an Oil and Gas Basin. *Nature* **2014,** *514* (7522), 351-354.

10. Pincock, R. E.; Kiovsky, T. E., Kinetics of Reactions in Frozen Solutions. *J. Chem. Educ.* **1966,** *43* (7), 358-360.
11. Shematovich, V. I., Formation of Complex Chemical Species in Astrochemistry (a Review). *Sol. Sys. Res.* **2012,** *46* (6), 391-407.
12. van Dishoeck, E. F., Astrochemistry of Dust, Ice and Gas: Introduction and Overview. *Faraday Discuss.* **2014,** *168*, 9-47.
13. Turco, R. P.; Toon, O. B.; Hamill, P., Heterogeneous Physicochemistry of the Polar Ozone Hole. *J. Geophys. Res. Atmos.* **1989,** *94* (D14), 16493-16510.
14. Molina, M. J.; Tso, T. L.; Molina, L. T.; Wang, F. C. Y., Antarctic Stratospheric Chemistry of Chlorine Nitrate, Hydrogen Chloride, and Ice: Release of Active Chlorine. *Science* **1987,** *238* (4831), 1253-1257.
15. Barrie, L. A.; Bottenheim, J. W.; Schnell, R. C.; Crutzen, P. J.; Rasmussen, R. A., Ozone Destruction and Photochemical Reactions at Polar Sunrise in the Lower Arctic Atmosphere. *Nature* **1988,** *334* (6178), 138-141.
16. Solberg, S.; Schmidbauer, N.; Semb, A.; Stordal, F.; Hov, O., Boundary-Layer Ozone Depletion as Seen in the Norwegian Arctic in Spring. *J. Atmos. Chem.* **1996,** *23* (3), 301-332.
17. Bottenheim, J. W.; Fuentes, J. D.; Tarasick, D. W.; Anlauf, K. G., Ozone in the Arctic Lower Troposphere During Winter and Spring 2000 (ALERT2000). *Atmos. Environ.* **2002,** *36* (15-16), 2535-2544.
18. Fan, S. M.; Jacob, D. J., Surface Ozone Depletion in Arctic Spring Sustained by Bromine. *Nature* **1992,** *359* (6395), 522-524.
19. Keene, W. C.; Sander, R.; Pszenny, A. A. P.; Vogt, R.; Crutzen, P. J.; Galloway, J. N., Aerosol pH in the Marine Boundary Layer: A Review and Model Evaluation. *J. Aerosol Sci.* **1998,** *29* (3), 339-356.
20. Michalowski, B. A.; Francisco, J. S.; Li, S. M.; Barrie, L. A.; Bottenheim, J. W.; Shepson, P. B., A Computer Model Study of Multiphase Chemistry in the Arctic Boundary Layer During Polar Sunrise. *J. Geophys. Res. Atmos.* **2000,** *105* (D12), 15131-15145.
21. Grannas, A. M.; Shepson, P. B.; Guimbaud, C.; Sumner, A. L.; Albert, M.; Simpson, W.; Domine, F.; Boudries, H.; Bottenheim, J.; Beine, H. J.; Honrath, R.; Zhou, X. L., A Study of Photochemical and Physical Processes Affecting Carbonyl Compounds in the Arctic Atmospheric Boundary Layer. *Atmos. Environ.* **2002,** *36* (15-16), 2733-2742.
22. Domine, F.; Shepson, P. B., Air-Snow Interactions and Atmospheric Chemistry. *Science* **2002,** *297* (5586), 1506-1510.
23. Yang, J.; Honrath, R. E.; Peterson, M. C.; Dibb, J. E.; Sumner, A. L.; Shepson, P. B.; Frey, M.; Jacobi, H. W.; Swanson, A.; Blake, N., Impacts of Snowpack Emissions on Deduced Levels of OH and Peroxy Radicals at Summit, Greenland. *Atmos. Environ.* **2002,** *36* (15-16), 2523-2534.
24. Lu, J. Y.; Schroeder, W. H.; Barrie, L. A.; Steffen, A.; Welch, H. E.; Martin, K.; Lockhart, L.; Hunt, R. V.; Boila, G.; Richter, A., Magnification of Atmospheric Mercury Deposition to Polar Regions in Springtime: the Link to Tropospheric Ozone Depletion Chemistry. *Geophys. Res. Lett.* **2001,** *28* (17), 3219-3222.
25. Lindberg, S. E.; Brooks, S.; Lin, C. J.; Scott, K. J.; Landis, M. S.; Stevens, R. K.; Goodsite, M.; Richter, A., Dynamic Oxidation of Gaseous Mercury in the Arctic Troposphere at Polar Sunrise. *Environ. Sci. Technol.* **2002,** *36* (6), 1245-1256.
26. Edwards, P. M.; Young, C. J.; Aikin, K.; deGouw, J.; Dube, W. P.; Geiger, F.; Gilman, J.; Helmig, D.; Holloway, J. S.; Kercher, J.; Lerner, B.; Martin, R.; McLaren, R.; Parrish, D. D.;

Peischl, J.; Roberts, J. M.; Ryerson, T. B.; Thornton, J.; Warneke, C.; Williams, E. J.; Brown, S. S., Ozone Photochemistry in an Oil and Natural Gas Extraction Region During Winter: Simulations of a Snow-Free Season in the Uintah Basin, Utah. *Atmos. Chem. Phys.* **2013,** *13* (17), 8955-8971.
27. Finlayson-Pitts, B. J., Halogens in the Troposphere. *Anal. Chem.* **2010,** *82* (3), 770-776.
28. Oltmans, S. J., Surface Ozone Measurements in Clean Air. *J. Geophys. Res. Oc. Atm.* **1981,** *86* (NC2), 1174-1180.
29. Bottenheim, J. W.; Gallant, A. G.; Brice, K. A., Measurements of NOY Species and O3 at 82° N Latitude. *Geophys. Res. Lett.* **1986,** *13* (2), 113-116.
30. Berg, W. W.; Sperry, P. D.; Rahn, K. A.; Gladney, E. S., Atmospheric Bromine in the Arctic. *J. Geophys. Res. Oc. Atm.* **1983,** *88* (NC11), 6719-6736.
31. Schroeder, W. H.; Keeler, G.; Kock, H.; Roussel, P.; Schneeberger, D.; Schaedlich, F., International Field Intercomparison of Atmospheric Mercury Measurement Methods. *Water Air Soil Poll.* **1995,** *80* (1-4), 611-620.
32. Schroeder, W. H.; Anlauf, K. G.; Barrie, L. A.; Lu, J. Y.; Steffen, A.; Schneeberger, D. R.; Berg, T., Arctic Springtime Depletion of Mercury. *Nature* **1998,** *394* (6691), 331-332.
33. Steffen, A.; Schroeder, W.; Macdonald, R.; Poissant, L.; Konoplev, A., Mercury in the Arctic Atmosphere: An Analysis of Eight Years of Measurements of GEM at Alert (Canada) and a Comparison with Observations at Amderma (Russia) and Kuujjuarapik (Canada). *Sci. Total Environ.* **2005,** *342* (1-3), 185-198.
34. Douglas, T. A.; Sturm, M.; Simpson, W. R.; Brooks, S.; Lindberg, S. E.; Perovich, D. K., Elevated Mercury Measured in Snow and Frost Flowers Near Arctic Sea Ice Leads. *Geophys. Res. Lett.* **2005,** *32* (4), 4.
35. Bargagli, R.; Agnorelli, C.; Borghini, F.; Monaci, F., Enhanced Deposition and Bioaccumulation of Mercury in Antarctic Terrestrial Ecosystems Facing a Coastal Polynya. *Environ. Sci. Technol.* **2005,** *39* (21), 8150-8155.
36. Ariya, P. A.; Dastoor, A. P.; Amyot, M.; Schroeder, W. H.; Barrie, L.; Anlauf, K.; Raofie, F.; Ryzhkov, A.; Davignon, D.; Lalonde, J.; Steffen, A., The Arctic: a Sink for Mercury. *Tellus B* **2004,** *56* (5), 397-403.
37. Banic, C. M.; Beauchamp, S. T.; Tordon, R. J.; Schroeder, W. H.; Steffen, A.; Anlauf, K. A.; Wong, H. K. T., Vertical Distribution of Gaseous Elemental Mercury in Canada. *J. Geophys. Res. Atmos.* **2003,** *108* (D9), 14.
38. Hylander, L. D.; Goodsite, M. E., Environmental Costs of Mercury Pollution. *Sci. Total Environ.* **2006,** *368* (1), 352-370.
39. Poulain, A. J.; Orihel, D. M.; Amyot, M.; Paterson, M. J.; Hintelmann, H.; Southworth, G. R., Relationship to Aquatic Between the Loading Rate of Inorganic Mercury Ecosystems and Dissolved Gaseous Mercury Production and Evasion. *Chemosphere* **2006,** *65* (11), 2199-2207.
40. Finlayson-Pitts, B. J.; Livingston, F. E.; Berko, H. N., Ozone Destruction and Bromine Photochemistry at Ground Level in the Arctic Spring. *Nature* **1990,** *343* (6259), 622-625.
41. Frinak, E. K.; Abbatt, J. P. D., Br(2) Production From the Heterogeneous Reaction of Gas-Phase OH with Aqueous Salt Solutions: Impacts of Acidity, Halide Concentration, and Organic Surfactants. *J. Phys. Chem. A* **2006,** *110* (35), 10456-10464.
42. Mozurkewich, M., Mechanisms for the Release of Halogens from Sea-Salt Particles by Free Radical Reactions. *J. Geophys. Res. Atmos.* **1995,** *100* (D7), 14199-14207.

43. Sjostedt, S. J.; Abbatt, J. P. D., Release of Gas-Phase Halogens from Sodium Halide Substrates: Heterogeneous Oxidation of Frozen Solutions and Desiccated Salts by Hydroxyl Radicals. *Environ. Res. Lett.* **2008,** *3* (4), 7.
44. Oldridge, N. W.; Abbatt, J. P. D., Formation of Gas-Phase Bromine from Interaction of Ozone with Frozen and Liquid NaCl/NaBr Solutions: Quantitative Separation of Surficial Chemistry from Bulk-Phase Reaction. *J. Phys. Chem. A* **2011,** *115* (12), 2590-2598.
45. Clifford, D.; Donaldson, D. J., Direct Experimental Evidence for a Heterogeneous Reaction of Ozone with Bromide at the Air-Aqueous Interface. *J. Phys. Chem. A* **2007,** *111* (39), 9809-9814.
46. Reeser, D. I.; George, C.; Donaldson, D. J., Photooxidation of Halides by Chlorophyll at the Air-Salt Water Interface. *J. Phys. Chem. A* **2009,** *113* (30), 8591-8595.
47. Oum, K. W.; Lakin, M. J.; Finlayson-Pitts, B. J., Bromine Activation in the Troposphere by the Dark Reaction of O-3 with Seawater Ice. *Geophys. Res. Lett.* **1998,** *25* (21), 3923-3926.
48. Simpson, W. R.; Alvarez-Aviles, L.; Douglas, T. A.; Sturm, M.; Domine, F., Halogens in the Coastal Snow Pack Near Barrow, Alaska: Evidence for Active Bromine Air-Snow Chemistry During Springtime. *Geophys. Res. Lett.* **2005,** *32* (4), 4.
49. Yang, J.; Yau, M. K., A New Triple-Moment Blowing Snow Model. *Bound.-Layer Meteorol.* **2008,** *126* (1), 137-155.
50. Jones, A. E.; Anderson, P. S.; Begoin, M.; Brough, N.; Hutterli, M. A.; Marshall, G. J.; Richter, A.; Roscoe, H. K.; Wolff, E. W., BrO, Blizzards, and Drivers of Polar Tropospheric Ozone Depletion Events. *Atmos. Chem. Phys.* **2009,** *9* (14), 4639-4652.
51. Koop, T.; Kapilashrami, A.; Molina, L. T.; Molina, M. J., Phase Transitions of Sea-Salt/Water Mixtures at Low Temperatures: Implications for Ozone Chemistry in the Polar Marine Boundary Layer. *J. Geophys. Res. Atmos.* **2000,** *105* (D21), 26393-26402.
52. Abbatt, J. P. D.; Lee, A. K. Y.; Thornton, J. A., Quantifying Trace Gas Uptake to Tropospheric Aerosol: Recent Advances and Remaining Challenges. *Chem. Soc. Rev.* **2012,** *41* (19), 6555-6581.
53. Chen, G.; Davis, D.; Crawford, J.; Nowak, J. B.; Eisele, F.; Mauldin, R. L.; Tanner, D.; Buhr, M.; Shetter, R.; Lefer, B.; Arimoto, R.; Hogan, A.; Blake, D., An Investigation of South Pole HOx Chemistry: Comparison of Model Results with ISCAT Observations. *Geophys. Res. Lett.* **2001,** *28* (19), 3633-3636.
54. Honrath, R. E.; Guo, S.; Peterson, M. C.; Dziobak, M. P.; Dibb, J. E.; Arsenault, M. A., Photochemical Production of Gas Phase NOx from Ice Crystal NO3. *J. Geophys. Res. Atmos.* **2000,** *105* (D19), 24183-24190.
55. Honrath, R. E.; Lu, Y.; Peterson, M. C.; Dibb, J. E.; Arsenault, M. A.; Cullen, N. J.; Steffen, K., Vertical Fluxes of NOx, HONO, and HNO3 Above the Snowpack at Summit, Greenland. *Atmos. Environ.* **2002,** *36* (15-16), 2629-2640.
56. Dubowski, Y.; Colussi, A. J.; Hoffmann, M. R., Nitrogen Dioxide Release in the 302 nm Band Photolysis of Spray-Frozen Aqueous Nitrate Solutions. Atmospheric Implications. *J. Phys. Chem. A* **2001,** *105* (20), 4928-4932.
57. Chu, L.; Anastasio, C., Quantum Yields of Hydroxyl Radical and Nitrogen Dioxide from the Photolysis of Nitrate on Ice. *J. Phys. Chem. A* **2003,** *107* (45), 9594-9602.
58. Cotter, E. S. N.; Jones, A. E.; Wolff, E. W.; Bauguitte, S. J. B., What Controls Photochemical NO and NO2 Production from Antarctic Snow? Laboratory Investigation Assessing the Wavelength and Temperature Dependence. *J. Geophys. Res. Atmos.* **2003,** *108* (D4), 10.

59. Yabushita, A.; Iida, D.; Hama, T.; Kawasaki, M., Direct Observation of OH Radicals Ejected from Water Ice Surface in the Photoirradiation of Nitrate Adsorbed on Ice at 100 K. *J. Phys. Chem. A* **2008,** *112* (40), 9763-9766.
60. Yabushita, A.; Kawanaka, N.; Kawasaki, M.; Hamer, P. D.; Shallcross, D. E., Release of Oxygen Atoms and Nitric Oxide Molecules from the Ultraviolet Photodissociation of Nitrate Adsorbed on Water Ice Films at 100 K. *J. Phys. Chem. A* **2007,** *111* (35), 8629-8634.
61. Beine, H.; Colussi, A. J.; Amoroso, A.; Esposito, G.; Montagnoli, M.; Hoffmann, M. R., HONO Emissions from Snow Surfaces. *Environ. Res. Lett.* **2008,** *3* (4), 6.
62. Qiu, R.; Green, S. A.; Honrath, R. E.; Peterson, M. C.; Lu, Y.; Dziobak, M., Measurements of J(NO3)(-) in Snow by Nitrate-Based Actinometry. *Atmos. Environ.* **2002,** *36* (15-16), 2563-2571.
63. Zhou, X. L.; Beine, H. J.; Honrath, R. E.; Fuentes, J. D.; Simpson, W.; Shepson, P. B.; Bottenheim, J. W., Snowpack Photochemical Production of HONO: a Major Source of OH in the Arctic Boundary Layer in Springtime. *Geophys. Res. Lett.* **2001,** *28* (21), 4087-4090.
64. King, M. D.; France, J. L.; Fisher, F. N.; Beine, H. J., Measurement and Modelling of UV Radiation Penetration and Photolysis Rates of Nitrate and Hydrogen Peroxide in Antarctic Sea Ice: An Estimate of the Production Rate of Hydroxyl Radicals in First-Year Sea Ice. *J. Photoch. Photobio. A* **2005,** *176* (1-3), 39-49.
65. France, J. L.; King, M. D.; Lee-Taylor, J., Hydroxyl (OH) Radical Production Rates in Snowpacks from Photolysis of Hydrogen Peroxide (H2O2) and Nitrate (NO3-). *Atmos. Environ.* **2007,** *41* (26), 5502-5509.
66. Jacobi, H. W.; Annor, T.; Quansah, E., Investigation of the Photochemical Decomposition of Nitrate, Hydrogen Peroxide, and Formaldehyde in Artificial Snow. *J. Photoch. Photobio. A* **2006,** *179* (3), 330-338.
67. Chu, L.; Anastasio, C., Formation of Hydroxyl Radical from the Photolysis of Frozen Hydrogen Peroxide. *J. Phys. Chem. A* **2005,** *109* (28), 6264-6271.
68. Chu, L.; Anastasio, C., Temperature and Wavelength Dependence of Nitrite Photolysis in Frozen and Aqueous Solutions. *Environ. Sci. Technol.* **2007,** *41* (10), 3626-3632.
69. France, J. L.; King, M. D.; Lee-Taylor, J.; Beine, H. J.; Ianniello, A.; Domine, F.; MacArthur, A., Calculations of In-Snow NO2 and OH radical Photochemical Production and Photolysis Rates: A Field and Radiative-Transfer Study of the Optical Properties of Arctic (Ny-Alesund, Svalbard) Snow. *J. Geophys. Res. Earth Surf.* **2011,** *116*, 16.
70. Anastasio, C.; Chu, L., Photochemistry of Nitrous Acid (HONO) and Nitrous Acidium Ion (H2ONO+) in Aqueous Solution and Ice. *Environ. Sci. Technol.* **2009,** *43* (4), 1108-1114.
71. France, J. L.; Reay, H. J.; King, M. D.; Voisin, D.; Jacobi, H. W.; Domine, F.; Beine, H.; Anastasio, C.; MacArthur, A.; Lee-Taylor, J., Hydroxyl Radical and NOx Production Rates, Black Carbon Concentrations and Light-Absorbing Impurities in Snow from Field Measurements of Light Penetration and Nadir Reflectivity of Onshore and Offshore Coastal Alaskan Snow. *J. Geophys. Res. Atmos.* **2012,** *117*, 21.
72. Blaha, L.; Klanova, J.; Klan, P.; Janosek, J.; Skarek, M.; Ruzicka, R., Toxicity Increases in Ice Containing Monochlorophenols Upon Photolysis: Environmental Consequences. *Environ. Sci. Technol.* **2004,** *38* (10), 2873-2878.
73. Klan, P.; Klanova, J.; Holoubek, I.; Cupr, P., Photochemical Activity of Organic Compounds in Ice Induced by Sunlight Irradiation: The Svalbard Project. *Geophys. Res. Lett.* **2003,** *30* (6), 4.

74. Klanova, J.; Klan, P.; Heger, D.; Holoubek, I., Comparison of the Effects of UV, H2O2/UV and Gamma-Irradiation Processes on Frozen and Liquid Water Solutions of Monochlorophenols. *Photochem. Photobiol. Sci.* **2003,** *2* (10), 1023-1031.
75. Klanova, J.; Klan, P.; Nosek, J.; Holoubek, I., Environmental Ice Photochemistry: Monochlorophenols. *Environ. Sci. Technol.* **2003,** *37* (8), 1568-1574.
76. Albert, M. R.; Grannas, A. M.; Bottenheim, J.; Shepson, P. B.; Perron, F. E., Processes and Properties of Snow-Air Transfer in the High Arctic with Application to Interstitial Ozone at Alert, Canada. *Atmos. Environ.* **2002,** *36* (15-16), 2779-2787.
77. Grannas, A. M.; Bausch, A. R.; Mahanna, K. M., Enhanced Aqueous Photochemical Reaction Rates after Freezing. *J. Phys. Chem. A* **2007,** *111* (43), 11043-11049.
78. Grannas, A. M.; Shepson, P. B.; Filley, T. R., Photochemistry and Nature of Organic Matter in Arctic and Antarctic Snow. *Global Biogeochem. Cy.* **2004,** *18* (1), 10.
79. Dubowski, Y.; Hoffmann, M. R., Photochemical Transformations in Ice: Implications for the Fate of Chemical Species. *Geophys. Res. Lett.* **2000,** *27* (20), 3321-3324.
80. Kahan, T. F.; Wren, S. N.; Donaldson, D. J., A Pinch of Salt Is All It Takes: Chemistry at the Frozen Water Surface. *Accounts Chem. Res.* **2014,** *47* (5), 1587-1594.
81. Kahan, T. F.; Donaldson, D. J., Photolysis of Polycyclic Aromatic Hydrocarbons on Water and Ice Surfaces. *J. Phys. Chem. A* **2007,** *111*, 1277-1285.
82. Kahan, T. F.; Donaldson, D. J., Benzene Photolysis on Ice: Implications for the Fate of Organic Contaminants in the Winter. *Environ. Sci. Technol.* **2010,** *44*, 3819-3824.
83. Kahan, T. F.; Kwamena, N. O. A.; Donaldson, D. J., Different Photolysis Kinetics at the Surface of Frozen Freshwater vs. Frozen Salt Solutions. *Atmos. Chem. Phys.* **2010,** *10*, 10917-10922.
84. Kahan, T. F.; Zhao, R.; Jumaa, K. B.; Donaldson, D. J., Anthracene Photolysis in Aqueous Solution and Ice: Photon Flux Dependence and Comparison of Kinetics in Bulk Ice and at the Air−Ice Interface. *Environ. Sci. Technol.* **2010,** *44* (4), 1302-1306.
85. Ram, K.; Anastasio, C., Photochemistry of Phenanthrene, Pyrene, and Fluoranthene in Ice and Snow. *Atmos. Environ.* **2009,** *43* (14), 2252-2259.
86. Priority Pollutant List. Agency, E. P., Ed.
87. Cancer, I. A. f. R. o., Certain Polycyclic Aromatic Hydrocarbons and Heterocyclic Compounds. *IARC Monographs on the Evaluation of the Carcinogenic Risks of Chemicals to Man* **1972,** *3*.
88. Kima, K.-H.; Jahan, S. A.; Kabir, E.; Brown, R. J. C., A Review of Airborne Polycyclic Aromatic Hydrocarbons (PAHs) and Their Human Health Effects. *Environ. Int.* **2013,** *60*, 71-80.
89. Sigman, M. E.; Schuler, P. F.; Ghosh, M. M.; Dabestani, R. T., Mechanism of Pyrene Photochemical Oxidation in Aqueous and Surfactant Solutions. *Environ. Sci. Technol.* **1998,** *32*, 3980-3985.
90. Bernstein, M. P.; Sandford, S. A.; Allamandola, L. J.; Gillette, J. S.; Clemett, S. J.; Zare, R. N., UV Irradiation of Polycyclic Aromatic Hydrocarbons in Ices: Production of Alcohols, Quinones, and Ethers. *Science* **1999,** *283*, 1135-1138.
91. Mill, T.; Mabey, W. R.; Lan, B. Y.; Baraze, A., Photolysis of Polycyclic Aromatic Hydrocarbons in Water. *Chemosphere* **1981,** *10* (11/12), 1281-1290.
92. Finlayson-Pitts, B. J.; Pitts, J. N., *Chemistry of the Upper and Lower Atmosphere*. Academic Press: San Diego, 2000.
93. Wozniak, B.; Dera, J., *Light Absorption in Sea Water*. Springer: New York, 2007; Vol. 33.

94. Neff, J., *Polycyclic Aromatic Hydrocarbons in the Aquatic Environment: Sources, Fates, and Biological Effects*. Applied Science Publishers: 1979.
95. Abdel-Shafy, H. I.; Mansour, M. S., A Review on Polycyclic Aromatic Hydrocarbons: Source, Environmental Impact, Effect on Human Health and Remediation. *Egypt. J. Pet.* **2016,** *25* (1), 107-123.
96. Gudipati, M. S.; Allamandola, L. J., Facile Generation and Storage of Polycyclic Aromatic Hydrocarbon Ions in Astrophysical Ices. *Astrophys. J.* **2003,** *596* (2), L195-L198.
97. Fasnacht, M. P.; Blough, N. V., Aqueous Photodegradation of Polycyclic Aromatic Hydrocarbons. *Environ. Sci. Technol.* **2002,** *36*, 4364-4369.
98. Fasnacht, M. P.; Blough, N. V., Mechanisms of the Aqueous Photodegradation of Polycyclic Aromatic Hydrocarbons. *Environ. Sci. Technol.* **2003,** *37* (24), 5767-5772.
99. Fasnacht, M. P.; Blough, N. V., Kinetic Analysis of the Photodegradation of Polycyclic Aromatic Hydrocarbons in Aqueous Solution. *Aquat. Sci.* **2003,** *65* (4), 352-358.
100. Sasaki, J.; Aschmann, S. M.; Kwok, E. S. C.; Atkinson, R.; Arey, J., Products of the Gas-Phase OH and NO3 Radical-Initiated Reactions of Naphthalene. *Environ. Sci. Technol.* **1997,** *31* (11), 3173-3179.
101. Grosovsky, A. J.; Sasaki, J.; Arey, J.; Eastmond, D. A.; Parks, K. K.; Atkinson, R., Evaluation of the Potential Health Effects of the Atmospheric Reaction Products of Polycyclic Aromatic Hydrocarbons. *Res. Rep. Health Eff. Inst.* **1999,** *84*, 1-27.
102. Sasaki, J. C.; Arey, J.; Eastmond, D. A.; Parks, K. K.; Grosovsky, A. J., Genotoxicity Induced in Human Lymphoblasts by Atmospheric Reaction Products of Naphthalene and Phenanthrene. *Mutat. Res-Gen. Tox. En.* **1997,** *393* (1-2), 23-35.
103. Brussol, C.; Duane, M.; Carlier, P.; Kotzias, D., Photo-Induced OH Reactions of Naphthalene and its Oxidation Products on SiO2. *Environ. Sci. Pollut. Res.* **1999,** *6* (3), 138-140.
104. Behymer, T. D.; Hites, R. A., Photolysis of Polycyclic Aromatic Hydrocarbons Adsorbed on Fly Ash. *Environ. Sci. Technol.* **1988,** *22* (11), 1311-1319.
105. Grossman, J. N.; Stern, A. P.; Kirich, M. L.; Kahan, T. F., Anthracene and Pyrene Photolysis Kinetics in Aqueous, Organic, and Mixed Aqueous-Organic Phases. *Atmos. Environ.* **2016,** *128*, 158-164.
106. Zepp, R. G.; Schlotzhauer., P. F., Photoreactivity of Selected Aromatic Hydrocarbons in Water. In *Polynuclear Aromatic Hydrocarbons*, Ann Arbor Science Publishers Inc.: 1979; pp 141-158.
107. Donaldson, D. J.; Kahan, T. F.; Kwamena, N. O. A.; Handley, S. R.; Barbier, C., Atmospheric Chemistry of Urban Surface Films. In *Atmospheric Aerosols*, American Chemical Society: 2009; pp 79-89.
108. Clark, B. R.; Lacey, E.; Gill, J. H.; Capon, R. J., The Effect of Halide Salts on the Production of Gymnoascus Reessii Polyenylpyrroles. *J. Nat. Prod.* **2007,** *70* (4), 665-667.
109. Prak, D. J. L.; Milewski, E. A.; Jedlicka, E. E.; Kersey, A. J.; O'Sullivan, D. W., Influence of pH, Temperature, Salinity, and Dissolved Organic Matter on the Photolysis of 2,4-Dinitrotoluene and 2,6-Dinitrotoluene in Seawater. *Mar. Chem.* **2013,** *157*, 233-241.
110. Mihas, O.; Kalogerakis, N.; Psillakis, E., Photolysis of 2,4-Dinitrotoluene in Various Water Solutions: Effect of Dissolved Species. *J. Hazard. Mater.* **2007,** *146* (3), 535-539.
111. de Bruyn, W. J.; Clark, C. D.; Ottelle, K.; Aiona, P., Photochemical Degradation of Phenanthrene as a Function of Natural Water Variables Modeling Freshwater to Marine Environments. *Mar. Pollut. Bull.* **2012,** *64* (3), 532-538.

112. Grebel, J. E.; Pignatello, J. J.; Mitch, W. A., Impact of Halide Ions on Natural Organic Matter-Sensitized Photolysis of 17 beta-Estradiol in Saline Waters. *Environ. Sci. Technol.* **2012,** *46* (13), 7128-7134.
113. Lam, M. W.; Tantuco, K.; Mabury, S. A., PhotoFate: A New Approach in Accounting for the Contribution of Indirect Photolysis of Pesticides and Pharmaceuticals in Surface Waters. *Environ. Sci. Technol.* **2003,** *37* (5), 899-907.
114. Russi, H.; Kotzias, D.; Korte, F., Photoinduced Hydroxylation Reactions of Organic Chemicals in Natural Waters, Nitrates as Potential Sources for OH Radicals. *Chemosphere* **1982,** *11* (10), 1041-1048.
115. Brezonik, P. L.; Fulkerson-Brekken, J., Nitrate-Induced Photolysis in Natural Waters: Controls on Concentrations of Hydroxyl Radical Photo-Intermediates by Natural Scavenging Agents. *Environ. Sci. Technol.* **1998,** *32* (19), 3004-3010.
116. Buxton, G. V.; Greenstock, C. L.; Helman, W. P.; Ross, A. B., Critical Review of Rate Constants for Reactions of Hydrated Electrons, Hydrogen Atoms and Hydroxyl Radicals (·OH/·O− in Aqueous Solution. *J. Phys. Chem. Ref. Data* **1988,** *17* (2), 513-886.
117. Mill, T.; Hendry, D. G.; Richardson, H., Free-Radical Oxidants in Natural Waters. *Science* **1980,** *207* (4433), 886-887.
118. Neta, P.; Huie, R. E.; Ross, A. B., Rate Constants for Reactions of Peroxyl Radicals in Fluid Solutions. *J. Phys. Chem. Ref. Data* **1990,** *19* (2), 413-513.
119. Haag, W. R.; Hoigne, J., Singlet Oxygen in Surface Waters. 3. Photochemical Formation and Steady-State Concentrations in Various Types of Waters. *Environ. Sci. Technol.* **1986,** *20* (4), 341-348.
120. Kotzias, D.; Herrmann, M.; Zsolnay, A.; Beyerlepfnur, R.; Parlar, H.; Korte, F., Photochemical Aging of Humic Substances. *Chemosphere* **1987,** *16* (7), 1463-1468.
121. Hassett, J. P.; Anderson, M. A., Effects of Dissolved Organic Matter on Adsorption of Hydrophobic Organic Compounds by River and Sewage-Borne Particles. *Water Res.* **1982,** *16* (5), 681-686.
122. Calza, P.; Vione, D.; Minero, C., The role of Humic and Fulvic Acids in the Phototransformation of Phenolic Compounds in Seawater. *Sci. Total Environ.* **2014,** *493*, 411-418.
123. Dash, J. G.; Rempel, A. W.; Wettlaufer, J. S., The Physics of Premelted Ice and its Geophysical Consequences. *Rev. Mod. Phys.* **2006,** *78* (3), 695-741.
124. Dash, J. G.; Fu, H. Y.; Wettlaufer, J. S., The Premelting of Ice and its Environmental Consequences. *Rep. Prog. Phys.* **1995,** *58* (1), 115-167.
125. Wettlaufer, J. S.; Worster, M. G., Premelting Dynamics. In *Annu. Rev. Fluid Mech.*, Annual Reviews: Palo Alto, 2006; Vol. 38, pp 427-452.
126. Rosenberg, R., Why is Ice Slippery? *Phys. Today* **2005,** *58* (12), 50-55.
127. Gladich, I.; Pfalzgraff, W.; Marsalek, O.; Jungwirth, P.; Roeselova, M.; Neshyba, S., Arrhenius Analysis of Anisotropic Surface Self-Diffusion on the Prismatic Facet of Ice. *Phys. Chem. Chem. Phys.* **2011,** *13* (44), 19960-19969.
128. Golecki, I.; Jaccard, C., Intrinsic Surface Disorder in Ice Near the Melting Point. *J. Phys. C Solid State* **1978,** *11* (20), 4229-4237.
129. Wang, S. Y., Photochemical Reactions in Frozen Solutions. *Nature* **1961,** *190* (477), 690-694.
130. Wang, S. Y., The Mechanism for Frozen Aqueous Solution Irradiation of Pyrimidines. *Photochem. Photobiol.* **1964,** *3* (4), 395-398.

131. Gross, G. W.; Gutjahr, A.; Caylor, K., Recent Experimental Work on Solute Redistribution at the Ice/Water Interface. Implications for Electrical Properties and Interface Processes. *J. Phys-Paris* **1987,** *48* (C-1), 527-533.
132. Smith, M.; Pounder, E. R., Impurity Concentration Profiles in Ice by an Anthrone Method. *Can. J. Phys.* **1960,** *38* (3), 354-368.
133. Cohen, S. R.; Weissbuch, I.; PopovitzBiro, R.; Majewski, J.; Mauder, H. P.; Lavi, R.; Leiserowitz, L.; Lahav, M., Spontaneous Assembly in Organic Thin Films Spread on Aqueous Subphase: A Scanning Force Microscope (SFM) Study. *Israel J. Chem.* **1996,** *36* (1), 97-110.
134. Finnegan, W. G.; Pitter, R. L., Ion-Induced Charge Separations in Growing Single Ice Crystals: Effects on Growth and Interaction Processes. *J. Colloid Interf. Sci.* **1997,** *189* (2), 322-327.
135. Petrenko, V.; Whitworth, R., *Physics of Ice*. OUP Oxford: 1999.
136. Giannelli, V.; Thomas, D. N.; Haas, C.; Kattner, G.; Kennedy, H.; Dieckmann, G. S., Behaviour of Dissolved Organic Matter and Inorganic Nutrients During Experimental Sea-Ice Formation. In *Annals of Glaciology, Vol 33*, Jeffries, M. O.; Eicken, H., Eds. Int Glaciological Soc: Cambridge, 2001; Vol. 33, pp 317-321.
137. Cho, H.; Shepson, P. B.; Barrie, L. A.; Cowin, J. P.; Zaveri, R., NMR Investigation of the Quasi-Brine Layer in Ice/Brine Mixtures. *J. Phys. Chem. B* **2002,** *106* (43), 11226-11232.
138. Heger, D.; Jirkovsky, J.; Klan, P., Aggregation of Methylene Blue in Frozen Aqueous Solutions Studied by Absorption Spectroscopy. *J. Phys. Chem. A* **2005,** *109* (30), 6702-6709.
139. Vrbka, L.; Jungwirth, P., Brine Rejection from Freezing Salt Solutions: A Molecular Dynamics Study. *Phys. Rev. Lett.* **2005,** *95* (14), 4.
140. Wren, S. N.; Donaldson, D. J., Exclusion of Nitrate to the Air-Ice Interface During Freezing. *J. Phys. Chem. Lett.* **2011,** *2* (16), 1967-1971.
141. Kahan, T. F.; Reid, J. P.; Donaldson, D. J., Spectroscopic Probes of the Quasi-Liquid Layer on Ice. *J. Phys. Chem. A* **2007,** *111* (43), 11006-11012.
142. Dosch, H.; Lied, A.; Bilgram, J. H., Glancing-Angle X-Ray Scattering Studies of the Premelting of Ice Surfaces. *Surf. Sci.* **1995,** *327* (1-2), 145-164.
143. Furukawa, Y.; Nada, H., Anisotropic Surface Melting of an Ice Crystal and its Relationship to Growth Forms. *J. Phys. Chem. B* **1997,** *101* (32), 6167-6170.
144. Conde, M. M.; Vega, C.; Patrykiejew, A., The thickness of a Liquid Layer on the Free Surface of Ice as Obtained from Computer Simulation. *J. Chem. Phys.* **2008,** *129* (1), 11.
145. Doppenschmidt, A.; Butt, H. J., Measuring the Thickness of the Liquid-Like Layer on Ice Surfaces with Atomic Force Microscopy. *Langmuir* **2000,** *16* (16), 6709-6714.
146. Pittenger, B.; Fain, S. C.; Cochran, M. J.; Donev, J. M. K.; Robertson, B. E.; Szuchmacher, A.; Overney, R. M., Premelting at Ice-Solid Interfaces Studied Via Velocity-Dependent Indentation With Force Microscope Tips. *Phys. Rev. B* **2001,** *63* (13), 15.
147. Carignano, M. A.; Baskaran, E.; Shepson, P. B.; Szleifer, I., Molecular Dynamics Simulation of Ice Growth from Supercooled Pure Water and From Salt Solution. In *Annals of Glaciology, Vol 44, 2006*, Langhorne, P.; Squire, V., Eds. Int Glaciological Soc: Cambridge, 2006; Vol. 44, pp 113-117.
148. Carignano, M. A.; Shepson, P. B.; Szleifer, I., Ions at the Ice/Vapor Interface. *Chem. Phys. Lett.* **2007,** *436* (1-3), 99-103.
149. Belzile, C.; Gibson, J. A. E.; Vincent, W. F., Colored Dissolved Organic Matter and Dissolved Organic Carbon Exclusion from Lake Ice: Implications for Irradiance Transmission and Carbon Cycling. *Limnol. Oceanogr.* **2002,** *47* (5), 1283-1293.

150. Desnoyers, J. E.; Billon, M.; Leger, S.; Perron, G.; Morel, J. P., Salting out of Alcohols by Alkali Halides at the Freezing Temperature. *J. Solution Chem.* **1976,** *5* (10), 681-691.
151. McNeill, V. F.; Geiger, F. M.; Loerting, T.; Trout, B. L.; Molina, L. T.; Molina, M. J., Interaction of Hydrogen Chloride with Ice Surfaces: The Effects of Grain Size, Surface Roughness, and Surface Disorder. *J. Phys. Chem. A* **2007,** *111* (28), 6274-6284.
152. McNeill, V. F.; Loerting, T.; Geiger, F. M.; Trout, B. L.; Molina, M. J., Hydrogen Chloride-Induced Surface Disordering on Ice. *P. Natl. Acad. Sci. USA* **2006,** *103* (25), 9422-9427.
153. Moussa, S. G.; Kuo, M. H.; McNeill, V. F., Nitric Acid-Induced Surface Disordering on Ice. *Phys. Chem. Chem. Phys.* **2013,** *15* (26), 10989-10995.
154. Takenaka, N.; Ueda, A.; Daimon, T.; Bandow, H.; Dohmaru, T.; Maeda, Y., Acceleration Mechanism of Chemical Reaction by Freezing: The Reaction of Nitrous Acid with Dissolved Oxygen. *J. Phys. Chem.* **1996,** *100* (32), 13874-13884.
155. Pruppacher, H.; JD, K., *Microphysics of Clouds and Precipitation: With an Introduction to Cloud Chemistry and Cloud Electricity*. Kluwer Academy: Dordrecht, Netherlands, 1997.
156. Kurkova, R.; Ray, D.; Nachtigallova, D.; Klan, P., Chemistry of Small Organic Molecules on Snow Grains: The Applicability of Artificial Snow for Environmental Studies. *Environ. Sci. Technol.* **2011,** *45* (8), 3430-3436.
157. Betterton, E. A.; Anderson, D. J., Autoxidation of N(III), S(IV), and Other Species in Frozen Solution - A Possible Pathway for Enhanced Chemical Transformation in Freezing Systems. *J. Atmos. Chem.* **2001,** *40* (2), 171-189.
158. O' Driscoll, P.; Lang, K.; Minogue, N.; Sodeau, J., Freezing Halide Ion Solutions and the Release of Interhalogens to the Atmosphere. *J. Phys. Chem. A* **2006,** *110* (14), 4615-4618.
159. O'Driscoll, P.; Minogue, N.; Takenaka, N.; Sodeau, J., Release of Nitric Oxide and Iodine to the Atmosphere from the Freezing of Sea-Salt Aerosol Components. *J. Phys. Chem. A* **2008,** *112* (8), 1677-1682.
160. Kawamura, K.; Suzuki, I., Ice Core Record of Polycyc|ic Aromalic Hydrocarbons over the Past 400 Years. *Naturwissenschaften* **1994,** *81*, 502-505.
161. Halsall, C. J.; Barrie, L. A.; Fellin, P.; Muir, D. C. G.; Billeck, B. N.; Lockhart, L.; Rovinsky, F. Y.; Kononov, E. Y.; Pastukhov, B., Spatial and Temporal Variation of Polycyclic Aromatic Hydrocarbons in the Arctic Atmosphere. *Environ. Sci. Technol.* **1997,** *31*, 3593-3599.
162. MacNaughton, D. a., Twentieth Century Petroleum Statistics 1991 Dallas, Texas, 1991; p 126.
163. Boom, A.; Marsalek, J., Accumulation of Polycyclic Aromatic Hydrocarbons (PAHs) in an Urban Snowpack. *Sci. Total Environ.* **1988,** *74*, 133-148.
164. Hautala, E. L.; Rekila, R.; Tarhanen, J.; Ruuskanen, J., Deposition of Motor Vehicle Emissions and Winter Maintenance Along Roadside Assessed by Snow Analyses. *Environ. Pollut.* **1995,** *87* (1), 45-49.
165. Reinosdotter, K.; Viklander, M.; Malmqvist, P. A., Polycyclic Aromatic Hydrocarbons and Metals in Snow Along a Highway. *Water Sci. Technol.* **2006,** *54* (6-7), 195-203.
166. Sharma, M.; McBean, E. A., PAH Deposition to Snow Surface - Chemical Analysis and Interpretation of Results. *Environ. Sci. Pollut. Res.* **2001,** *8* (1), 11-18.
167. Schrimpff, E.; Thomas, W.; Herrmann, R., Regional Patterns of Contaminants (PAH, Pesticides and Trace Metals) in Snow of Northeast Bavaria and Their Relationship to Human Influence and Orographic Effects. *Water Air Soil Poll.* **1979,** *11* (4), 481-497.

168. Franz, T. P.; Eisenreich, S. J., Accumulation of Polychlorinated Biphenyls and Polycyclic Aromatic Hydrocarbons in the Snowpack of Minnesota and Lake Superior. *J. Great Lakes Res.* **2000,** *26* (2), 220-234.
169. Carrera, G.; Fernandez, P.; Vilanova, R. M.; Grimalt, J. O., Persistent Organic Pollutants in Snow from European High Mountain Areas. *Atmos. Environ.* **2001,** *35* (2), 245-254.
170. Fernandez, P.; Carrera, G.; Grimalt, J. O.; Ventura, M.; Camarero, L.; Catalan, J.; Nickus, U.; Thies, H.; Psenner, R., Factors Governing the Atmospheric Deposition of Polycyclic Aromatic Hydrocarbons to Remote Areas. *Environ. Sci. Technol.* **2003,** *37* (15), 3261-3267.
171. Wania, F., Assessing the Potential of Persistent Organic Chemicals for Long-Range Transport and Accumulation in Polar Regions. *Environ. Sci. Technol.* **2003,** *37* (7), 1344-1351.
172. Li, Y. F.; Macdonald, R. W.; Jantunen, L. M. M.; Harner, T.; Bidleman, T. F.; Strachan, W. M. J., The Transport of Beta-Hexachlorocyclohexane to the Western Arctic Ocean: a Contrast to Alpha-HCH. *Sci. Total Environ.* **2002,** *291* (1-3), 229-246.
173. Wania, F.; Mackay, D., Global Fractionation and Cold Condensation of Low Volatility Organochlorine Compounds in Polar Regions. *Ambio* **1993,** *22* (1), 10-18.
174. Wania, F.; Mackay, D., Modelling the Global Distribution of Toxaphene: A Discussion of Feasibility and Desirability. *Chemosphere* **1993,** *27* (10), 2079-2094.
175. Wania, F.; Mackay, D., A Global Distribution Model for Persistent Organic Chemicals. *Sci. Total Environ.* **1995,** *160-61*, 211-232.
176. Peterle, T. J., DDT in Antarctic Snow. *Nature* **1969,** *224* (5219), 620-&.
177. Peel, D. A., Organochlorine Residues in Antarctic Snow. *Nature* **1975,** *254* (5498), 324-325.
178. Risebrough, R. W.; Walker, W.; Schmidt, T. T.; Delappe, B. W.; Connors, C. W., Transfer of Chlorinated Biphenyls to Antarctica. *Nature* **1976,** *264* (5588), 738-739.
179. Wania, F.; Mackay, D., Tracking the Distribution of Persistent Organic Pollutants. *Environ. Sci. Technol.* **1996,** *30* (9), 390-396.
180. Pruppacher, H. R.; Klett, J. D., Hydrodynamics of Single Cloud and Precipitation Particles. In *Microphysics of Clouds and Precipitation*, Springer Netherlands: 1978; pp 282-346.
181. Wania, F.; Hoff, J. T.; Jia, C. Q.; Mackay, D., The Effects of Snow and Ice on the Environmental Behaviour of Hydrophobic Organic Chemicals. *Environ. Pollut.* **1998,** *102* (1), 25-41.
182. Bartels-Rausch, T.; Bergeron, V.; Cartwright, J. H. E.; Escribano, R.; Finney, J. L.; Grothe, H.; Gutierrez, P. J.; Haapala, J.; Kuhs, W. F.; Pettersson, J. B. C.; Price, S. D.; Sainz-Diaz, C. I.; Stokes, D. J.; Strazzulla, G.; Thomson, E. S.; Trinks, H.; Uras-Aytemiz, N., Ice Structures, Patterns, and Processes: A View Across the Icefields. *Rev. Mod. Phys.* **2012,** *84* (2), 885-944.
183. Domine, F.; Taillandier, A. S.; Simpson, W. R., A Parameterization of the Specific Surface Area of Seasonal Snow for Field Use and for Models of Snowpack Evolution. *J. Geophys. Res. Earth Surf.* **2007,** *112* (F2), 13.
184. Lei, Y. D.; Wania, F., Is Rain or Snow a More Efficient Scavenger of Organic Chemicals? *Atmos. Environ.* **2004,** *38* (22), 3557-3571.
185. Blais, J. M.; Schindler, D. W.; Muir, D. C. G.; Kimpe, L. E.; Donald, D. B.; Rosenberg, B., Accumulation of Persistent Organochlorine Compounds in Mountains of Western Canada. *Nature* **1998,** *395* (6702), 585-588.
186. Kuhn, M., The Nutrient Cycle Through Snow and Ice, a Review. *Aquat. Sci.* **2001,** *63* (2), 150-167.

187. Macdonald, R. W.; Mackay, D.; Li, Y. F.; Hickie, B., How Will Global Climate Change Affect Risks from Long-Range Transport of Persistent Organic Pollutants? *Hum. Ecol. Risk Assess.* **2003,** *9* (3), 643-660.
188. Stocker, J.; Scheringer, M.; Wegmann, F.; Hungerbuhler, K., Modeling the Effect of Snow and Ice on the Global Environmental Fate and Long-Range Transport Potential of Semivolatile Organic Compounds. *Environ. Sci. Technol.* **2007,** *41* (17), 6192-6198.
189. Ardura, D.; Kahan, T. F.; Donaldson, D. J., Self-Association of Naphthalene at the Air-Ice Interface. *J. Phys. Chem. A* **2009,** *113*, 7353-7359.
190. Domine, F.; Bock, J.; Voisin, D.; Donaldson, D. J., Can We Model Snow Photochemistry? Problems with the Current Approaches. *J. Phys. Chem. A* **2013,** *117* (23), 4733-4749.
191. Domine, F.; Gallet, J. C.; Bock, J.; Morin, S., Structure, Specific Surface Area and Thermal Conductivity of the Snowpack Around Barrow, Alaska. *J. Geophys. Res. Atmos.* **2012,** *117*, 12.
192. Beine, H.; Anastasio, C.; Domine, F.; Douglas, T.; Barret, M.; France, J.; King, M.; Hall, S.; Ullmann, K., Soluble Chromophores in Marine Snow, Seawater, Sea Ice and Frost Flowers Near Barrow, Alaska. *J. Geophys. Res. Atmos.* **2012,** *117*, 12.
193. Richard, C.; Trubetskaya, O.; Trubetskoj, O.; Reznikova, O.; Afanas'eva, G.; Aguer, J. P.; Guyot, G., Key Role of the Low Molecular Size Fraction of Soil Humic Acids for Fluorescence and Photoinductive Activity. *Environ. Sci. Technol.* **2004,** *38* (7), 2052-2057.
194. Canonica, S.; Jans, U.; Stemmler, K.; Hoigne, J., Transformation Kinetics of Phenols in Water: Photosensitization by Dissolved Natural Organic Material and Aromatic Ketones. *Environ. Sci. Technol.* **1995,** *29*, 1822-1831.
195. Aguer, J.-P.; Richard, C., Reactive Species Produced on Irradiation at 365 nm of Aqueous Solutions of Humic Acids. *J. Photoch. Photobio. A* **1996,** *93*, 193-198.
196. Hoigné, J.; Faust, B. C.; Haag, W. R.; Scully, F. E.; Zepp, R. G., Aquatic Humic Substances as Sources and Sinks of Photochemically Produced Transient Reactants. *ACS Sym. Ser.* **1989,** *219*, 363-381.
197. Zepp, R. G.; Baughman, G. L.; Schlotzhauer, P. F., Comparison of Photochemical Behavior of Various Humic Substances in Water: I. Sunlight Induced Reactions of Aquatic Pollutants Photosensitized by Humic Substances. *Chemosphere* **1981,** *10* (1), 109-117.
198. Grannas, A. M.; Pagano, L. P.; Pierce, B. C.; Bobby, R.; Fede, A., Role of Dissolved Organic Matter in Ice Photochemistry. *Environ. Sci. Technol.* **2014,** *48*, 10725-10733.
199. Liyana-Arachchi, T. P.; Valsaraj, K. T.; Hung, F. R., Adsorption of Naphthalene and Ozone on Atmospheric Air/Ice Interfaces Coated with Surfactants: a Molecular Simulation Study. *J. Phys. Chem. A* **2012,** *116* (10), 2519-28.

Chapter Two:

Non-Chromophoric Organic Matter Suppresses Polycyclic Aromatic Hydrocarbon Photolysis in Ice and at Ice Surfaces

Reproduced with permission from:

Malley, Philip PA, and Kahan, Tara F. "Nonchromophoric Organic Matter Suppresses Polycyclic Aromatic Hydrocarbon Photolysis in Ice and at Ice Surfaces." *The Journal of Physical Chemistry A* 118.9 (2014): 1638-1643.

2.1 Abstract

We have investigated the effects of organic matter (OM) that does not absorb sunlight ("non-chromophoric") on the reactive environment presented by bulk ice and ice surfaces. Fluorescence spectroscopy showed that the presence of as little as 2.5×10^{-5} M octanol or decanol reduces the extent to which naphthalene self-associates at ice surfaces, which indicates that naphthalene partitions between ice and organic phases present there. We also measured photolysis kinetics of the polycyclic aromatic hydrocarbons (PAHs) anthracene, pyrene, and phenanthrene in bulk ice and at ice surfaces containing 2.5×10^{-5} M to 7.5×10^{-3} M OM. In bulk ice, even the lowest concentrations of OM reduced photolysis kinetics to below our detection limits. Organic matter also reduced measured photolysis kinetics of PAHs at ice surfaces, but generally to a lesser extent than in bulk ice. Our results support previous reports that bulk ice and ice surfaces present distinct reaction environments, and show for the first time that OM can affect PAH photolysis kinetics by altering the physical environment within bulk ice and at ice surfaces.

2.2 Introduction

A wide range of atmospherically-important reactions occur in snow and ice at Earth's surface (e.g. refs 1-6). Reactions in ice occur primarily in two compartments: Veins and pockets within the ice bulk, which contain liquid water,[7] and at the ice surface, which has physicochemical properties that are distinct from both bulk ice and liquid water (e.g. refs 7-11). Some reactions have been shown to proceed at different rates in these two regions.[12-13]

Reaction kinetics in ice have been measured primarily in samples prepared from deionized water. This minimizes experimental artifacts and simplifies the reaction system, but

may not accurately represent the reaction environment that ice presents in much of the world. Although some ice (such as that in remote inland polar regions) contains very low solute concentrations, snow in most of the world contains high concentrations of solutes such as halide salts and organic matter (OM). Solute concentrations in veins and pockets within ice and at ice surfaces can be significantly higher than in the pre-frozen solution due to exclusion from the ice matrix during freezing.[8]

Aromatic pollutants such as pesticides and polycyclic aromatic hydrocarbons (PAHs) are found in snow both in urban centers and remote regions (e.g. Ref 14). Many aromatic pollutants have carcinogenic and mutagenic properties; their toxicity often increases after photolysis (e.g. ref 15). Some recent studies have measured photolysis kinetics of aromatic pollutants in ice. Studies that probed bulk ice (or liquid regions therein) generally reported photolysis kinetics that were similar to those measured in liquid water.[13, 16] However, studies that probed the ice surface reported much faster photolysis rates.[13, 17-19] In bulk ice, solutes that photolyze to form hydroxyl radicals increased measured PAH reaction rates,[12, 16, 20] but no enhancement was observed at ice surfaces.[12, 17] Sodium chloride and sodium bromide have been shown to decrease photolysis rates of the aromatic compound harmine at ice surfaces due to the formation of a liquid brine at the ice surface; at high salt concentrations, harmine photolysis kinetics were the same as those measured in liquid water.[19] These studies show that solutes can greatly alter the reaction environment in ice and at ice surfaces.

Organic species are often associated with natural waters and with snow and ice in the atmosphere (e.g. refs 5, 21). Immiscible organic species form coatings at water surfaces that can significantly affect reaction kinetics there. The mass transfer of gas-phase species to water can be enhanced or suppressed by organic films, as can heterogeneous reactions such as hydrolysis and

ozonation (e.g. refs 22-26). Chromophoric dissolved organic matter (cDOM) absorbs solar radiation, and so can affect photochemistry in aqueous solution by filtering sunlight, by acting as a photosensitizer, or by producing reactive species such as hydroxyl radicals (e.g. ref 27). Organic matter that does not absorb sunlight (non-chromophoric OM) may also affect photochemistry: We have recently shown that PAH photolysis in aqueous solution is suppressed by miscible organic species such as methanol.[28] Immiscible OM may also affect photochemistry by forming microenvironments in natural waters to which hydrophobic pollutants can partition; the fate of hydrophobic pollutants in these organic environments may be substantially different from that in aqueous solution (e.g. ref 27). PAH photolysis is significantly slower in the water-immiscible organic solvents octanol and decanol than in aqueous solution.[28-29] However, we have recently shown that photolysis in aqueous solutions containing several mM octanol or decanol (corresponding to one to several monolayers at the water surface) proceeds at similar rates as in pure deionized water.[28] This suggests that PAH photolysis kinetics are regulated by total OM concentration rather than by surface excess.

Organic pollutants such as PAHs are thought to be strongly associated with OM in snow and ice.[21] However, the effects of OM on environmental reactions in ice have not been investigated. In this work, we examine the effects of immiscible non-chromophoric OM on the photolysis kinetics of PAHs in ice and at ice surfaces.

2.3 Experimental

2.3.1 Sample Preparation

Samples of phenanthrene (Aldrich, ≥ 99.5%), pyrene (Alfa Aesar, 98%), anthracene (Acros organics, 98%), and naphthalene (Fluka, ≥ 99%) were prepared by stirring a few mg of

solid PAH in 100 mL of water overnight and then diluting the solution to 1.2×10^{-6} M (phenanthrene), 1.0×10^{-7} M (pyrene), 6.3×10^{-8} M (anthracene), or 1.2×10^{-4} M (naphthalene). The samples were then frozen in 10 mL aliquots in ice cube trays ("ice cubes"). Some ice cubes were crushed to 2 mm diameter crystals ("ice granules") prior to photolysis. For some experiments, aqueous solutions containing a PAH and 25 μM to 7.5 mM octanol (Acros Organics, 99%) or decanol (Alfa Aesar, ≥ 98%) were prepared.

Samples of phenanthrene and anthracene in frozen decanol were prepared by dissolving a few mg of PAH in liquid decanol and diluting the solution to the same concentrations as described for the aqueous solutions, then freezing the solution in an ice cube tray. The resulting samples were powdery solids with similar diameters to the ice granules described above.

2.3.2 Photolysis

Samples containing phenanthrene were irradiated with the output of a 450 W xenon arc lamp, and samples containing pyrene and anthracene were irradiated by a 150 W lamp. The output of the lamp passed through a 295 nm long-pass cut-off filter, through a quartz flat-bottomed dish filled with deionized water acting as an IR filter, and through aluminum mesh that was used as a neutral density filter. The average lamp power reaching the sample was measured to be 26.3 mW using a power meter centered at 310 nm. The filtered output of the lamp was reflected downward onto the sample which was contained in a copper vessel. Temperatures within the vessel were varied between 23 °C and –25 °C (with expected variations within the sample holder of less than 2 °C with a recirculating chiller attached to the copper vessel. Dark runs were conducted for all experiments by shielding samples from the lamp during the course of the experiment.

Photolysis kinetics were determined by measuring the change in PAH fluorescence intensity over time. After a known time period of irradiation, samples were removed from the copper vessel and melted into a 1 cm quartz cuvette. This was repeated at known time intervals ranging from 1 minute to 2 hours. Fluorescence spectra were acquired on a commercial fluorimeter using excitation wavelengths of 252 nm for anthracene and phenanthrene and 261 nm for pyrene. Photolysis rate constants were determined from the slope of the best-fit line to either $ln(I)$ vs. time (first-order kinetics) or I^{-1} vs. time (second-order kinetics), where I is fluorescence intensity of the PAH. Fluorescence intensity was monitored at 401 nm (anthracene), 364 nm (phenanthrene), or 372 nm (pyrene). Each experiment was repeated at least three times.

2.3.3 Fluorescence spectra

Naphthalene fluorescence spectra in ice granules were acquired at −15 °C by connecting a recirculating chiller to the sample holder of a commercial fluorimeter. Ice granules containing naphthalene were placed in a 1 cm quartz cuvette. The cuvette was placed in the fluorimeter and emission spectra were acquired. Samples were excited at 266 nm and fluorescence was acquired between 300 and 500 nm with 1 nm steps. Samples were allowed to sit for several minutes before spectra acquisition to achieve thermal equilibrium.

2.4 Results and Discussion

2.4.1 Clean ice

2.4.1.1 Spectra

Figure 2.1 shows naphthalene fluorescence spectra in liquid water and in ice granules with average diameters of 2 mm and 4 mm respectively. The surface-area-to volume (SAV) ratios of the smaller ice granules are approximately two times greater than the larger granules.

Naphthalene emission in aqueous solution does not extend to wavelengths longer than about 390 nm, but in the ice granules significant emission is observed between 380 and 500 nm. This emission at long wavelengths is due to excimers, which form from self-associated naphthalene.[30] We also acquired emission spectra of ice granules that did not contain naphthalene. The spectra did not contain features resembling monomeric or excimeric naphthalene emission. However, the sharp peaks in the ice samples in Figure 2.1 at approximately 340 nm, 450 nm, 470 nm, and 485 nm are due to scattering from the ice rather than to naphthalene emission.

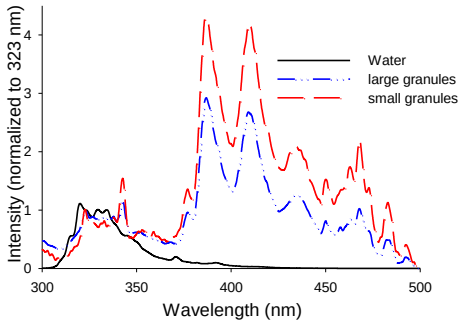

Figure 2.1. Fluorescence spectra of naphthalene in liquid water and in ice granules with diameters of 2 mm ("small granules") and 4 mm ("large granules"). Shown spectra are the average of 3 individual spectra.

Excimeric emission from naphthalene and other aromatic hydrocarbons has been measured at ice surfaces using surface-sensitive laser-induced fluorescence.[17-18, 31] Aromatic species are thought to self-associate at ice surfaces due to unfavorable interactions with water molecules in the disordered surface region.[32] Our fluorescence measurements are not inherently selective to ice surfaces (compared to ice bulk), but we can increase our surface selectivity by increasing the SAV of our samples. Naphthalene in ice is likely distributed between the air-ice interface and liquid regions within bulk ice. As the SAV ratio of ice samples increases, so too does the fraction of solutes at the air-ice interface. Studies have recently shown that reaction kinetics in ice granules with high SAV ratios are similar to those measured directly at ice

surfaces.[12-13] The fact that we observe excimeric emission from naphthalene in ice granules, and that the intensity of excimer emission relative to monomer emission intensity increases with decreasing ice granule size (i.e. with increasing SAV) indicates that we can probe naphthalene at ice surfaces using a commercial fluorimeter.

2.4.1.2 Photolysis Kinetics

Table 2.1 shows the average photolysis rate constants of phenanthrene, pyrene, and anthracene in liquid water, ice cubes (SAV = 2.9 cm^{-1}), and ice granules (SAV = 30 cm^{-1}). Photolysis was better described by first-order than by second-order kinetics in all cases.

Table 2.1. Photolysis rate constants of PAHs in water at 23 °C and in ice samples at –15 °C. The stated error represents the standard deviation about the mean for at least 3 trials.

	First-order Rate Constant (10^{-4} s^{-1})		
Environment	**Phenanthrene**	**Pyrene**	**Anthracene**
Water	0.8 ± 0.3	2.3 ± 0.5	1.3 ± 0.5
Ice cubes	--[a]	4.4 ± 0.4	3 ± 2
Ice granules	2 ± 1	3 ± 1	6 ± 3

a) Fewer than half of the experiments yielded measurable photolysis rate constants. The experiments with measurable kinetics yielded a rate constant of $(5 \pm 3) \times 10^{-5}$ s^{-1}. We define this rate constant as our lower limit of detection.

Photolysis kinetics measured in ice cubes were within a factor of 2.3 of those measured in aqueous solution in all cases. This is in agreement with previous reports of similar photolysis kinetics of anthracene, phenanthrene, and pyrene in bulk ice and in aqueous solution.[13, 16] The photolysis rate constants we measured in ice granules were faster than those measured in aqueous solution for all three PAHs, in agreement with reports that photolysis of aromatic compounds proceeds more quickly at ice surfaces than in aqueous solution.[17, 19] Photolysis of anthracene and phenanthrene proceeded more quickly in ice granules than ice cubes, consistent with reactivity being different in bulk ice and at ice surfaces.[12-13] Pyrene photolysis was more

rapid in ice cubes than in ice granules, although photolysis in both samples was faster than in aqueous solution. We have previously observed a reduction in pyrene photolysis kinetics in aqueous solution at concentrations that exceed saturation;[28] the similar kinetics in bulk ice and at ice surfaces may be due to a combination of rate-enhancing effects of the ice surface and rate-suppressing effects of pyrene self-association.

2.4.2 Effects of organics

2.4.2.1 Spectra

Figure 2.2 shows fluorescence spectra of naphthalene in aqueous solution, in solid decanol granules (diameter = 2 mm), and in ice granules (diameter = 2 mm). Emission from excimeric naphthalene is not observed in aqueous solution, but dominates in ice granules due to self-association at the ice surface. No excimeric emission is observed in solid decanol. This is in agreement with an earlier study that reported only monomeric emission from naphthalene at the surface of solid decanol.[17] Self-association at ice surfaces is thought to be due to unfavorable interactions between aromatic compounds and surfacial water molecules;[32] since naphthalene interacts much more favorably with decanol than with water, we do not expect excimers to form at liquid or solid decanol surfaces.

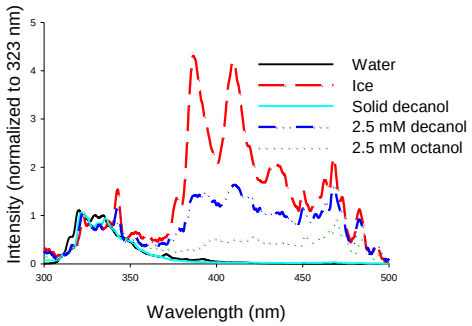

Figure 2.2. Fluorescence spectra of naphthalene in liquid water, in solid decanol, and in ice granules (2 mm diameter) prepared from deionized water and from aqueous solutions containing 2.5 mM decanol or octanol. Shown spectra are the average of 3 individual samples.

Figure 2.2 also shows the effects of incorporating 2.5 mM octanol or decanol in aqueous solutions prior to freezing on naphthalene fluorescence. In the presence of OM, excimeric naphthalene emission is observed, but to a lesser extent than in pure ice granules. This shows that OM is present at the ice surface, and that it creates a physical environment that is distinct from that at pristine air-ice interfaces.

In aqueous solution, an octanol monolayer is formed at the water surface at bulk concentrations of approximately 2.5 mM.[33-34] We acquired naphthalene emission spectra in ice granules containing octanol concentrations ranging from 0.25 – 7.5 mM. We determined the relative degree of self-association at ice surfaces by taking the ratio of excimer fluorescence intensity (the total intensity from 365 – 440 nm) to monomer fluorescence intensity (310 – 335 nm). As shown in Figure 2.3, the degree of self-association decreases dramatically in the presence of 0.25 mM octanol compared to in pure water ice. Increasing the octanol concentration further causes only minor decreases in the ratio up to at least 7.5 mM. The lowest excimer:monomer intensity ratio observed (at an octanol concentration of 7.5 mM) is 1.3 ± 0.5, which is approximately 6.5 times greater than the ratio measured in solid decanol (0.197 ± 0.009), and approximately 5.6 times greater than that measured in aqueous solution (0.228 ± 0.002). This suggests that in the presence of OM, the environment that PAHs encounter at ice surfaces is between that of the pristine ice surface and the surface of solid OM, and that OM does not completely shield naphthalene from the ice surface even at multilayer coverage. This is in agreement with recent molecular dynamics (MD) simulations that predicted that octanol and other aliphatic hydrocarbons will form an organic layer above the disordered surface region of ice, and that naphthalene will reside deep within the organic layer, in occasional contact with the

ice surface.[35] That study predicted little effect of OM films on the degree of naphthalene self-association; our results show that the effect is in fact significant.

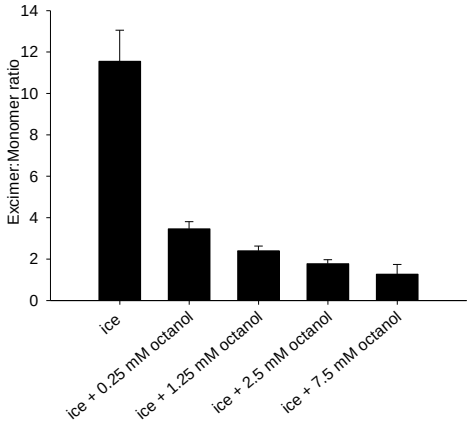

Figure 2.3. Effects of octanol on the average excimer:monomer ratio of naphthalene in ice granules at −15 °C. The error represents the standard deviation about the mean of 3 samples.

We also measured excimer:monomer ratios in large granules (4 mm diameters). Octanol and decanol had a greater effect on the ratio in large granules than in small granules. The excimer:monomer ratio in large granules containing 7.5 mM octanol was 17% of that in pure ice, compared to 24% for small granules. Likewise, the excimer:monomer ratio in large granules containing 7.5 mM decanol was 41% that in pure ice, compared to 55% in small granules. This suggests that as SAV decreases, more of the naphthalene is in contact with the OM, likely within liquid regions in bulk ice.

2.4.2.2 Photolysis Kinetics in Bulk Ice (Ice Cubes)

We measured anthracene and pyrene photolysis kinetics in ice cubes (SAV = 2.9 cm^{-1}) in the presence of 7.5 mM octanol or decanol. In the presence of OM, photolysis was too slow to measure. We also varied the octanol concentration in the pre-frozen solution between 0.025 and 7.5 mM. No anthracene photolysis was observed in the presence of octanol at concentrations

equal to or greater than 0.25 mM. In ice cubes prepared from solutions containing 0.025 mM octanol, no photolysis was observed in three of the six experiments, while the other three experiments yielded a rate constant of $(3 \pm 1) \times 10^{-4}$ s^{-1}, which is similar to that measured in ice cubes in the absence of OM.

These results suggest that OM and PAHs are co-excluded during freezing to liquid regions within the ice, and that photolysis occurs in a primarily organic phase. The rate constants of anthracene and pyrene measured in liquid octanol and decanol are below 5×10^{-5} s^{-1};[28-29] if photolysis kinetics are similar in ice cubes containing octanol and decanol, they will be below our detection limit. It is possible that at the lowest OM concentration (0.025 mM), PAHs in some samples are excluded to different regions than the octanol during freezing. This would explain the fact that 50% of experiments showed photolysis kinetics similar to those measured in pure ice samples, while the remaining experiments did not show any photolysis.

2.4.2.3 Photolysis Kinetics at Ice Surfaces (Ice Granules)

Table 2.2 summarizes the effects of octanol and decanol on the photolysis rate constants of anthracene, pyrene, and phenanthrene in ice granules (SAV = 30 cm^{-1}). Octanol had little effect on PAH photolysis rates. The presence of 7.5 mM decanol reduced phenanthrene and anthracene photolysis rate constants by a factor of two, and reduced pyrene photolysis rate constants to below our detection limit (so by at least a factor of six). Phenanthrene and anthracene photolysis kinetics were also measured in frozen decanol; no photolysis was observed in these experiments. Anthracene photolysis at the surface of frozen decanol was reported to be 2.7 times faster than at the surface of liquid decanol.[17] The rate constant for anthracene photolysis in liquid decanol was well below 5×10^{-5} s^{-1},[28] so we do not expect to detect photolysis at solid decanol surfaces even with the reported rate enhancement.

Table 2.2. Effects of 7.5 mM octanol and decanol on photolysis rate constants of PAHs in ice granules at −15 °C. The stated error represents the standard deviation about the mean of at least 3 trials.

Measured First-order Rate Constants (10^{-4} s^{-1})			
Environment	**Phenanthrene**	**Pyrene**	**Anthracene**
Ice	2 ± 1	3 ± 1	6 ± 3
Ice and octanol	2.0 ± 0.9	3 ± 1	4 ± 1
Ice and decanol	0.9 ± 0.8	--[a]	3 ± 1
Solid decanol	--[a]	n/a[b]	--[a]

a) Photolysis was not observed. We assign an upper limit to the rate constant of 5 x 10^{-5} s^{-1}.

b) Experiment was not performed.

In bulk ice, PAH photolysis was significantly suppressed by OM, suggesting that PAHs largely resided within liquid or solid pockets of OM and were not in contact with liquid water or ice. The smaller effect of OM at ice surfaces suggests that PAHs there are still in contact with ice, and do not exist completely in an organic phase. This is in agreement with the fluorescence spectra we acquired that show excimeric naphthalene emission even in ice granules containing OM concentrations corresponding to multilayer coatings in liquid solution. The greater effect of OM on excimer:monomer ratios in larger granules also supports this conclusion; in ice cubes, which have a much smaller SAV than large ice granules (2.9 cm^{-1} and 15 cm^{-1} respectively), we expect the effects of OM to be much greater.

At the lamp powers used in our experiments, PAH photolysis kinetics depend on photon flux.[13] If the presence of OM decreases the photon flux reaching the sample, this could explain the suppressed photolysis. We investigated this possibility by placing 12 mL each of octanol and water in the quartz dish used as an IR filter, forming aqueous and organic layers of approximately 3 mm in depth. The total volume of liquid in the quartz bowl was the same as in the previously-described experiments. The power of the lamp passing through this dish was not

significantly different from that measured when only water was in the dish, and photolysis kinetics of anthracene in aqueous solution at room temperature were similar to those measured with only water in the quartz dish. If OM suppresses PAH photolysis kinetics in ice cubes and ice granules by reducing the photon flux, we would expect the photolysis rate constant to decrease when the light passed through a layer of octanol before reaching the sample. Based on these results, we do not believe that non-chromophoric OM reduces PAH photolysis kinetics in ice and at ice surfaces by reducing the photon flux.

The suppression of photolysis at ice surfaces in the presence of NaCl and NaBr has been ascribed to the formation of a liquid brine at the ice surface due to freezing point suppression caused by the salts.[19] In that study, photolysis at the surface of frozen 100 mM NaCl solutions was half as fast as at frozen freshwater surfaces. In the current study, anthracene and phenanthrene photolysis rates were suppressed to a similar extent in the presence of less than 7.5 mM decanol or octanol; pyrene photolysis rates were suppressed even more significantly by OM. It is unlikely that OM is more than an order of magnitude more efficient at depressing water's freezing point than NaCl. Therefore, we suggest that our results are not due primarily to surface melting, but rather are due to the formation of a distinct phase at the ice surface. This is in agreement with MD simulations which suggest that the thickness of the surfacial disordered layer is in fact *reduced* by organic surfactants, rather than increased as would be expected if the surface was melting.[35]

We investigated the effects of temperature on anthracene photolysis kinetics. Table 2.3 lists anthracene photolysis kinetics in ice granules at −15 and −25 °C. Reducing the temperature of pure ice samples does not affect the measured kinetics, in agreement with previous work.[17] Likewise, in the presence of 7.5 mM decanol, no change in reaction rate is observed at the two

temperatures. However, in the presence of 7.5 mM octanol, reducing the temperature from −15 to −25 °C decreases the photolysis rate to a value that is below our detection limit. Our estimated maximum rate constant of 5×10^{-5} s^{-1} corresponds to the reaction being at least eight times slower at -25 ºC than at -15 ºC. Similarly, we were unable to measure pyrene photolysis in the presence of 7.5 mM octanol at −25 °C. This difference in octanol's effects at the two temperatures is likely due to a change in octanol's phase: With a melting point of −16 °C, octanol is a liquid at −15 °C and a solid at −25 °C. This suggests that the more significant suppression of PAH photolysis by decanol than octanol at −15 °C (as shown in Table 2.2) may be due to the fact that decanol is a solid at that temperature (m.p. = 6.4 °C). This would also explain the fact that octanol's effect is greater at the lower temperature, while decanol's effect remains unchanged. We therefore suggest that solid OM may reduce photolysis kinetics more significantly than liquid OM. The reason for this behavior is not clear. It is possible that solid OM reduces photolysis kinetics by sequestering the PAHs from the underlying ice surface more effectively than liquid OM. However, naphthalene excimer:monomer ratios in ice granules containing octanol were lower than those containing the same concentration of decanol at −15 °C, indicating that the liquid OM (octanol) sequestered the PAH more effectively than the solid. Further, excimer:monomer ratios in ice granules containing 7.5 mM octanol were higher at −25 °C than at −15 °C (1.9 ± 0.7 and 1.3 ± 0.5 respectively), which again suggests that naphthalene has more contact with the ice surface when decanol is in the solid rather than in the liquid phase. The enhanced suppression of photolysis by solid OM may have implications for the fate of PAHs in snow associated with particulate organic matter versus dissolved organic matter, and warrants further study.

Table 2.3. Anthracene photolysis kinetics in snow at varying temperatures. The stated error represents the standard deviation about the mean of at least 3 trials.

Temperature (°C)	Measured First-order Rate Constants (10^{-4} s^{-1})		
	0 mM OM	7.5 mM octanol	7.5 mM decanol
–15	6±3	4±1	3±1
–25	6±3	--[a]	3±1

a) Photolysis was not observed. We assign an upper limit to the rate constant of 5×10^{-5} s^{-1}.

2.5 Conclusions and Atmospheric Implications

We have investigated the effects of non-chromophoric OM on the physical environment encountered by PAHs associated with ice, and to its effects on PAH photolysis kinetics in bulk ice and at ice surfaces. Our results suggest that OM can create unique reaction environments within bulk ice and at ice surfaces, and can alter PAH reactivity. Non-chromophoric OM reduces PAH photolysis kinetics significantly in bulk ice, and to varying degrees at ice surfaces. Solid OM appears to suppress photolysis more effectively than liquid OM. Although the photolysis kinetics of PAHs do not display a temperature dependence, their lifetimes in snow-covered environments may display a temperature dependence due to phase-transitions of OM associated with the snow. Further, our results suggest that particulate OM may suppress PAH photolysis kinetics more effectively than dissolved OM in snow and ice.

These results show that photolysis in "dirty" ice, such as is present in most urban centers, may occur quite differently than in pristine ice, which has been primarily used in laboratory experiments. The results also show that OM does not need to absorb sunlight in order to affect pollutant photolysis kinetics. To our knowledge this possibility has not previously been considered.

Atmospheric lifetimes of PAHs in snow at Summit, Greenland, have been reported to be much longer than laboratory-measured photolysis kinetics predict.[16] It has been suggested that

this could be due to PAHs being associated with soot and organic aerosols, rather than with snow and ice.[16, 21] Our results demonstrate that PAHs associated with an organic phase will photolyze less rapidly than those associated with a pure ice phase. These findings may help to reconcile predictions and measurements of PAH concentrations in snow and ice.

Our observations that OM suppresses PAH photolysis kinetics less efficiently at ice surfaces than in liquid regions within bulk ice supports the idea that different reaction environments exist in liquid regions within bulk ice and at ice surfaces (e.g. refs 12-13). Our results suggest that in order to accurately predict the chemical fate of organic pollutants such as PAHs in winter environments, the composition of snow and ice must be taken into account. Further, the distribution of solutes within the snow and ice must be considered, since different reaction rates (both in the presence and absence of OM) will be observed within bulk ice and at ice surfaces. Finally, we suggest that the effects of other solutes on photochemical kinetics in and on ice should be investigated to improve our understanding of environmentally-relevant chemistry in solute-containing snow and ice.

2.6 References

1. Abbatt, J. P. D.; Thomas, J. L.; Abrahamsson, K.; Boxe, C.; Granfors, A.; Jones, A. E.; King, M. D.; Saiz-Lopez, A.; Shepson, P. B.; Sodeau, J., *et al.*, Halogen Activation Via Interactions with Environmental Ice and Snow in the Polar Lower Troposphere and Other Regions *Atmos. Chem. Phys.* **2012,** *12*, 6237-6271.
2. Bartels-Rausch, T., Ten Things We Need to Know About Ice and Snow *Nature* **2013,** *494*, 27-29.
3. Domine, F.; Albert, M.; Huthwelker, T.; Jacobi, H. W.; Kokhanovsky, A. A.; Lehning, M.; Picard, G.; Simpson, W. R., Snow Physics as Relevant to Snow Photochemistry *Atmos. Chem. Phys.* **2008,** *8*, 171-208.
4. Grannas, A. M.; Jones, A. E.; Dibb, J.; Ammann, M.; Anastasio, C.; Beine, H. J.; Bergin, M.; Bottenheim, J.; Boxe, C. S.; Carver, G., *et al.*, An Overview of Snow Photochemistry: Evidence, Mechanisms and Impacts *Atmos. Chem. Phys.* **2007,** *7*, 4329-4373.

5. McNeill, V. F.; Grannas, A. M.; Abbatt, J. P. D.; Ammann, M.; Ariya, P.; Bartels-Rausch, T.; Domine, F.; Donaldson, D. J.; Guzman, M. I.; Heger, D., *et al.*, Organics in Environmental Ices: Sources, Chemistry, and Impacts *Atmos. Chem. Phys.* **2012,** *12*, 9653-9678.
6. Simpson, W. R.; von Glasow, R.; Riedel, K.; Anderson, P.; Ariya, P.; Bottenheim, J.; Burrows, J.; Carpenter, L.; Friess, U.; Goodsite, M. E., *et al.*, Halogens and Their Role in Polar Boundary-Layer Ozone Depletion *Atmos. Chem. Phys. Discuss.* **2007,** *7*, 4285-4403.
7. Dash, J. G.; Rempel, A. W.; Wettlaufer, J. S., The Physics of Premelted Ice and Its Geophysical Consequences *Rev. Mod. Phys.* **2006,** *78*, 695-741.
8. Bartels-Rausch, T.; Jacobi, H. W.; Kahan, T. F.; Thomas, J. L.; Thomson, E. S.; Abbatt, J. P. D.; Ammann, M.; Blackford, R. R.; Bluhm, H.; Boxe, C., *et al.*, A Review of Air-Ice Chemical and Physical Interactions (AICI): Liquid, Quasi-Liquid, and Solid Ice in Snow *Atmos. Chem. Phys.* **accepted**.
9. Dash, J. G.; Fu, H. Y.; Wettlaufer, J. S., The Premelting of Ice and Its Environmental Consequences *Rep. Prog. Phys.* **1995,** *58*, 115-167.
10. Wettlaufer, J. S.; Worster, M. G., Premelting Dynamics *Annu. Rev. Fluid Mech.* **2006,** *38*, 427-452.
11. Rosenberg, R., Why Is Ice Slippery? *Phys. Today* **2005,** *58*, 50-55.
12. Kahan, T. F.; Zhao, R.; Donaldson, D. J., Hydroxyl Radical Reactivity at the Air-Ice Interface *Atmos. Chem. Phys.* **2010,** *10*, 843-854.
13. Kahan, T. F.; Zhao, R.; Jumaa, K. B.; Donaldson, D. J., Anthracene Photolysis in Aqueous Solution and Ice: Photon Flux Dependence and Comparison of Kinetics in Bulk Ice and at the Air-Ice Interface *Environ. Sci. Technol.* **2010,** *44*, 1302-1306.
14. Grannas, A. M.; Bogdal, C.; Hageman, K. J.; Halsall, C.; Harner, T.; Hung, H.; Kallenborn, R.; Klan, P.; Klanova, J.; Macdonald, R. W., *et al.*, The Role of the Global Cryosphere in the Fate of Organic Contaminants *Atmos. Chem. Phys.* **2013,** *13*, 3271-3305.
15. Finlayson-Pitts, B. J.; Pitts, J. N., *Chemistry of the Upper and Lower Atmosphere*. Academic Press: San Diego, 2000; p 969.
16. Ram, K.; Anastasio, C., Photochemistry of Phenanthrene, Pyrene, and Fluoranthene in Ice and Snow *Atmos. Environ.* **2009,** *43*, 2252-2259.
17. Kahan, T. F.; Donaldson, D. J., Photolysis of Polycyclic Aromatic Hydrocarbons on Water and Ice Surfaces *J. Phys. Chem. A* **2007,** *111*, 1277-1285.
18. Kahan, T. F.; Donaldson, D. J., Benzene Photolysis on Ice: Implications for the Fate of Organic Contaminants in the Winter *Environ. Sci. Technol.* **2010,** *44*, 3819-3824.
19. Kahan, T. F.; Kwamena, N. O. A.; Donaldson, D. J., Different Photolysis Kinetics at the Surface of Frozen Freshwater Vs. Frozen Salt Solutions *Atmos. Chem. Phys.* **2010,** *10*, 10917-10922.
20. Klanova, J.; Klan, P.; Heger, D.; Holoubek, I., Comparison of the Effects of Uv, H_2O_2/Uv and Gamma-Irradiation Processes on Frozen and Liquid Water Solutions of Monochlorophenols *Photochem. Photobiol. Sci.* **2003,** *2*, 1023-1031.
21. Domine, F.; Bock, J.; Voisin, D.; Donaldson, D. J., Can We Model Snow Photochemistry? Problems with the Current Approaches *J. Phys. Chem. A* **2013,** *117*, 4733-49.
22. Mmereki, B. T.; Chaudhuri, S. R.; Donaldson, D. J., Enhanced Uptake of Pahs by Organic-Coated Aqueous Surfaces *J. Phys. Chem. A* **2003,** *107*, 2264-2269.
23. Donaldson, D. J.; Vaida, V., The Influence of Organic Films at the Air-Aqueous Boundary on Atmospheric Processes *Chem. Rev.* **2006,** *106*, 1445-1461.

24. Donaldson, D. J.; Valsaraj, K. T., Adsorption and Reaction of Trace Gas-Phase Organic Compounds on Atmospheric Water Film Surfaces: A Critical Review *Environ. Sci. Technol.* **2010,** *44*, 865-873.
25. Schwier, A.; Mitroo, D.; McNeill, V. F., Surface Tension Depression by Low-Solubility Organic Material in Aqueous Aerosol Mimics *Atmos. Environ.* **2012,** *54*, 490-495.
26. Burden, D. K.; Johnson, A. M.; Nathanson, G. M., Surfactant Control of Gas Transport and Reactions at the Surface of Sulfuric Acid *Abstracts of Papers of the American Chemical Society* **2010,** *240*.
27. Hassett, J. P., Chemistry - Dissolved Natural Organic Matter as a Microreactor *Science* **2006,** *311*, 1723-1724.
28. Grossman, J.; Kirrich, M.; Stern, A.; Kahan, T. F., Photolysis Kinetics of Aqueus-Phase Polycyclic Aromatic Hydrocarbons in the Presence of Organic Matter and Halide Salts **in preparation**.
29. Donaldson, D. J.; Kahan, T. F.; Kwamena, N.-O. A.; Handley, S. R.; Barbier, C., Atmospheric Chemistry of Urban Surface Films. 2009.
30. Kawakubo, T.; Okada, M.; Shibata, T., Excimer (Excited Dimer) Fluorescence of Naphthalene at 77ºk in Rigid Media *J. Phys. Soc. Jpn.* **1966,** *21*, 1469-1470.
31. Kahan, T. F.; Donaldson, D. J., Heterogeneous Ozonation Kinetics of Phenanthrene at the Air-Ice Interface *Environ. Res. Lett.* **2008,** *3*, 045006.
32. Ardura, D.; Kahan, T. F.; Donaldson, D. J., Self-Association of Naphthalene at the Air-Ice Interface *J. Phys. Chem. A* **2009,** *113*, 7353-7359.
33. Mmereki, B. T.; Donaldson, D. J., Direct Observation of the Kinetics of an Atmospherically Important Reaction at the Air-Aqueous Interface *J. Phys. Chem. A* **2003,** *107*, 11038-11042.
34. Lin, S. Y.; Wang, W. J.; Hsu, C. T., Adsorption Kinetics of 1-Octanol at the Air-Water Interface *Langmuir* **1997,** *13*, 6211-6218.
35. Liyana-Arachchi, T. P.; Valsaraj, K. T.; Hung, F. R., Adsorption of Naphthalene and Ozone on Atmospheric Air/Ice Interfaces Coated with Surfactants: A Molecular Simulation Study *J. Phys. Chem. A* **2012,** *116*, 2519-2528.

Chapter Three

Effects of Chromophoric Dissolved Organic Matter on Anthracene Photolysis Kinetics in Aqueous Solution and Ice

3.1 Abstract

We have investigated the effects of chromophoric dissolved organic matter (CDOM) on the photolysis kinetics of the polycyclic aromatic hydrocarbon (PAH) anthracene in liquid water, ice cubes (representative of reactions occurring in liquid regions within bulk ice), and ice granules (representative of reactions occurring at ice surfaces). Fulvic acid (FA) and natural organic matter (NOM) suppressed anthracene photolysis in all three media. In liquid water, competitive photon absorption (the "inner filter effect") played a negligible role in the observed suppression; quenching of excited anthracene is likely the dominant effect of CDOM. Conversely, competitive photon absorption did suppress anthracene photolysis in ice cubes and ice granules. Physical interactions between CDOM and anthracene (such as quenching of excited anthracene and suppression of excimer formation) may also reduce anthracene photolysis rate constants in ice and at ice surfaces. We also investigated possible causes for faster anthracene photolysis at ice surfaces than in aqueous solution. We determined that enhanced local photon fluxes caused by light scattering can account for only ~20% of the observed enhancement. Self-association of anthracene at ice surfaces appears to lead to different photolysis mechanisms than in the liquid phase, and may explain the faster photolysis as ice surfaces.

3.2 Introduction

Aromatic pollutants such as polycyclic aromatic hydrocarbons (PAHs) are emitted primarily in industrialized regions, but are found even in the most remote parts of the earth due to long range transport.[1-2] These pollutants often increase in toxicity after undergoing chemical processing in the environment; their health effects therefore depend on their reaction kinetics. Since reactivity can vary greatly between different environments, accurate rate constants in relevant environmental media are required to accurately predict PAH fate and toxicity.[3]

Over the past decade, photolysis has been recognized as an important transformation pathway for PAHs in snow and ice.[4-7] A number of aromatic pollutants, including several PAHs, have been reported to photolyze more rapidly at ice surfaces than in aqueous solution.[4-9] In some cases, this appears to be due to self-association leading to red shifts in the pollutants' absorbance spectra.[8, 10] For other pollutants, however, the reason for faster photolysis at ice surfaces remains unknown.[4] This uncertainty makes it difficult to predict pollutant fate in snow-covered regions. Additional uncertainty is added by the fact that photolysis of some species has been reported to proceed at different rates in different compartments within ice. Specifically, the disordered region at ice surfaces appears to present a distinct physical environment from liquid regions within bulk ice; reaction kinetics can be very different in these two regions.[11-12] For example, the photolysis rate constant of the PAH anthracene in liquid regions within ice is similar to (or slightly larger than) that in aqueous solution, while the rate constant at ice surfaces is up to six times greater.[4-5, 7] Benzene, toluene, ethylbenzene, and xylenes do not photolyze in aqueous solution or in liquid regions within bulk ice because their absorbance spectra do not overlap with sunlight at Earth's surface. However, at ice surfaces each of these molecules undergoes photolysis due to red-shifted absorption spectra caused by self-association.[8-9]

Ice is a complex reaction environment, and its effects on the photochemical fate of aromatic pollutants remain poorly understood. Further complexity and uncertainty is introduced by the presence of solutes. Most investigations of aromatic pollutant photolysis kinetics in snow and ice have been performed in samples frozen from deionized water without added solutes. However, ice in the environment often contains non-negligible solute concentrations, which can affect reaction kinetics in non-straightforward ways. For example, common solutes such as nitrate, nitrite, and hydrogen peroxide photolyze in water and ice to form hydroxyl radicals

(OH). However, there is some indication that OH reactivity toward aromatic pollutants is much lower at ice surfaces than in liquid water.[4, 13-14] Other solutes can decrease photolysis rate constants of aromatic species in ice or at ice surfaces by changing the physical properties of the local environment. Halide salts have been reported to suppress photolysis of the aromatic molecule harmine at ice surfaces by creating a liquid brine, and we have reported that octanol and decanol suppress PAH photolysis in liquid regions within bulk ice and at ice surfaces by forming a nonpolar environment due to co-exclusion of solutes.[5, 12]

Chromophoric dissolved organic matter (CDOM) is an important environmental solute that could affect photolysis kinetics both by altering the physical properties of the local environment and by participating in photochemistry. CDOM, which refers to environmental organic matter that can absorb sunlight, is present in surface waters at concentrations that generally range from a few to tens of mg L^{-1}.[15-16] It is also present in snow and ice, and recent measurements in Barrow, Alaska suggest that absorption of sunlight in snow and ice is dominated by organic molecules.[17] In surface waters, CDOM forms nonpolar microenvironments to which hydrophobic pollutants partition and react.[18-19] Since CDOM absorbs solar photons, it can affect photolysis rate constants of other aquatic species by competitively absorbing photons (the inner filter effect). It can also produce reactive species such as OH, singlet oxygen ($^1O_2$), organic peroxy radicals (RO_2), and excited triplet state CDOM upon absorbing light.[20-24] CDOM has variable effects on the photochemical fate of pollutants in aqueous solution; the dominant effects depend on the overlap of the pollutant's absorbance spectrum with sunlight, its reactivity toward the various oxidizers produced by CDOM, and its susceptibility to photosensitization; photolysis can be either enhanced or suppressed by CDOM.[23, 25-26]

The effects of CDOM on pollutant photolysis in snow and ice are largely unknown; a

single study has reported that the insecticide aldrin photolyzed more rapidly in ice containing CDOM due to singlet oxygen production and photosensitization.[17] Given the varied effects of CDOM on pollutant photolysis kinetics in liquid water, it is likely that different pollutants will also be affected in different ways by CDOM in ice. In this work we measure rate constants of the PAH anthracene in aqueous solution, in bulk ice, and at ice surfaces in the presence and absence of CDOM to investigate (1) the reasons for faster photolysis at ice surfaces compared to in aqueous solution, and (2) the effects of CDOM on anthracene photolysis kinetics in aqueous solution, in liquid regions within bulk ice, and at ice surfaces.

3.3 Experimental

3.3.1 Chemicals

Anthracene (Acros Organics, 98%), pyrene (Alfa Aesar, 98%), methanol (Sigma—Aldrich, ≥99.8%), fulvic acid (FA, Suwannee River Standard I, International Humic Substances Society), Suwannee River natural organic matter (NOM, International Humic Substances Society), 2-nitrobenzaldehyde (2NB, Alfa Aesar, 98+%), and furfuryl alcohol (FFA, Acros Organics, 98%) were used without further purification.

3.3.2 Sample Preparation

For most experiments, solutions were prepared by stirring a few mg of solid anthracene in 100 mL of deionized water (18 MΩ cm) overnight. This saturated stock solution was diluted with deionized water to a final anthracene concentration of 6.3×10^{-8} M. For concentration dependence experiments and for experiments using anthracene concentrations greater than the saturation limit, anthracene was dissolved in methanol and then diluted 99:1 with deionized water. Fulvic acid or NOM was dissolved in deionized water at concentrations up to 30 mg L^{-1}.

Samples were frozen in 4 or 5 mL aliquots in ice cube trays. Some samples were irradiated after being removed from the tray without further processing ("ice cubes"), and some were crushed to 2 mm diameter "ice granules" prior to photolysis.

3.3.3 Photolysis

Samples were irradiated by the output of a 150 W xenon arc lamp. For most experiments, the output of the lamp passed through a 295 nm long pass cutoff filter and through a flat-bottomed quartz dish filled with deionized water that acted as an IR filter. The beam was then reflected downward onto the sample. Aqueous samples were contained in a quartz cuvette at room temperature (23 °C); ice samples were contained in a stainless steel vessel that was maintained at -15 °C using a recirculating chiller. The photon flux in aqueous solution (which is assumed to be the same as the incident photon flux) was determined to be $(3.15 \pm 0.08) \times 10^{13}$ photons cm^{-2} s^{-1} by chemical actinometry (*vide infra*). Experiments investigating anthracene's concentration dependence were conducted using a different 150 W xenon arc lamp with a configuration described previously and a photon flux of 1.4×10^{14} photons cm^{-2} s^{-1}.[27] Dark control experiments were performed for each set of experimental conditions; no decrease in anthracene concentration was observed in the absence of light.

Photolysis rate constants were determined by measuring the change in anthracene fluorescence intensity over time. After irradiation for a time interval ranging from 1 to 80 minutes, the sample was removed from the light, and ice samples were melted in the dark. Once the sample reached room temperature, an emission spectrum of the melt-water was acquired on a commercial fluorimeter (Photon Technology International QuantaMaster 40) using an excitation wavelength of 252 nm. The photolysis rate constant was calculated from the slope of the best-fit line to either $\ln(I/I_0)$ vs. time (first-order kinetics) or I^{-1} (second-order kinetics), where I is

fluorescence intensity of anthracene after an irradiation time t and I_0 is fluorescence intensity at t = 0. Each experiment was repeated at least 3 times. Fluorescence intensity was monitored at 401 nm.

3.3.4 Chemical Actinometry

Solutions of 2NB were prepared in deionized water at concentrations of approximately 1.3×10^{-5} M. Some samples were frozen in 4 mL aliquots in stainless steel ice cube trays and covered with Parafilm; ice cubes and ice granules were prepared as described above. Photolysis was effected in 30 second increments. Irradiated samples were melted in sealed glass jars and diluted with an equal volume of methanol, and then 2NB concentrations were determined using High Performance Liquid Chromatography (HPLC) on an isocratic Shimadzu Prominence-i LC-2030 with UV detection at 277 nm. A C-18 reverse-phase column (Restek, 150 mm × 4.6 mm, 5 μm particle size) was used; the column temperature was maintained at 40 °C. The mobile phase was 30/70 v/v deionized water to acetonitrile with a 0.6 mL min^{-1} flow rate. Total photon fluxes were determined from the rate of 2NB loss as described in McFall and Anastasio.[28]

3.3.5 Singlet Oxygen Detection

In some experiments, 0.01 M FFA was incorporated into the sample as a singlet oxygen trap. Ice granules containing FFA (in the presence and absence of anthracene) were irradiated for 10 minutes and the concentration of 6-hydroxy-2,3-dihydro-6H-pyrano-3-one ("pyranone"), which is formed from the reaction of FFA and $^1O_2$, was determined via HPLC of the meltwater. The column temperature was 40 °C and the mobile phase was 50/50 methanol/water with a flow rate of 1 mL min^{-1}, and absorbance was measured at 219 nm.

3.4 Results and Discussion

3.4.1 Photolysis in Liquid Water

Figure 3.1a shows emission spectra from an aqueous solution containing 6.3×10^{-8} M anthracene and 30 mg L^{-1} FA after various irradiation times, and Figure 3.1b shows emission spectra of solutions containing either anthracene or FA. While there is significant spectral overlap in emission from anthracene and FA, the three resolved peaks at 380 nm, 401 nm, and 425 nm in Figure 3.1a are clearly from anthracene. These peaks decrease in intensity during irradiation, and their shapes remain distinct even at long irradiation times, whereas the featureless emission at wavelengths longer than ~450 nm does not decrease appreciably even after 60 minutes of irradiation. This suggests that we do not need to separate the components of the reaction mixture in order to measure anthracene photolysis kinetics using fluorescence spectroscopy. To ensure that FA photolysis does not contribute to the measured photolysis rate constant of anthracene, we irradiated aqueous solutions containing only FA. We measured a rate constant for FA photolysis of $(8.6 \pm 0.5) \times 10^{-6}$ s^{-1} which was determined to be the limit of detection for our study. This value is in good agreement with previously reported CDOM photolysis rate constants.[29] The smallest anthracene photolysis rate constant measured when CDOM was present in the reaction mixture in this study was 8.4×10^{-5} s^{-1} (*vide infra*), which is close to an order of magnitude larger than that measured for FA. We therefore conclude that the contribution of FA photolysis to our reported anthracene photolysis rate constants in this study is negligible.

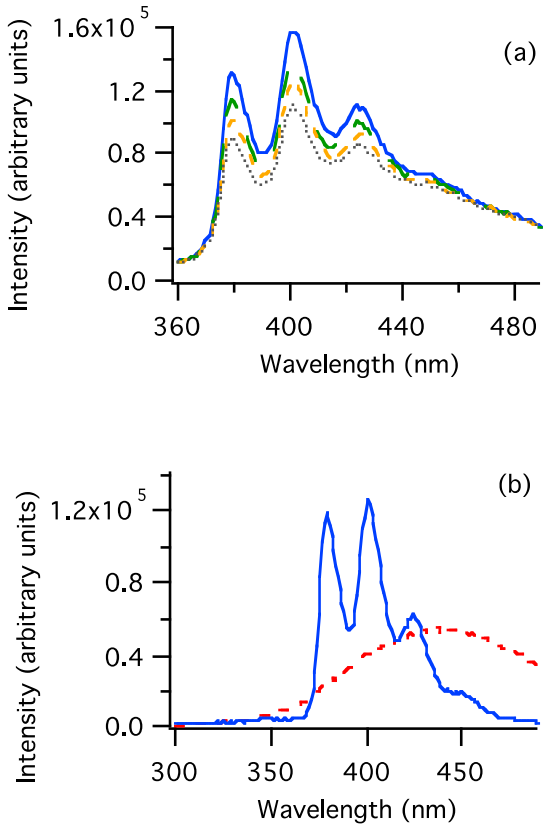

Figure 3.1. Emission spectra of aqueous solutions excited at 252 nm: (a) 6.3×10^{-8} M anthracene and 30 mg L^{-1} FA at irradiation times of 0 min (solid blue trace), 20 min (long dashed green trace), 40 min (short dashed orange trace), and 60 min (dotted grey trace); and (b) individual solutions containing 6.3×10^{-8} M anthracene (solid blue trace) and 30 mg L^{-1} FA (dashed red trace).

We measured anthracene photolysis rate constants in the presence of FA and NOM under two sets of conditions. In the first, CDOM was contained in the reaction solution, and could affect anthracene photolysis either through intermolecular interactions (such as production of reactive species or energy transfer) or competitive photon absorption. In the second, CDOM was contained in the quartz dish used as an IR filter suspended above the sample; in this case competitive photon absorption was the only means by which it could affect anthracene photolysis. As shown in Figure 3.2, anthracene photolysis rate constants were inversely correlated with FA concentration when FA was in solution with anthracene, and anthracene photolysis was suppressed to a similar extent by FA and NOM. When FA solutions were

suspended above the reaction solution, very little suppression of anthracene photolysis was observed, even at high FA concentrations. Photolysis kinetics of several PAHs have been measured in the presence of FA at environmentally relevant wavelengths.[25] Although anthracene photolysis was reported to be slightly enhanced by 5 mg L^{-1} FA, the authors concluded that the only important role of CDOM in PAH photochemistry is light attenuation. Our results suggest that CDOM suppresses anthracene photolysis, but that light attenuation is not the dominant mechanism.

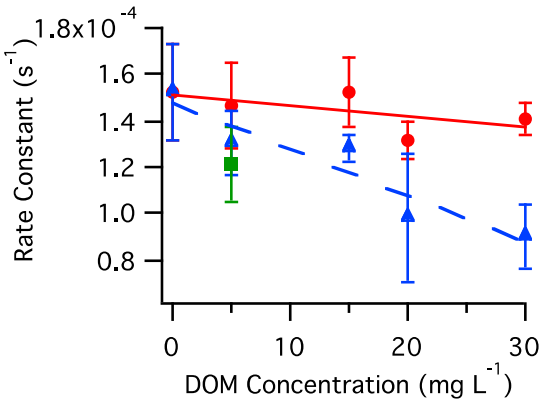

Figure 3.2. Anthracene photolysis rate constants measured in the presence of 5 mg L^{-1} FA suspended above the reaction solution (red circles) and contained in the reaction solution (blue triangles), as well as in the presence of 5 mg L^{-1} NOM in the reaction solution (green square). Error bars represent the standard deviation about the mean of at least three trials. The solid red and dashed blue traces are linear fits to the data. The slopes are -4.2×10^{-7} L mg^{-1} s^{-1} and -2.0×10^{-6} L mg^{-1} s^{-1}.

We have previously reported that the organic compounds octanol and decanol suppress PAH photolysis in liquid water and in ice by reducing local polarity.[5, 27] To determine whether the suppressing effect of CDOM on anthracene photolysis shown in Figure 32 was due to decreased polarity, we acquired emission spectra of pyrene, a fluorescing polarity probe, in the presence and absence of FA; full details are provided in the Supplementary Information (SI). The emission spectra (Figure S1 in the SI) indicate that the polarity of an aqueous 30 mg L^{-1} FA solution was not significantly different from that of deionized water. Polarity changes are therefore not responsible for the observed suppression of anthracene photolysis by CDOM; other

factors, such as quenching of anthracene excited states, are likely responsible.

3.4.2 Photolysis in Ice Cubes and Ice Granules

Table 3.1 shows anthracene photolysis rate constants measured in liquid water, ice cubes, and ice granules; these values are in agreement with previous measurements.[5, 7] Several aromatic compounds have been reported to photolyze more rapidly at ice surfaces than in aqueous solution.[5, 7-9, 13, 30-34] Rate constants of reactions occurring in ice granules largely reflect reactions at ice surfaces due to the high surface-area-to-volume ratios, whereas rate constants acquired from experiments performed with ice cubes largely reflect reactivity in liquid water, since reagents are primarily confined to liquid inclusions within the bulk ice.[5, 7, 9, 12, 14]

Table 3.1. Photolysis rate constants of anthracene in water at 23°C and in ice cubes and ice granules at -15°C. The stated uncertainty represents the standard deviation about the mean of at least three trials.

environment	rate constant (10^{-4} s^{-1})
water	1.5 ± 0.2
ice cubes	3.1 ± 0.5
ice granules	7.5 ± 1.2

3.4.3 Local Photon Fluxes in Aqueous Solution, Ice Cubes, and Ice Granules

Light scattering in small particles such as aerosols can increase local photon fluxes and lead to faster-than-expected photolysis.[35] This could partially account for faster anthracene photolysis in ice cubes and ice granules. Indeed, photon fluxes in ice disks and ice granules prepared similarly to our ice cubes and ice granules have recently been reported to be approximately 40% and 80% greater than photon fluxes in aqueous solution.[28] We measured local photon fluxes in aqueous solution, ice granules, and ice cubes using 2NB actinometry.[28] The molar absorptivity and photolysis quantum yield of 2NB do not show a significant dependence on temperature or phase, so the photolysis rate constant of 2NB is directly

proportional to the local photon flux, which may differ from the incident photon flux due to scattering.[36] Figure 3.3 shows local photon fluxes within each sample type at the same incident photon flux. Photon fluxes were 29% and 66% greater in the ice cubes and ice granules than in aqueous solution, in good agreement with previous observations.[28] These results suggest that up to 20% of the enhancement in anthracene's photolysis rate constant in ice granules may be due to scattering, but that the majority of the enhancement is due to other factors.

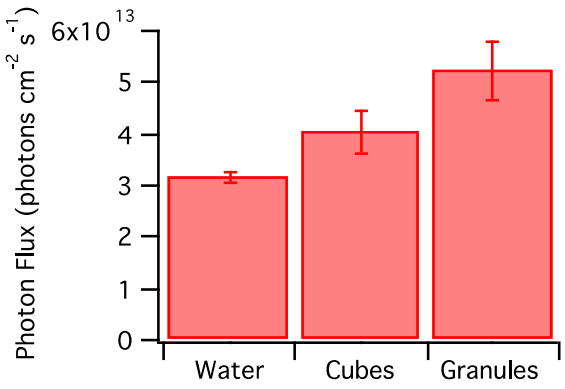

Figure 3.3. Local photon fluxes measured in water, ice cubes, and ice granules at the same incident photon flux. Error bars represent the standard deviation about the mean of at least 3 trials.

3.4.4 Role of Anthracene Self-Association on Photolysis Kinetics

Many aromatic species, including anthracene, undergo self-association at ice surfaces, even at submonolayer coverages.[4, 8, 37] The resulting red shifts in the absorbance spectra (due to excimer formation) have been reported to enable photolysis of benzene and substituted benzenes, which do not absorb solar photons in their monomeric forms.[8-9] Anthracene excimers have red-shifted absorbance compared to monomers, but this red shift does not contribute significantly to faster photolysis at ice surfaces.[4] Self-association could lead to faster photolysis for reasons other than red-shifted absorption spectra, however.

Singlet oxygen has been reported to be generated from the irradiation of concentrated PAH solutions in organic solvents.[38-39] It is possible that high local anthracene concentrations resulting from freeze exclusion are forming $^1O_2$ in ice cubes and granules in our experiments. We irradiated ice granules containing the $^1O_2$ trap FFA to determine whether this was the case. After irradiating ice granules containing FFA for 10 minutes, no pyranone product was detected regardless of whether anthracene was present in the sample. This suggests that $^1O_2$ formation is not responsible for the faster anthracene photolysis observed in ice cubes and granules in this work.

To determine whether self-association increases anthracene photolysis rates, we measured photolysis rate constants of 3.0×10^{-5} M anthracene in aqueous solution. Anthracene's solubility limit in water is 2.5×10^{-7} M, so we expect significant self-association in these samples.[40] As shown in Table 3.2, anthracene photolyzed more than three times more rapidly in the saturated solution than in dilute solution. To ensure that this was an effect of self-association rather than concentration, we also measured anthracene photolysis kinetics at a concentration of 3.0×10^{-5} M in methanol and in a 50% v/v mixture of methanol and water. Anthracene photolyzes less rapidly in methanol and methanol-water mixtures than in aqueous solution due to lower polarity.[27] In methanol and methanol-water mixtures, anthracene photolysis rate constants at the two concentrations were the same within experimental uncertainty. At the higher concentration, anthracene is well above the solubility limit of 2.5×10^{-7} M in water, but is soluble in methanol and the methanol-water mixture.[41] This indicates that it is self-association, rather than high concentrations, that enhances anthracene reactivity.

Table 3.2. Anthracene photolysis rate constants at low and high concentrations in aqueous solution, methanol, and water-methanol mixtures. The stated uncertainty represents the standard deviation about the mean of at least three trials.

	rate constant (10^{-5} s^{-1})	
	1.5×10^{-7} M	**3.0×10^{-5} M**
water	25 ± 2	85 ± 4
methanol	2.3 ± 1.6	3.4 ± 1.0
mixture[a]	10 ± 2	9.5 ± 1.4

a) 50% v/v methanol / water

Anthracene excimers can be detected by a reduction in fluorescence intensity of the shortest wavelength emission peak (~380 nm, "Peak 1") relative to that of the second (~405 nm, "Peak 2").[42] Figure S2 in the SI shows anthracene emission spectra in aqueous and organic solutions at low concentrations where excimer formation is expected to be minimal; the Peak 2:Peak 1 ratio in each solution is between 1.0 and 1.3. Figure 3.4 shows that at a concentration of 3.0×10^{-5} M, there is little evidence of excimers in methanol or methanol-water mixtures (Peak 2:Peak 1 ratios are 1.0 and 1.2 respectively), but that there is extensive excimer formation in water (with a Peak 2:Peak 1 ratio of 4.0). This confirms that anthracene photolysis is enhanced by self-association.

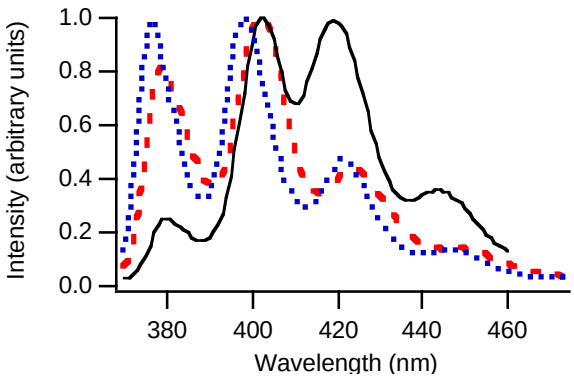

Figure 3.4. Intensity-normalized emission spectra of 3.0×10^{-5} M anthracene excited at 356 nm in water (solid black trace), methanol (dotted blue trace), and a 50/50% v/v methanol-water mixture (dashed red trace).

To further investigate the effects of self-association on anthracene photolysis kinetics, we measured photolysis rate constants in aqueous solution over a range of concentrations below and above the solubility limit. As shown in Figure 3.5a, the rate constant was independent of concentration below approximately 8×10^{-6} M, but increased at higher concentrations. Figure 3.5b shows relative excimer fractions as a function of anthracene concentration. Excimeric content displays a very similar concentration dependence as anthracene photolysis rate constants, adding further evidence that faster anthracene photolysis at high concentrations is due to self-association.

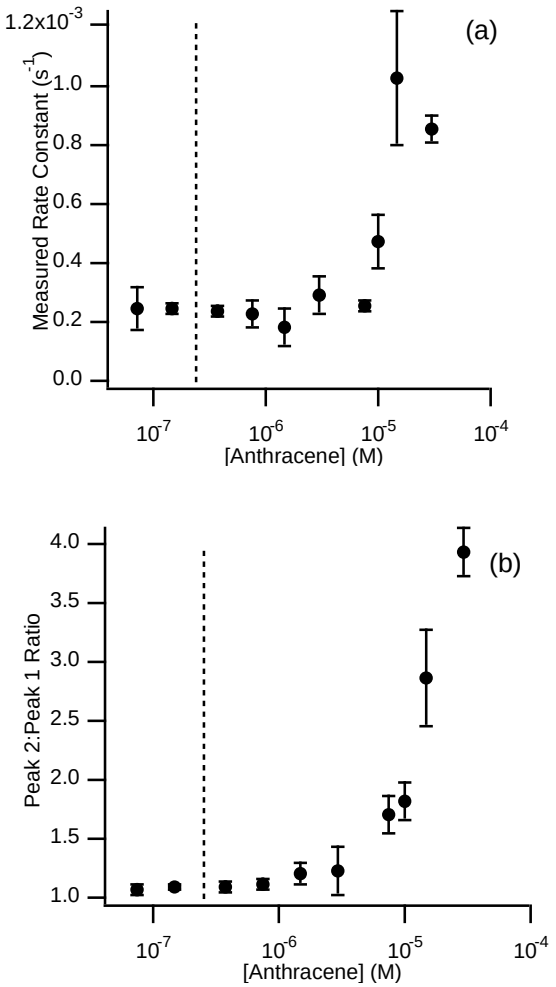

Figure 3.5. Effect of anthracene concentration on (a) first-order anthracene photolysis rate constants, and (b) excimer content in aqueous solutions containing 1% methanol (v/v). The vertical dashed traces denote anthracene's saturated concentration in aqueous solution.[40] The error bars represent the standard deviation about the mean of at least 3 trials.

Using the method of initial rates, we determined that anthracene photolysis was first order at anthracene concentrations up to approximately 7.5×10^{-6} M, and second order at higher concentrations. This shift to second order kinetics coincides with the concentrations at which we observe an increase in the apparent first order rate constant, which suggests that anthracene photolysis in solutions containing large excimer concentrations (and perhaps at ice surfaces) is faster than photolysis in dilute aqueous solutions, and that it proceeds via a different mechanism. This transition from first- to second-order kinetics was only detectable via initial rates analysis;

first order fits to the data were excellent at all concentrations. This is demonstrated in Figure S3 in the SI, which shows fits to 1st and 2nd order photolysis kinetics in water at low and high concentrations. We were not able to determine the reaction order at ice surfaces as we did in aqueous solution using the method of initial rates since local concentrations at ice surfaces can not be predicted from the concentration in solution prior to freezing. Fits to first and second order rate constants were both very good in frozen media.

We note that while the increase in photolysis rate constants correlated well with the fraction of excimers (as shown in Figure 3.5), this does not necessarily indicate that the faster photolysis is due to the excimers themselves. It is possible that anthracene excimers photolyze more rapidly than monomers (due perhaps to larger absorption cross sections or photolysis quantum yields). However, faster photolysis may also arise from the close proximity of anthracene molecules under conditions that give rise to excimer emission. For example, energy transfer between adjacent anthracene molecules (self photosensitization) could also explain the observed photolysis kinetics.

3.4.5 Effects of CDOM on Anthracene Photolysis in Ice and at Ice Surfaces

Figure 3.6 shows anthracene photolysis rate constants in aqueous solution, ice cubes, and ice granules in the presence and absence of 5 mg L^{-1} CDOM. Rate constants measured in the presence of FA and NOM were the same within experimental uncertainty in each medium. While competitive photon absorption by CDOM had little effect on anthracene photolysis kinetics in liquid water, photolysis in ice cubes and ice granules was suppressed when aqueous 5 mg L^{-1} FA solutions were suspended above the reaction chamber; the rate constants in ice cubes and granules were reduced to 70% and 44% of those measured in the absence of FA. Incorporating the CDOM into the ice cubes and ice granules containing anthracene suppressed photolysis

further. Rate constants in ice cubes and ice granules containing FA or NOM were 39% and 24% of those in the absence of CDOM. Approximately 48% and 74% of the reduction in anthracene's rate constant when CDOM was present in ice cubes and ice granules can be attributed to competitive photon absorbance. The additional suppression observed when CDOM was in the sample (as opposed to when it was suspended above the sample) may be due to several factors, which we discuss below.

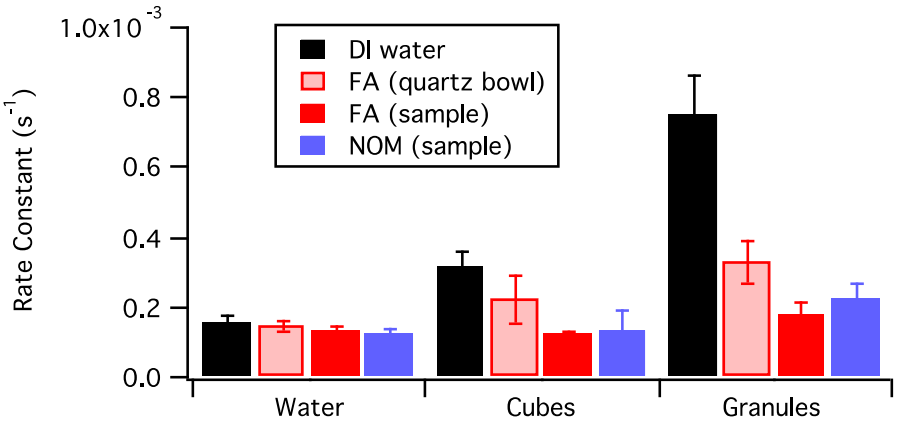

Figure 3.6. Effects of 5 mg L^{-1} FA and NOM on anthracene photolysis rate constants in water, ice cubes, and ice granules. Error bars indicate the standard deviation about the mean of at least 3 trials. "Quartz bowl" indicates that aqueous CDOM solutions were suspended above the reaction chamber, and "sample" indicates that the CDOM was incorporated into the anthracene solution.

We have previously reported the effects of organic matter that does not absorb sunlight ("non-chromophoric OM") on PAH photolysis kinetics.[5] Octanol and decanol suppressed PAH photolysis rate constants in ice cubes to values below our detection limits at OM concentrations as low as 0.25 mM (32.6 mg L^{-1}). Octanol did not greatly suppress photolysis at ice surfaces (in ice granules), but 2.5 mM decanol reduced anthracene's photolysis rate constant by 50%, and suppressed pyrene photolysis below our detection limit. A key difference between octanol and decanol is that at the temperature of those experiments (-15 ºC), octanol is a liquid and decanol is a solid. In that work, suppression of PAH photolysis was attributed to co-exclusion of PAHs and

OM leading to reaction environments with high local organic concentrations; we have reported that anthracene and other PAHs photolyze much less rapidly in nonpolar organics than in aqueous solution.[27] Co-exclusion of anthracene and CDOM may also be responsible for some of the suppression observed in the current work. Reduced local polarity could explain some of the observed suppression, but it could also be due to other factors. For example, high local CDOM concentrations could lead to enhanced inner filter effects, as well as to increased quenching of excited anthracene molecules. Freeze exclusion could also lead to organic microenvironments within bulk ice and at ice surfaces; self-association may be suppressed in these organic regions, leading to photolysis occurring via unimolecular rather than bimolecular pathways.

The observed suppression of anthracene photolysis by CDOM is in contrast with a recent study that reported increased photolysis rate constants of the insecticide aldrin in the presence of various types of CDOM (including Suwannee River fulvic acid) in liquid water and ice.[17] The different effects of CDOM on these two pollutants is likely due to the fact that aldrin absorbs sunlight very weakly, and so singlet oxygen production and photosensitization are CDOM's dominant effects on the photolysis kinetics. Anthracene absorbs sunlight much more strongly than aldrin, and CDOM's main effects will be competitive photon absorption (at least in frozen media) and quenching of excited anthracene molecules. This illustrates the complexity of predicting the effects of CDOM on the fate of aromatic pollutants in liquid and frozen aqueous environments.

3.5 Conclusions

Anthracene photolyzes more rapidly at ice surfaces than in aqueous solution; the majority of this enhancement can not be explained by light scattering. The observed enhancement

correlates with excimer concentration, and may be explained by larger photolysis rate constants of excimeric anthracene than of monomeric anthracene, or by interactions such as energy transfer between adjacent anthracene molecules. The observation that anthracene photolysis becomes more rapid and switches to second order kinetics in aqueous solutions at concentrations that give rise to excimer emission supports this hypothesis.

Chromophoric dissolved organic matter (in the form of FA and NOM) slightly suppressed anthracene photolysis in aqueous solution. This appears to be due primarily to physical interactions between CDOM and anthracene rather than to competitive photon absorption. Conversely, competitive photon absorption by CDOM decreased anthracene photolysis rate constants in liquid regions within ice and at ice surfaces. Further suppression of anthracene photolysis when CDOM was in the reaction mixture could be due to physical interactions between anthracene and CDOM or to enhanced competitive photon absorption by CDOM due to high local concentrations. Our results, along with those of Grannas et al., demonstrate the wide range of effects that CDOM can have on pollutant photolysis in snow and ice.[17] This work increases our understanding of chemistry in the cryosphere, and will improve predictions of pollutant fate in snow-covered regions.

3.6 Supporting Information. Polarity measurements; emission spectra of anthracene in water and organic solvents; fits of fluorescence intensity as a function of irradiation time to first and second order kinetics.

3.7 References

1. Wania, F.; Mackay, D., Tracking the Distribution of Persistent Organic Pollutants. *Environ. Sci. Technol.* **1996,** *30* (9), 390-396.

2. Grannas, A. M.; Bogdal, C.; Hageman, K. J.; Halsall, C.; Harner, T.; Hung, H.; Kallenborn, R.; Klán, P.; Klánová, J.; Macdonald, R. W.; Meyer, T.; Wania, F., The Role of the Global Cryosphere in the Fate of Organic Contaminants. *Atmos. Chem. Phys.* **2013,** *13* (6), 3271-3305.
3. Finlayson-Pitts, B. J.; Pitts, J. N., *Chemistry of the Upper and Lower Atmosphere*. Academic Press: San Diego, 2000.
4. Kahan, T. F.; Donaldson, D. J., Photolysis of Polycyclic Aromatic Hydrocarbons on Water and Ice Surfaces. *J. Phys. Chem. A* **2007,** *111*, 1277-1285.
5. Malley, P. P. A.; Kahan, T. F., Nonchromophoric Organic Matter Suppresses Polycyclic Aromatic Hydrocarbon Photolysis in Ice and at Ice Surfaces. *J. Phys. Chem. A* **2014,** *118* (9), 1638-1643.
6. Ram, K.; Anastasio, C., Photochemistry of Phenanthrene, Pyrene, and Fluoranthene in Ice and Snow. *Atmos. Environ.* **2009,** *43* (14), 2252-2259.
7. Kahan, T. F.; Zhao, R.; Jumaa, K. B.; Donaldson, D. J., Anthracene Photolysis in Aqueous Solution and Ice: Photon Flux Dependence and Comparison of Kinetics in Bulk Ice and at the Air−Ice Interface. *Environ. Sci. Technol.* **2010,** *44* (4), 1302-1306.
8. Kahan, T. F.; Donaldson, D. J., Benzene Photolysis on Ice: Implications for the Fate of Organic Contaminants in the Winter. *Environ. Sci. Technol.* **2010,** *44*, 3819-3824.
9. Stathis, A. A.; Hendrickson-Stives, A. K.; Kahan, T. F., Photolysis Kinetics of Toluene, Ethylbenzene, and Xylenes at Ice Surfaces. *J. Phys. Chem. A* **2016,** *120*, 6693-6697.
10. Ardura, D.; Kahan, T. F.; Donaldson, D. J., Self-Association of Naphthalene at the Air-Ice Interface. *J. Phys. Chem. A* **2009,** *113*, 7353-7359.
11. Bartels-Rausch, T.; Jacobi, H. W.; Kahan, T. F.; Thomas, J. L.; Thomson, E. S.; Abbatt, J. P. D.; Ammann, M.; Blackford, J. R.; Bluhm, H.; Boxe, C.; Domine, F.; Frey, M. M.; Gladich, I.; Guzman, M. I.; Heger, D.; Huthwelker, T.; Klan, P.; Kuhs, W. F.; Kuo, M. H.; Maus, S.; Moussa, S. G.; McNeill, V. F.; Newberg, J. T.; Pettersson, J. B. C.; Roeselova, M.; Sodeau, J. R., A Review of Air-Ice Chemical and Physical Interactions (AICI): Liquids, Quasi-Liquids, and Solids in Snow. *Atmos. Chem. Phys.* **2014,** *14* (3), 1587-1633.
12. Kahan, T. F.; Wren, S. N.; Donaldson, D. J., A Pinch of Salt Is All It Takes: Chemistry at the Frozen Water Surface. *Accounts Chem. Res.* **2014,** *47* (5), 1587-1594.
13. Klanova, J.; Klan, P.; Heger, D.; Holoubek, I., Comparison of the Effects of UV, H2O2/UV and Gamma-Irradiation Processes on Frozen and Liquid Water Solutions of Monochlorophenols. *Photochem. Photobiol. Sci.* **2003,** *2* (10), 1023-1031.
14. Kahan, T. F.; Zhao, R.; Donaldson, D. J., Hydroxyl Radical Reactivity at the Air-Ice Interface. *Atmos. Chem. Phys.* **2010,** *10*, 843-854.
15. Serkiz, S. M.; Perdue, E. M., Isolation of Dissolved Organic-Matter from the Suwannee River Using Reverse-Osmosis. *Water Res.* **1990,** *24* (7), 911-916.
16. Mantoura, R. F. C.; Woodward, E. M. S., Conservative Behaviour of Riverine Dissolved Organic Carbon in the Severn Estuary: Chemical and Geochemical Implications. *Geochim. Cosmochim. Acta* **1983,** *47* (7), 1293-1309.
17. Grannas, A. M.; Pagano, L. P.; Pierce, B. C.; Bobby, R.; Fede, A., Role of Dissolved Organic Matter in Ice Photochemistry. *Environ. Sci. Technol.* **2014,** *48*, 10725-10733.
18. Hassett, J. P.; Anderson, M. A., Effects of Dissolved Organic Matter on Adsorption of Hydrophobic Organic Compounds by River and Sewage-Borne Particles. *Water Res.* **1982,** *16* (5), 681-686.

19. Hassett, J. P., Chemistry - Dissolved Natural Organic Matter as a Microreactor. *Science* **2006,** *311* (5768), 1723-1724.
20. Hoigné, J.; Faust, B. C.; Haag, W. R.; Scully, F. E.; Zepp, R. G., Aquatic Humic Substances as Sources and Sinks of Photochemically Produced Transient Reactants. In *Aquatic Humic Substances: Influence on Fate and Treatment of Pollutants*, American Chemical Society: Washington, DC, 2009; pp 363-381.
21. Aguer, J.-P.; Richard, C., Reactive Species Produced on Irradiation at 365 nm of Aqueous Solutions of Humic Acids. *J. Photoch. Photobio. A* **1996,** *93*, 193-198.
22. Canonica, S.; Jans, U.; Stemmler, K.; Hoigne, J., Transformation Kinetics of Phenols in Water: Photosensitization by Dissolved Natural Organic Material and Aromatic Ketones. *Environ. Sci. Technol.* **1995,** *29*, 1822-1831.
23. Lam, M. W.; Tantuco, K.; Mabury, S. A., PhotoFate: A New Approach in Accounting for the Contribution of Indirect Photolysis of Pesticides and Pharmaceuticals in Surface Waters. *Environ. Sci. Technol.* **2003,** *37* (5), 899-907.
24. McNeill, K.; Canonica, S., Triplet State Dissolved Organic Matter in Aquatic Photochemistry: Reaction Mechanisms, Substrate Scope, and Photophysical Properties. *Environ. Sci.-Process. Impacts* **2016,** *18* (11), 1381-1399.
25. Fasnacht, M. P.; Blough, N. V., Aqueous Photodegradation of Polycyclic Aromatic Hydrocarbons. *Environ. Sci. Technol.* **2002,** *36*, 4364-4369.
26. Janssen, E. M. L.; Erickson, P. R.; McNeill, K., Dual Roles of Dissolved Organic Matter as Sensitizer and Quencher in the Photooxidation of Tryptophan. *Environ. Sci. Technol.* **2014,** *48* (9), 4916-4924.
27. Grossman, J. N.; Stern, A. P.; Kirich, M. L.; Kahan, T. F., Anthracene and Pyrene Photolysis Kinetics in Aqueous, Organic, and Mixed Aqueous-Organic Phases. *Atmos. Environ.* **2016,** *128*, 158-164.
28. McFall, A. S.; Anastasio, C., Photon Flux Dependence on Solute Environment in Water Ices. *Envir. Chem.* **2016,** *13* (4), 682-687.
29. Wu, F. C.; Mills, R. B.; Cai, Y. R.; Evans, R. D.; Dillon, P. J., Photodegradation-Induced Changes in Dissolved Organic Matter in Acidic Waters. *Can. J. Fish Aquat. Sci.* **2005,** *62*, 1019-1027.
30. Blaha, L.; Klanova, J.; Klan, P.; Janosek, J.; Skarek, M.; Ruzicka, R., Toxicity Increases in Ice Containing Monochlorophenols Upon Photolysis: Environmental Consequences. *Environ. Sci. Technol.* **2004,** *38* (10), 2873-2878.
31. Klan, P.; Klanova, J.; Holoubek, I.; Cupr, P., Photochemical Activity of Organic Compounds in Ice Induced by Sunlight Irradiation: The Svalbard Project. *Geophys. Res. Lett.* **2003,** *30* (6), 4.
32. Klanova, J.; Klan, P.; Nosek, J.; Holoubek, I., Environmental Ice Photochemistry: Monochlorophenols. *Environ. Sci. Technol.* **2003,** *37* (8), 1568-1574.
33. Grannas, A. M.; Bausch, A. R.; Mahanna, K. M., Enhanced Aqueous Photochemical Reaction Rates after Freezing. *J. Phys. Chem. A* **2007,** *111* (43), 11043-11049.
34. Kahan, T. F.; Kwamena, N.-O. A.; Donaldson, D. J., Different Photolysis Kinetics at the Surface of Frozen Freshwater vs. Frozen Salt Solutions. *Atmos. Chem. Phys.* **2010,** *10*, 10917-10922.
35. Nissenson, P.; Knox, C. J. H.; Finlayson-Pitts, B. J.; Phillips, L. F.; Dabdub, D., Enhanced Photolysis in Aerosols: Evidence for Important Surface Effects. *Phys. Chem. Chem. Phys.* **2006,** *8* (40), 4700-4710.

36. Galbavy, E. S.; Ram, K.; Anastasio, C., 2-Nitrobenzaldehyde as a Chemical Actinometer for Solution and Ice Photochemistry. *J. Photoch. Photobio. A* **2010,** *209*, 186-192.
37. Kahan, T. F.; Donaldson, D. J., Heterogeneous Ozonation Kinetics of Phenanthrene at the Air–Ice Interface. *Environ. Res. Lett.* **2008,** *3* (4).
38. Gorman, A. A.; Gould, I. R.; Hamblett, I., The Triplet Sensitized Reaction of Singlet Oxygen with 2,5-Ditertiarybutylfuran: Yield Evidence for Inefficient Triplet Energy Transfer from Benzophenone to Oxygen. *Tetrahedron Lett.* **1980,** *21* (11), 1087-1090.
39. Gorman, A. A.; Hamblett, I.; Lambert, C.; Prescott, A. L.; Rodgers, M. A. J.; Spence, H. M., Aromatic Ketone-Naphthalene Systems as Absolute Standards for the Triplet-Sensitized Formation of Singlet Oxygen, O2(1.DELTA.g), in Organic and Aqueous Media. A Time-Resolved Luminescence Study. *J. Am. Chem. Soc.* **1987,** *109* (10), 3091-3097.
40. Pearlman, R. S.; Yalkowsky, S. H.; Banerjee, S., Water Solubilities of Polynuclear Aromatic and Heteroaromatic Compounds. *Journal of Physical and Chemical Reference Data* **1984,** *13* (2), 555-562.
41. Seidell, A.; Linke, W. F., *Solubilities of Inorganic and Organic Compounds*. 2nd ed.; D. Van Nostrand Company: New York, 1919.
42. Dabestani, R.; Ellis, K. J.; Sigman, M. E., Photodecomposition of Anthracene on Dry Surfaces: Products and Mechanism. *J. Photoch. Photobio. A* **1995,** *86* (1-3), 231-239.

Chapter Four:

Physical Characterization of Frozen Saltwater Solutions Using Raman Microscopy

4.1 Abstract:

We have investigated the surface of frozen salt water solutions containing 0.02M and 0.6M NaCl, as well as frozen Sargasso Sea samples using Raman microscopy. At temperatures above the eutectic temperature (-21.1°C), the ice surfaces were incompletely wetted at all temperatures in the presence of 0.02M NaCl, and at all but the highest temperatures studied (approximately -5°C) for 0.6M NaCl and Sargasso Sea water. Liquid water generally took the form of channels at the ice surface, although in some cases (at the lowest temperatures for 0.6M NaCl and Sargasso Sea water, and at all temperatures for 0.02M NaCl) liquid water was observed in "islands" distributed across the ice surface. Fractional surface coverage of liquid was very similar for 0.6M NaCl and Sargasso Sea water at all temperatures, which suggests that Cl^- accounts for the majority of surface melting of sea ice. Liquid fractions ranged from approximately 20% to 85% for frozen 0.6M NaCl solutions and Sargasso Sea water between -21 and -5°C. Channel widths were approximately 10 μm at -21°C, and were immeasurably large at -5°C, where the surface was almost completely wetted. Surface wetting was much less extensive for frozen 0.02M NaCl solutions, with only 39% of the surface wetted even at -5°C, and channels generally not being observed even at this high temperature. 3-dimensional maps indicated that liquid water (and therefore Cl^-) is distributed relatively evenly throughout the ice bulk (at least to depths of ~100 μM). Liquid fractions and channel widths were similar at all depths investigated as at the surface for each sample type. Below -21.1°C, no liquid was observed in any sample. Instead, $NaCl{\cdot}2H_2O$ ("hydrohalite") was observed at ice surfaces at low temperatures. Surface coverages were independent of temperature (to at least -30°C), and ranged from 40% to greater than 70% for 0.6M NaCl and Sargasso Sea water samples, and from 13 – 20 % for 0.02M NaCl solutions.

4.2 Introduction

The physical properties of ice surfaces have been a matter of scientific interest since Michael Faraday observed in 1850 that two ice cubes, when pressed against one another, would fuse together.[1] In the years since then, numerous techniques have been applied to the investigation of the physicochemical nature of ice surfaces. It is currently agreed that, near ice's melting point, the surface is coated in a layer of disordered water molecules, but that is where the agreement ends. The physical properties of this disordered surface region are a subject of debate: Values of parameters such as density, degree of orientational disorder, and depth as a function of temperature vary widely. As an example, experimentally-measured thicknesses of the disordered region at -1°C range from less than 1 nm to over 100 nm.[2]

The above discussion highlights the complexity of ice surfaces. Interestingly, ice surfaces are expected to become more easily understood as compositional complexity increases. This is because solutes cause surface melting, and at high enough solute concentrations the ice surface is expected to be coated by a liquid film; the properties of this film will be those of a concentrated aqueous solution. The composition of the liquid fraction of frozen aqueous solutions can be determined from phase diagrams, and the liquid volume fraction of the frozen sample can be calculated by a thermodynamic expression, illustrated by Equation 4.1.[3]

Equation 4.1: $\phi_{(H_2O)}(T) = [NaCl]_0 / [NaCl]_{FPD,T}$

The liquid fraction ($\phi_{(H_2O)}(T)$) can be determined by dividing the concentration of the salt in a completely melted sample ($[NaCl]_0$) by the concentration of the liquid brine in the ice $[NaCl]_{FPD,T}$. Knowing the liquid volume fraction of an ice sample is useful, but it doesn't fully

describe the environment at ice surfaces. Phase diagrams and Equation 4.1 tell us how much liquid is present in a sample, and what its solute concentrations are, but it does not tell us *where* the liquid is located. While many atmospheric models assume that all solutes are excluded to the ice surface (and that therefore all liquid is at the surface), there is no reason that this should be the case, since multi-crystalline ice (as it tends to be in the environment) contains many liquid regions at grain boundaries, triple points, and defect sites.[2, 4-6] Recent experiments report that the concentrations of solutes such as Cl^- and NO_3^- measured at ice surfaces are significantly lower than they should be if all of the solute was excluded to the ice surface.[7-9]

Knowing where solutes are located (and their concentrations) is important for two reasons. First, solutes may be involved in chemistry. A prime example is bromide, which undergoes heterogeneous reactions at ice surfaces to form reactive bromine compounds which are implicated in catalytic ozone and mercury depletion in polar regions.[10-23] This chemistry is made possible in part by the high bromide concentrations at sea ice surfaces due to freeze exclusion. A second reason is that solutes can change the physicochemical properties of ice surfaces, even if they are not themselves involved in reactions there. Many physical and chemical processes occur very differently at liquid and frozen water surfaces. For example, a number of aromatic pollutants have been reported to photolyze more rapidly at ice surfaces than at liquid water surfaces, and some aromatic pollutants that do not photolyze in aqueous solution can photolyze at ice surfaces.[24-28] Heterogeneous reaction kinetics have also been reported to differ at frozen and liquid water surfaces: Ozonation of phenanthrene was reported to be much faster at ice surfaces than at liquid water surfaces, while hydroxyl radicals (OH), which react rapidly with aromatic species at liquid water surfaces, have been reported to be unreactive toward a range of aromatic species at ice surfaces.[29-30] If solutes cause the surface to be coated in

a liquid “brine”, then these physical and chemical processes will occur as though the surface is a liquid rather than a solid, and can be modelled as such. There is some evidence that this might be the case: The photolysis rate constant of the aromatic dye harmine at frozen freshwater surfaces was larger than in aqueous solution, but at the surface of frozen NaCl solutions (at initial NaCl concentrations greater than 0.2M) it was the same as in aqueous solution. These results were interpreted as indicating that the reaction environment experienced by harmine transitioned from that of an ice surface to a liquid brine as the NaCl concentration increased.[26]

Halides are major solutes in many environmental ices. This is obviously true in sea ice, but even remote inland snowpacks such as Summit, Greenland (72.5796° N, 38.4592° W) have halide concentrations of 1-4 ppbv due to transported sea spray aerosols.[31] Halide-water phase diagrams are well-known, and calculating the liquid volume fraction using Equation 4.1 is straightforward. Several studies have characterized the surfaces of frozen halide salt solutions. Most studies have not reported spatially-resolved data; the emphasis has been on the existence and thickness of the liquid layer.[3, 7, 32-33] A few studies have investigated the characteristics of frozen saltwater solutions using techniques that enable spatial resolution. Scanning Electron Microscopy (SEM) studies of sintered frozen NaCl solutions showed isolated liquid patches at grain surfaces and at grain boundaries above the eutectic temperature, and “webs” of solid salt below the eutectic temperature.[34] An Atomic Force Microscopy (AFM) study reported isolated “clumps” or islands of solid salt surrounded by bare ice at temperatures below the eutectic (measurements above the eutectic were not reported).[35] A recent x-ray fluorescence study reported that frozen solutions containing NaCl and transition metals had channels at the surface at temperatures above the eutectic.[36]

The studies discussed above suggest that not all liquid is excluded to the surface, and that liquid may not evenly coat the ice surface. However, the spatially-resolved studies had some limitations with respect to applying them to environmental conditions. First, some of the techniques require low pressures, which may produce non-atmospherically relevant results. Second, low salt concentrations (generally sub-mM) were used in these experiments; these concentrations are relevant to inland snows, but not to sea ice. At higher salt concentrations, more liquid will be present, which might result in greater surface coverage. Third, only one study presented spatially-resolved information both below and above the eutectic temperature.[34] The cryosphere often reaches temperatures below -21°C; frozen saltwater surfaces may present very different reaction environments below this temperature. As a final point, a Nuclear Magnetic Resonance (NMR) study reported the existence of liquid water in frozen saltwater solutions at temperatures below the eutectic.[3] If liquid water is present at these temperatures, it would have significant implications for reactions at cold frozen saltwater surfaces. In this work, we use Raman microscopy to determine the location of liquid water at frozen salt solutions at a range of NaCl concentrations at temperatures above and below the eutectic. We also present volume maps to investigate the distribution of liquid water between the ice surface and bulk.

4.3 Methods

4.3.1 Samples:

Sodium chloride (Sigma Aldrich ≥99.5%) solutions were prepared by dissolving a measured quantity of NaCl in deionized water to a concentration of 0.6M or 0.02M. Solutions were kept in a sealed jar. Frozen sea ice was prepared with Sargasso Sea water obtained from Dr. David J. Kieber at SUNY ESF.[37]

4.3.2 Freezing Technique:

A custom-built cold chamber was used for all experiments. The chamber consisted of a stainless steel plate attached to a Peltier device. A circulating chiller set at 0°C continuously flowed a 50/50 v/v mixture of water and ethylene glycol through the copper chamber to remove heat produced on the underside of the Peltier. Once the temperature was stabilized, the stainless steel surface was wiped of any excess condensation with a Kimwipe. A drop of solution (approximately 100 μL) was placed on the surface, and a tightly-fitting stainless steel cover with a quartz window in the ceiling was placed over the sample. A thermocouple was inserted through an entrance on the side of the cover and into the drop to record the temperature of the ice. The temperature of the sample chamber was controlled by varying the current applied to the Peltier device. Frozen samples were allowed to equilibrate for 10 minutes prior to acquiring spectra.

4.3.3 Raman Mapping:

Raman images were acquired with a confocal Raman microscope (Renishaw, InVia) using a 532 nm continuous wave laser with a 50× long working distance objective. The microscope was focused at the sample surface prior to each experiment, and an optical image was acquired. Scattered light was collected through the microscope objective and imaged onto a CCD camera. Spectra were acquired between 2502 and 3824 cm^{-1}.

Map dimensions were 150 μm × 150 μm and spectra were taken in 3 μm steps along the x and y axis with an acquisition time of 0.25 s per spectrm. 3-dimensional ("volume") maps were obtained using the same parameters as the surface area maps but were repeated in 10 μm steps along the z-axis from the ice surface (z=0 μm) to a depth of -100 μm. The presence of hydrohalite ($NaCl{\cdot}2H_2O$), liquid water (or "brine"), and solid ice was determined based on

criteria expressed by the ratios of the intensity at 3421 cm^{-1} to the intensity at 3300 cm^{-1}, and the ratio of intensities at 3300 cm^{-1} to 3135 cm^{-1}. Table 4.1 contains a detailed list of these defined criteria. Several experiments were performed to ensure that exposure to the laser beam did not alter the physical properties of the ice surface. These are discussed in the Supplementary Information (SI).

Table 4.1. Criteria for classifying spectra as being due to hydrohalite, liquid brine, or solid ice.

	3300 cm^{-1}/3135 cm^{-1}	**3421 cm^{-1}/3300 cm^{-1}**
Hydrohalite	<0.7	>1.05
Aqueous solution (liquid)	>0.7	>0.82
Ice (solid)	<0.7	<1.05

4.4 Results and Discussion:

4.4.1 Spectra:

Figure 4.1a shows Raman spectra of the OH stretch region of deionized water and 0.6 M NaCl solutions. With salt present in solution, the intensity at lower energy is reduced due to the salt ions disrupting the hydrogen bonding network.[38] Figure 4.1b shows the Raman spectra of pristine ice and of a frozen 0.6 M NaCl solution above and below the eutectic temperature (-21.1°C). Above the eutectic temperature, the greatest intensity is observed at 3421 cm^{-1}, which is similar to that observed in aqueous solution (3425 cm^{-1}). The sharp peaks in frozen salt solution below the eutectic temperature at 3421 cm^{-1} and 3543 cm^{-1} are indicative of $NaCl{\cdot}2H_2O$.[39-40]

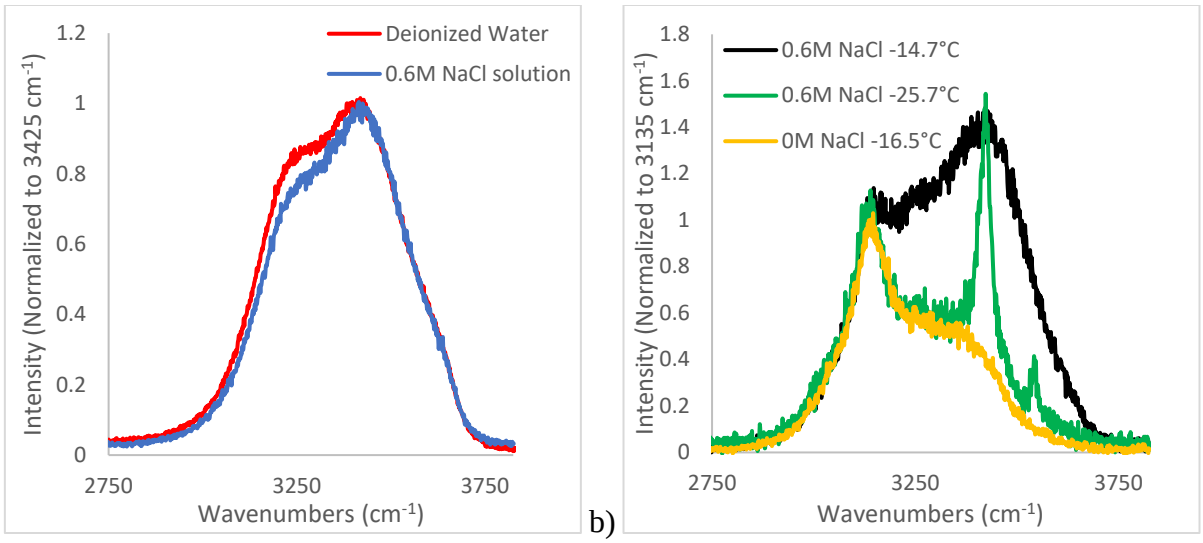

Figure 4.1. Raman spectra of (a) deionized water and 0.6M NaCl solution normalized to the intensity at 3425 cm^{-1} acquired at 25°C and (b) Raman spectra of pristine ice at -16.7°C and a frozen 0.6M NaCl solution at -14.7°C and -25.7°C.

4.4.2 Frozen Surfaces at Temperatures Above the Eutectic:

4.4.2.1 0.6M NaCl

Figure 4.2 shows optical images and Raman maps acquired at the surface of frozen 0.6 M NaCl solutions at 3 different temperatures. At all but the highest temperature (-5.2°C), we observe distinct regions of solid ice and liquid water. These results are in agreement with previous studies that suggest incomplete wetting of ice surfaces by NaCl.[41-42] This is the first study to show this at seawater NaCl concentrations, however. Further surface maps are available in the SI.

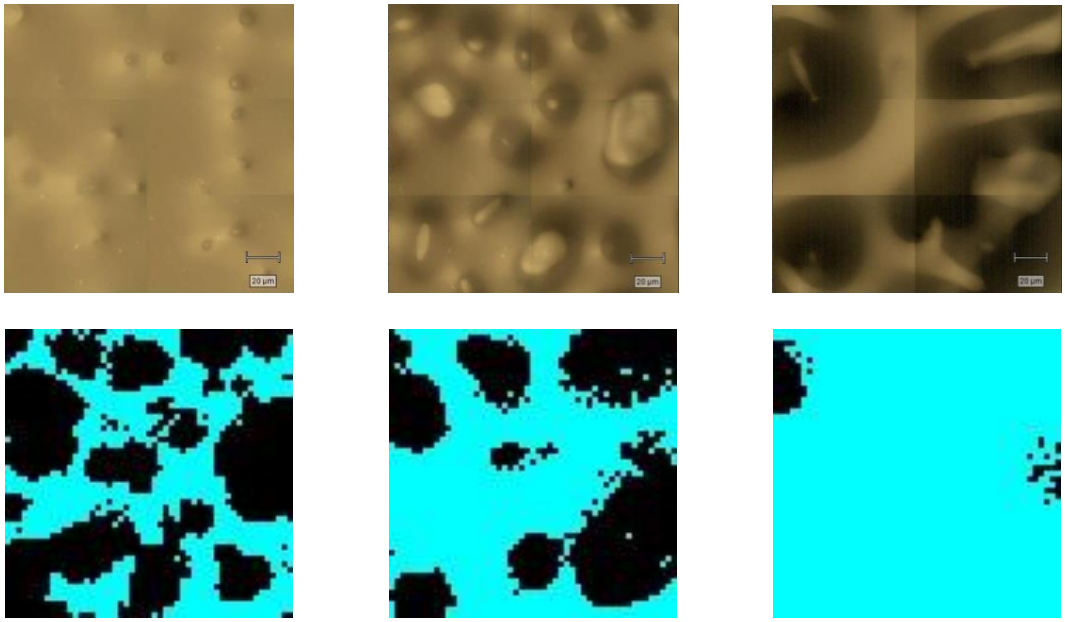

Figure 4.2. Optical images and Raman maps of a 0.6M NaCl ice surface at -15.4°C, -10.6°C, and -5.4°C from left to right.

In general, liquid regions at the ice surface took the form of channels. This is in agreement with a recent x-ray fluorescence study which reported the formation of y-shaped liquid channels at the surfaces of frozen aqueous solutions containing NaCl and transition metals.[36] As the temperature increases, so does the fraction of liquid at the ice surface; at -5°C almost the entire surface is wetted. For comparison, at the surface of frozen deionized water samples in the absence of salt, no liquid was detected at -15°C, and at -5°C 1.8 ± 0.7% of the surface was covered in liquid. Maps of frozen deionized water surfaces are shown in the SI. These results indicate that the majority (and at some temperatures, all) of the observed liquid at the ice surface is due to NaCl. Figure 4.3 shows average liquid fraction and channel width as a function of temperature. At ~-5°C, almost the entire surface is covered in liquid, and it is impossible to measure channel widths. It should also be noted that at temperatures just above the eutectic, channels are not always present and the liquid is often in the form of isolated patches at the surface.

a)

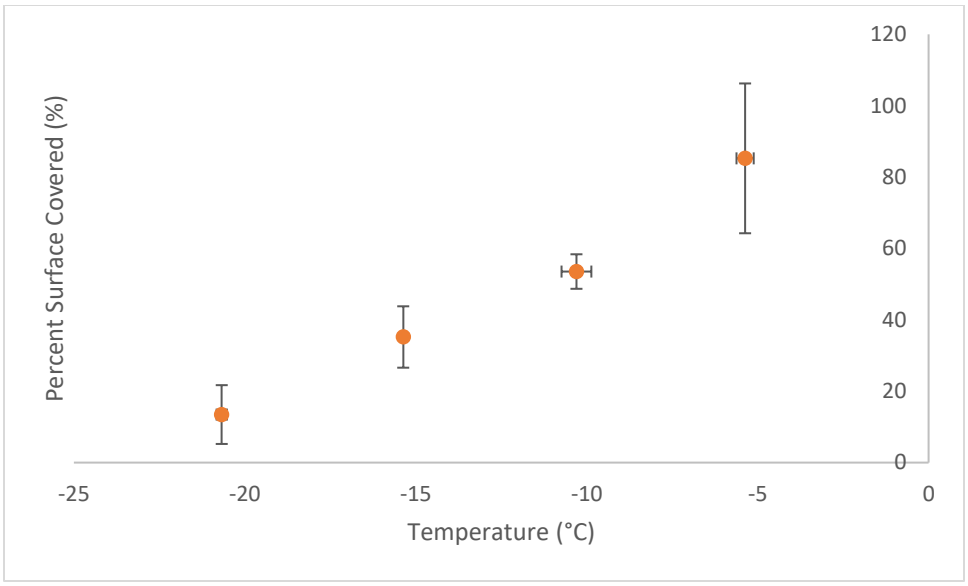

b)

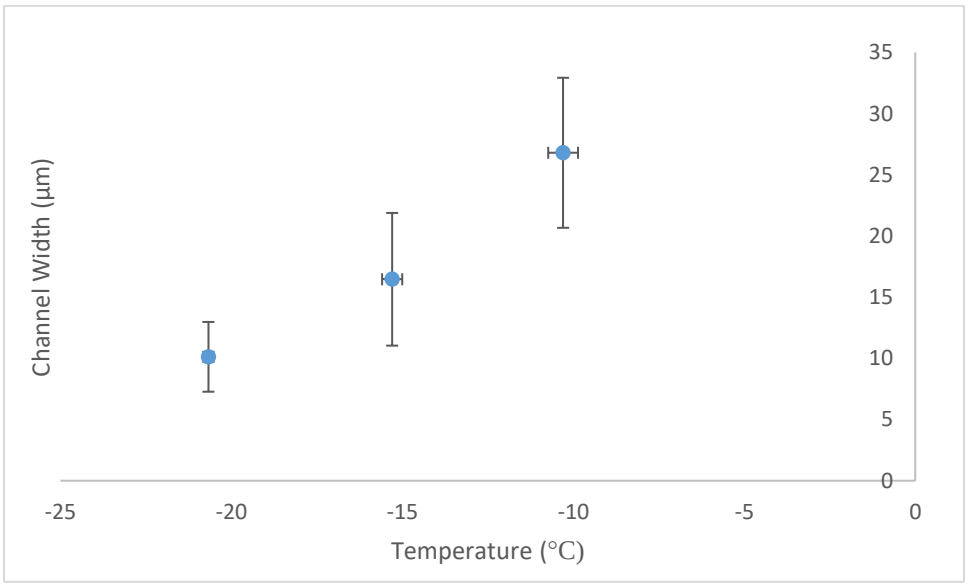

Figure 4.3. Temperature dependence of (a) percent coverage of liquid, and (b) average channel width at the surface of frozen 0.6M NaCl solutions. Error bars indicate the standard deviation of at least 3 trials.

We noted that the method of sample preparation affected the fraction of the surface covered by liquid at a given temperature. This variability is demonstrated in Figure 4.4. When the temperature was lowered directly to -15°C ("no warming," either rapidly or slowly), liquid was observed to cover 51 ± 8% of the surface. If the ice was first frozen at a temperature below the eutectic (around -30°C), and then warmed up quickly ("fast warming," 0.5°C/s), the liquid

coverage was determined to be 65 ± 4%, which is larger than the coverage when samples were frozen directly to -15°C. However, if the temperature was increased very gradually over the eutectic range ("slow warming," 0.5°C/min), the fractional coverage was only 32 ± 7%. These results suggest that temperature fluctuations may significantly affect the extent of surface wetting in the environment. For the purposes of reproducibility between experiments, all reported results correspond to the latter method of sample preparation unless otherwise specified.

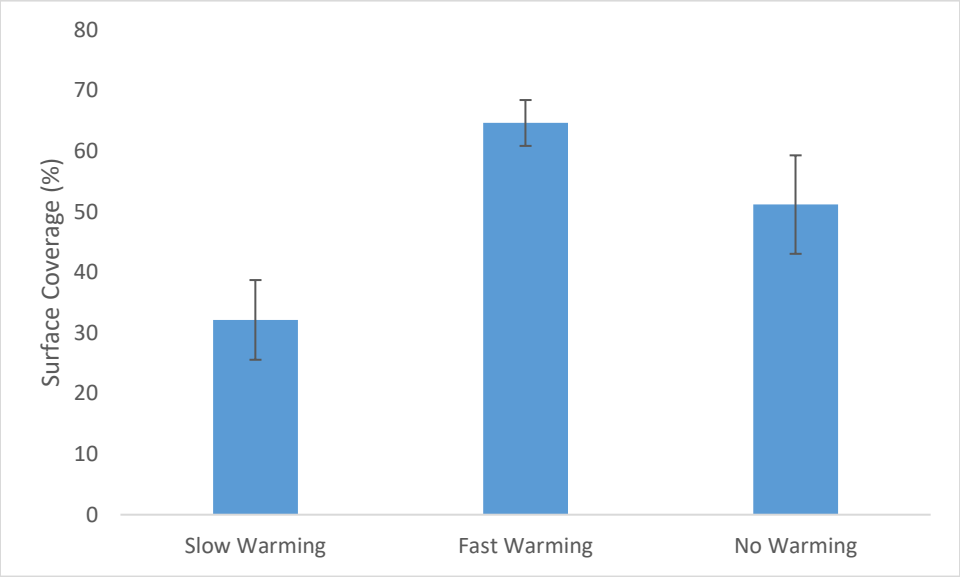

Figure 4.4. Effect of sample preparation on liquid coverage of ice surfaces at -15°C. The error bars indicate the standard deviation of at least 3 trials.

We acquired volume (3-dimensional) maps at several temperatures above the eutectic. Figure 4.5 shows slices along the x-y plane acquired at 20 μm increments along the z-axis, as well as vertical slices along the x and y axes for a 0.6 M NaCl solution at -15.4°C. Liquid regions were observed at all depths. We calculated the liquid fraction at depths of -40 and -80 μm; they were 29 ± 13% and 36 ± 6%, which are in good agreement with the fractional coverage of 32 ± 7% measured at the ice surface. Channel widths at the two depths were 15 ± 9 μm and 16 ± 6 μm, which are also in excellent agreement with the width of 16 ± 5 μm measured at the surface at the same temperature. Two main conclusions can be drawn from these results: First,

that not all solutes are excluded to the ice surface; and second, that liquid channels extend throughout at least the top 100 µm of ice (and likely deeper). As shown in the SI, volume maps of frozen deionized water did not show any liquid at any depth, which indicates that the liquid observed in these experiments is due to the NaCl. Additional volume maps can be found in the SI.

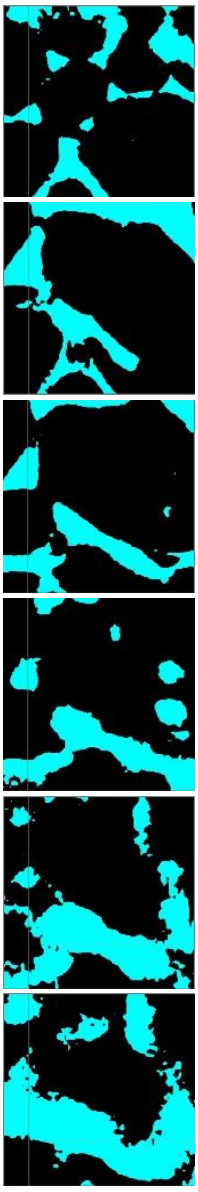

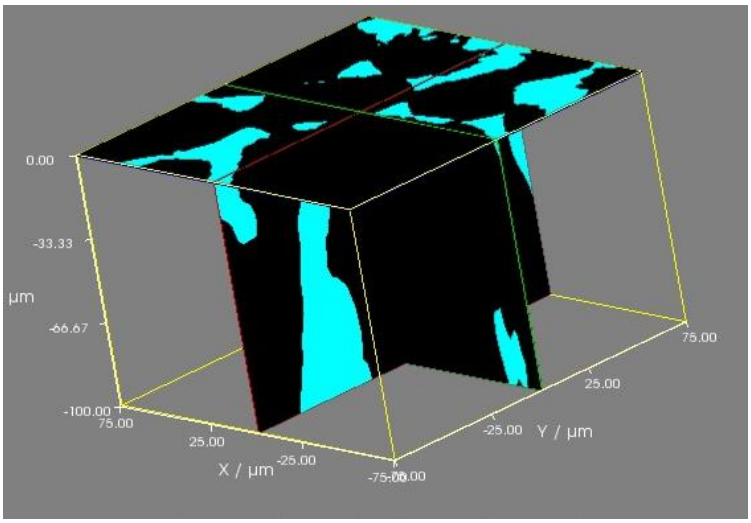

Figure 4.5. Image slices taken of a volume map for a 0.6M NaCl solution at -15.4°C. The left-hand column shows slices along the x-y plane at 20 µm steps. The right-hand column shows images at the surface (along the x-y plane), as well as slices extending 100 µm into the sample along the x-z and y-z planes.

4.4.2.2 0.02M NaCl

Chloride's concentration in seawater is 0.6M, but lower concentrations are observed in many environmental snowpacks. We acquired Raman maps of frozen 0.02M NaCl solutions, which corresponds to the chloride concentration reported in snow contaminated with road salt.[43] Figure 4.6 shows maps of the ice surface of a 0.02M NaCl solution at -15.0°C and -5.7°C. There is clearly less liquid at the surface of the frozen 0.02M solutions than the 0.6M solutions, and the liquid that is present at the surface of the frozen 0.02M surfaces takes the form of isolated patches rather than channels. Surface coverages at -15°C and -5°C for the 0.02 M solution were 8.9 ± 4.0% and 39 ± 11%, compared to 35 ± 9% and 85 ± 21% for the 0.6M solutions. Recall that at -5°C, 1.8% of the surface of frozen deionized water was covered in liquid; even 0.02 M NaCl has a significant effect on the surface liquid coverage.

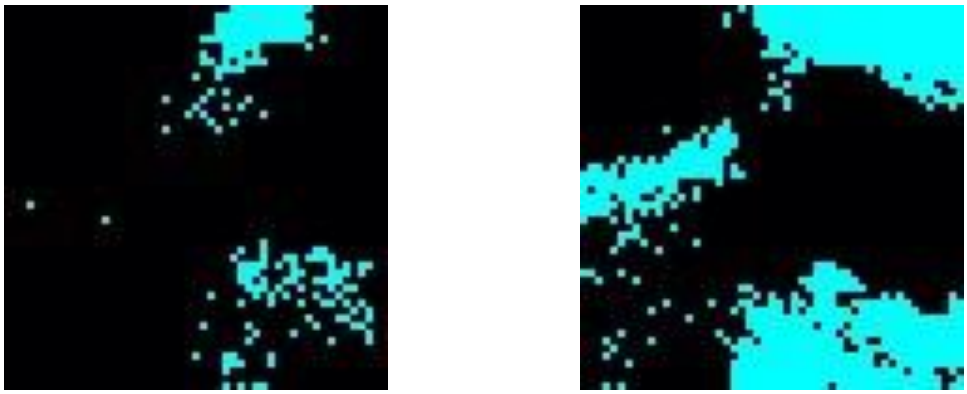

Figure 4.6. Surface map of 0.02M NaCl at (left) -15.0°C and (right) -5.7°C.

Figure 4.7 shows volume maps of a frozen 0.02M NaCl solution at -15.5°C. Again, the amount of liquid is significantly lower than that in the 0.6M solutions. While the liquid in the 0.6M frozen solutions formed channels throughout the ice bulk, this is largely not the case for the 0.02M solutions. The degree of interconnection between different liquid regions is much lower in the 0.02M solutions. Additional volume maps can be found in the SI.

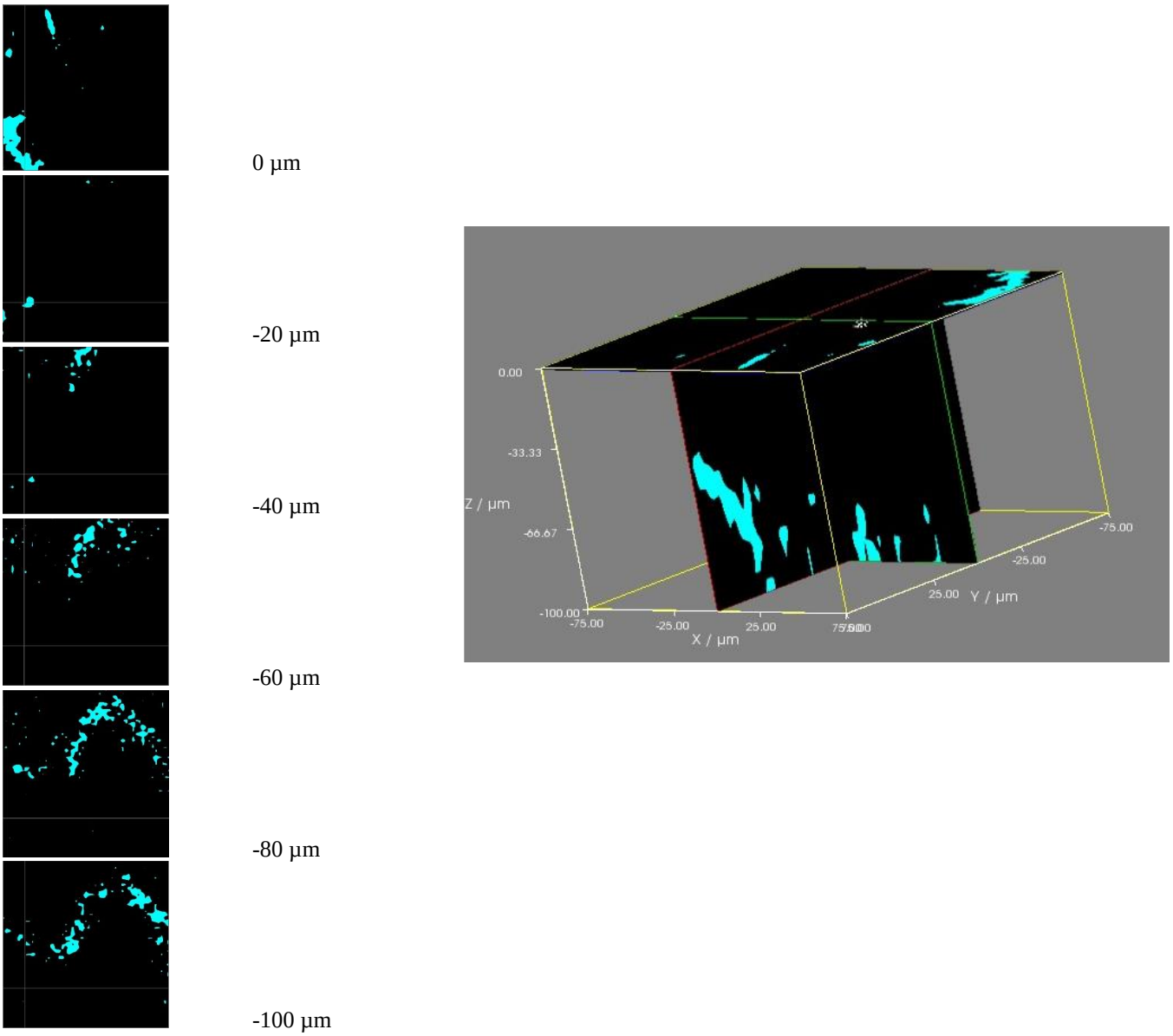

Figure 4.7. Image slices taken of a volume map for a 0.02M NaCl solution at -15.5°C. The left-hand column shows slices along the x-y plane at 20 µm steps. The right-hand column shows images at the surface (along the x-y plane), as well as slices extending 100 µm into the sample along the x-z and y-z planes.

4.4.2.3 Sargasso Sea Water

We acquired Raman maps of Sargasso Sea water to determine whether solutes other than NaCl affect the liquid content of frozen solutions under atmospherically relevant conditions. This work presents, to our knowledge, the first reported spatially-resolved analysis of the physical

properties of frozen sea water surfaces. Figure 4.8 shows a volume map of a frozen Sargasso Sea water solution at -15°C. Looking at the surface map, it is clear that liquid covers a significant fraction of the surface in the form of channels. The surface coverage was 35 ± 4% for the Sargasso Sea water, which is the same as that measured at the surface of frozen 0.6M NaCl solutions at the same temperature (35 ± 9%). This suggests that NaCl is responsible for the majority of surface melting observed in sea ice, despite the presence of other solutes. As with the 0.6M NaCl solutions, frozen Sargasso Sea water solutions showed significant liquid content well below the surface in the form of interconnected channels. Additional volume maps can be found in the SI.

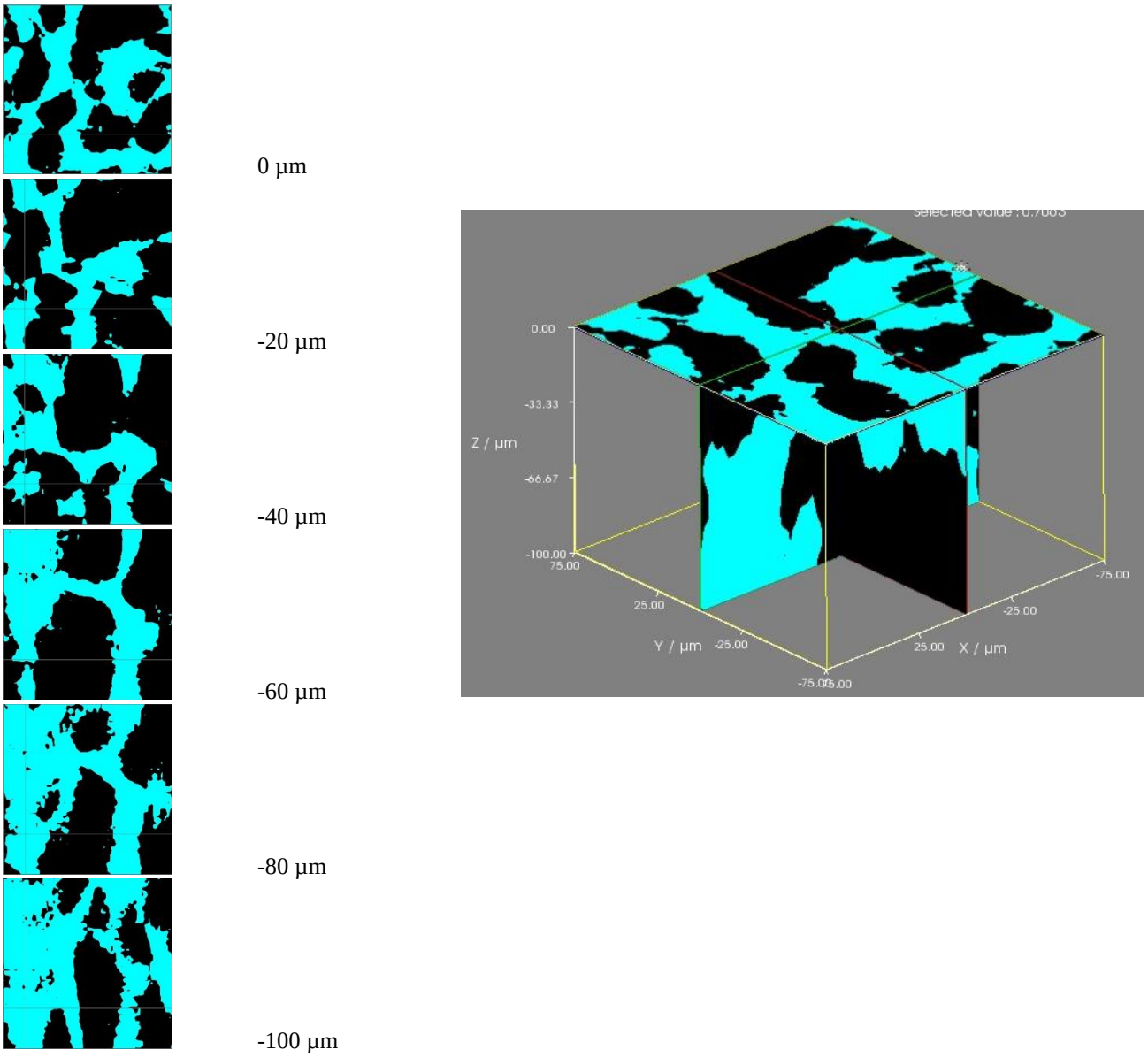

Figure 4.8. Image slices taken of a volume map for a Sargasso Sea Water solution at -15.6°C. The left-hand column shows slices along the x-y plane at 20 µm steps. The right-hand column shows images at the surface (along the x-y plane), as well as slices extending 100 µm into the sample along the x-z and y-z planes.

4.4.3 Below the Eutectic Temperature

At temperatures below the eutectic (-21.1°C), the NaCl–H_2O phase diagram predicts a combination of solid ice and solid salt (including the hydrohalite, $NaCl{\cdot}2H_2O$). Liquid water (or brine) is not expected to be present, although an NMR study reported the presence of liquid

water to temperatures as low as -45°C in frozen 0.5M NaCl solutions.[3] Figure 4.9 shows surface maps of frozen NaCl and Sargasso Sea water solutions at approximately -31°C. At this temperature, we do not see any evidence of liquid (which would be represented in blue on the maps if it was detected). Instead, we see distinct regions of pristine ice and hydrohalite. The surface coverage of hydrohalite varied significantly between samples and ranged from 40 to 100% for the 0.6M NaCl solutions and 45 to 80% for the Sargasso Seawater solutions. Coverage was much lower for the 0.02M NaCl solutions, ranging from 13 to 20%. At temperatures lower than the eutectic, the ice is opaque due to the presence of hydrohalite, and volume maps could not be obtained.

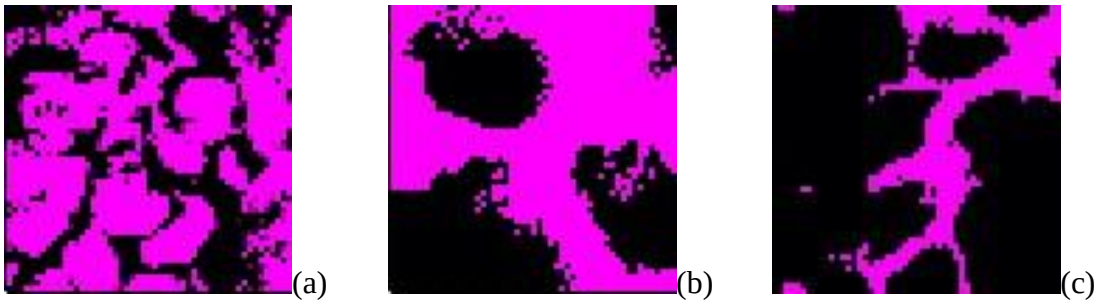

Figure 4.9. Surface map of (a) 0.6 M NaCl (-32.0°C), (b) Sargasso Sea Water (-29.5°C), and (c) 0.02 M NaCl (-30.9°C). Magenta is hydrohalite, black is ice, and blue is liquid aqueous solution.

4.4.4 Near the Eutectic Temperature

We performed a series of experiments to investigate the transition between liquid brine and hydrohalite near the eutectic temperature using 0.6M NaCl solutions. For these experiments, the temperature was increased and decreased in small increments about the eutectic temperature, and Raman maps of the surface were acquired at each temperature. Figure 4.10 illustrates the amount of hydrohalite present at the ice surface at each temperature. The hydrohalite coverage remained constant at temperatures between -32 and -21.7°C. As the temperature increased to -21.1°C, the extent of hydrohalite coverage decreased rapidly. Negligible hydrohalite was

detected at temperatures above the eutectic. After bringing the sample temperature up to approximately -15°C, we acquired surface maps of the same sample as the temperature was decreased incrementally. As we cooled the sample, we observed a reproducible hysteresis: hydrohalite was not observed until the temperature decreased below -22°C – a full degree lower than the eutectic temperature. This supercooling is likely due to the fact that hydrohalite formation requires the proper conformation of salt and water molecules. Similar hystereses are reported for several atmospheric processes such as the efflorescence of aqueous aerosols and the homogeneous freezing of water.[44-46] This trend was consistent whether the solution was cooled slowly, or at a rapid rate (0.5°C/min or 0.5°C/s).

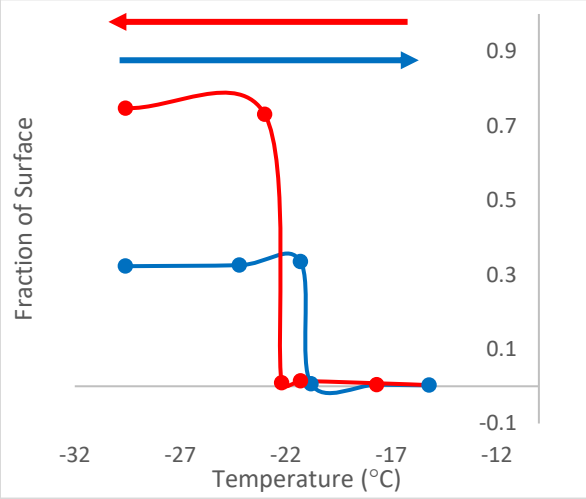

Figure 4.10. Average fraction of the surface covered with hydrohalite as a function of sample temperature. Blue circles indicate increasing temperature, and red circles indicate decreasing temperature.

Figure 4.11 shows the fraction of the ice surface covered by liquid at each temperature. The same hysteresis reported for hydrohalite formation is observed in these data. Whereas the surface coverage of hydrohalite was constant at temperatures below the eutectic, the liquid fraction increased with increasing temperature above the eutectic, as shown in Figure 4.11 and discussed above.

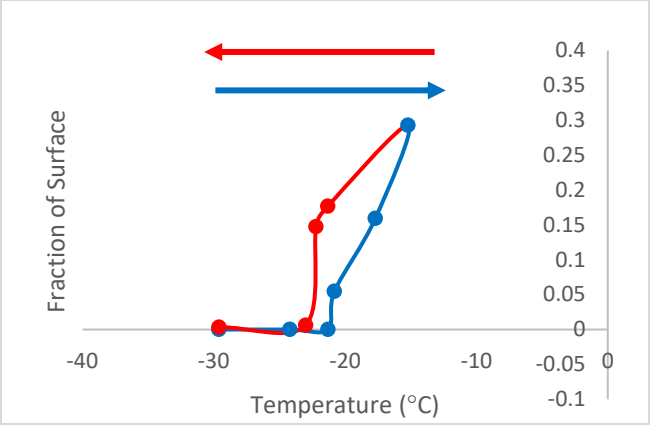

Figure 4.11. Fraction of the surface covered with liquid as a function of sample temperature. Blue circles indicate increasing temperature, and red circles indicate decreasing temperature.

Figure 4.12 shows surface maps acquired at temperatures near the eutectic temperature. The transition from liquid brine to solid hydrohalite is evident both in the optical images and the Raman maps. At all temperatures investigated, hydrohalite and liquid were never observed simultaneously.

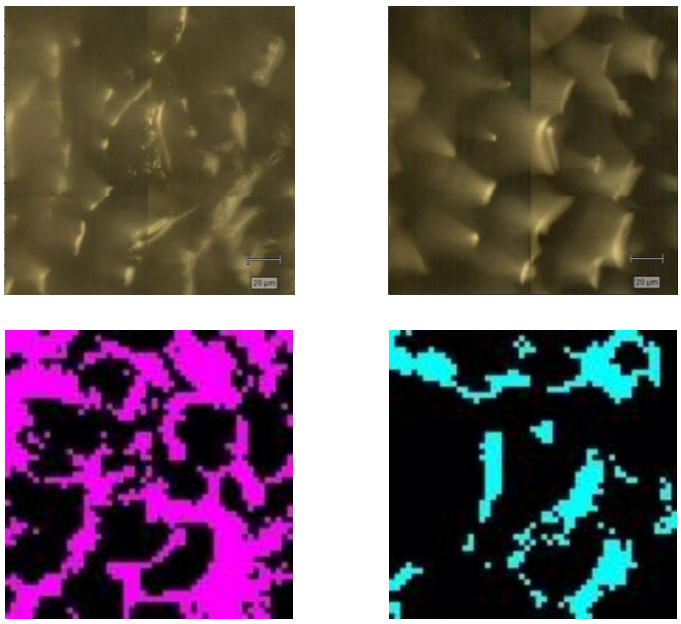

Figure 4.12. Optical images and Raman maps of a 0.6M NaCl solution at -21.8°C and -18.7°C. Magenta is hydrohalite, blue is solution, and black is ice.

4.5 Atmospheric Implications

Except at temperatures very near the melting point, the ice surface is incompletely wetted at seawater salt concentrations, and incomplete wetting is observed at all temperatures at road salt concentrations. Volume maps have shown that not all solutes are excluded to the surface and are present at depths of at least 100 μm below the ice surface. In addition, salt channels are not homogenous throughout the ice bulk. At temperatures below the eutectic, liquid was not observed and hydrohalite covers large fractions of the ice surface, typically at greater coverage than the preexisting salt solution before it refroze. These results have implications for the reactive environment presented by frozen saltwater solutions.

4.6 Acknowledgments:

We would like to thank Dr. David J. Kieber for providing Sargasso Sea Water for our experiments.

4.7 Supporting Information. Analysis performed to monitor the effect of the laser on the physical properties of ice; deionized water Raman maps; additional 0.6M NaCl, 0.02M NaCl, and Sargasso Sea Water maps at -15°C and -5°C as well as volume maps at -15°C; 0.6M NaCl Raman maps below eutectic temperature.

4.8 References

1. Faraday, M., *Experimental Researches in Chemistry and Physics*. Taylor and Francis: London, 1859.
2. Bartels-Rausch, T.; Jacobi, H. W.; Kahan, T. F.; Thomas, J. L.; Thomson, E. S.; Abbatt, J. P. D.; Ammann, M.; Blackford, J. R.; Bluhm, H.; Boxe, C.; Domine, F.; Frey, M. M.; Gladich, I.; Guzman, M. I.; Heger, D.; Huthwelker, T.; Klan, P.; Kuhs, W. F.; Kuo, M. H.; Maus, S.; Moussa, S. G.; McNeill, V. F.; Newberg, J. T.; Pettersson, J. B. C.; Roeselova, M.; Sodeau, J. R.,

A Review of Air-Ice Chemical and Physical Interactions (AICI): Liquids, Quasi-Liquids, and Solids in Snow. *Atmos. Chem. Phys.* **2014,** *14* (3), 1587-1633.
3. Cho, H.; Shepson, P. B.; Barrie, L. A.; Cowin, J. P.; Zaveri, R., NMR Investigation of the Quasi-Brine Layer in Ice/Brine Mixtures. *J. Phys. Chem. B* **2002,** *106* (43), 11226-11232.
4. McNeill, V. F.; Geiger, F. M.; Loerting, T.; Trout, B. L.; Molina, L. T.; Molina, M. J., Interaction of Hydrogen Chloride with Ice Surfaces: The Effects of Grain Size, Surface Roughness, and Surface Disorder. *J. Phys. Chem. A* **2007,** *111* (28), 6274-6284.
5. Kurkova, R.; Ray, D.; Nachtigallova, D.; Klan, P., Chemistry of Small Organic Molecules on Snow Grains: The Applicability of Artificial Snow for Environmental Studies. *Environ. Sci. Technol.* **2011,** *45* (8), 3430-3436.
6. Dash, J. G.; Rempel, A. W.; Wettlaufer, J. S., The Physics of Premelted Ice and its Geophysical Consequences. *Rev. Mod. Phys.* **2006,** *78* (3), 695-741.
7. Walker, R. L.; Searles, K.; Willard, J. A.; Michelsen, R. R. H., Total Reflection Infrared Spectroscopy of Water-Ice and Frozen Aqueous NaCl Solutions. *J. Chem. Phys.* **2013,** *139* (24), 8.
8. Kahan, T. F.; Wren, S. N.; Donaldson, D. J., A Pinch of Salt Is All It Takes: Chemistry at the Frozen Water Surface. *Accounts Chem. Res.* **2014,** *47* (5), 1587-1594.
9. Wren, S. N.; Donaldson, D. J., Exclusion of Nitrate to the Air-Ice Interface During Freezing. *J. Phys. Chem. Lett.* **2011,** *2* (16), 1967-1971.
10. Finlayson-Pitts, B. J.; Livingston, F. E.; Berko, H. N., Ozone Destruction and Bromine Photochemistry at Ground Level in the Arctic Spring. *Nature* **1990,** *343* (6259), 622-625.
11. Frinak, E. K.; Abbatt, J. P. D., Br(2) Production From the Heterogeneous Reaction of Gas-Phase OH with Aqueous Salt Solutions: Impacts of Acidity, Halide Concentration, and Organic Surfactants. *J. Phys. Chem. A* **2006,** *110* (35), 10456-10464.
12. Sjostedt, S. J.; Abbatt, J. P. D., Release of Gas-Phase Halogens from Sodium Halide Substrates: Heterogeneous Oxidation of Frozen Solutions and Desiccated Salts by Hydroxyl Radicals. *Environ. Res. Lett.* **2008,** *3* (4), 7.
13. Mozurkewich, M., Mechanisms for the Release of Halogens from Sea-Salt Particles by Free Radical Reactions. *J. Geophys. Res. Atmos.* **1995,** *100* (D7), 14199-14207.
14. Oldridge, N. W.; Abbatt, J. P. D., Formation of Gas-Phase Bromine from Interaction of Ozone with Frozen and Liquid NaCl/NaBr Solutions: Quantitative Separation of Surficial Chemistry from Bulk-Phase Reaction. *J. Phys. Chem. A* **2011,** *115* (12), 2590-2598.
15. Clifford, D.; Donaldson, D. J., Direct Experimental Evidence for a Heterogeneous Reaction of Ozone with Bromide at the Air-Aqueous Interface. *J. Phys. Chem. A* **2007,** *111* (39), 9809-9814.
16. Reeser, D. I.; George, C.; Donaldson, D. J., Photooxidation of Halides by Chlorophyll at the Air-Salt Water Interface. *J. Phys. Chem. A* **2009,** *113* (30), 8591-8595.
17. Oum, K. W.; Lakin, M. J.; Finlayson-Pitts, B. J., Bromine Activation in the Troposphere by the Dark Reaction of O-3 with Seawater Ice. *Geophys. Res. Lett.* **1998,** *25* (21), 3923-3926.
18. Schroeder, W. H.; Anlauf, K. G.; Barrie, L. A.; Lu, J. Y.; Steffen, A.; Schneeberger, D. R.; Berg, T., Arctic Springtime Depletion of Mercury. *Nature* **1998,** *394* (6691), 331-332.
19. Steffen, A.; Schroeder, W.; Macdonald, R.; Poissant, L.; Konoplev, A., Mercury in the Arctic Atmosphere: An Analysis of Eight Years of Measurements of GEM at Alert (Canada) and a Comparison with Observations at Amderma (Russia) and Kuujjuarapik (Canada). *Sci. Total Environ.* **2005,** *342* (1-3), 185-198.

20. Douglas, T. A.; Sturm, M.; Simpson, W. R.; Brooks, S.; Lindberg, S. E.; Perovich, D. K., Elevated Mercury Measured in Snow and Frost Flowers Near Arctic Sea Ice Leads. *Geophys. Res. Lett.* **2005,** *32* (4), 4.
21. Bargagli, R.; Agnorelli, C.; Borghini, F.; Monaci, F., Enhanced Deposition and Bioaccumulation of Mercury in Antarctic Terrestrial Ecosystems Facing a Coastal Polynya. *Environ. Sci. Technol.* **2005,** *39* (21), 8150-8155.
22. Ariya, P. A.; Dastoor, A. P.; Amyot, M.; Schroeder, W. H.; Barrie, L.; Anlauf, K.; Raofie, F.; Ryzhkov, A.; Davignon, D.; Lalonde, J.; Steffen, A., The Arctic: a Sink for Mercury. *Tellus B* **2004,** *56* (5), 397-403.
23. Banic, C. M.; Beauchamp, S. T.; Tordon, R. J.; Schroeder, W. H.; Steffen, A.; Anlauf, K. A.; Wong, H. K. T., Vertical Distribution of Gaseous Elemental Mercury in Canada. *J. Geophys. Res. Atmos.* **2003,** *108* (D9), 14.
24. Kahan, T. F.; Donaldson, D. J., Benzene Photolysis on Ice: Implications for the Fate of Organic Contaminants in the Winter. *Environ. Sci. Technol.* **2010,** *44*, 3819-3824.
25. Stathis, A. A.; Hendrickson-Stives, A. K.; Kahan, T. F., Photolysis Kinetics of Toluene, Ethylbenzene, and Xylenes at Ice Surfaces. *J. Phys. Chem. A* **2016,** *120*, 6693-6697.
26. Kahan, T. F.; Kwamena, N.-O. A.; Donaldson, D. J., Different Photolysis Kinetics at the Surface of Frozen Freshwater vs. Frozen Salt Solutions. *Atmos. Chem. Phys.* **2010,** *10*, 10917-10922.
27. Kahan, T. F.; Zhao, R.; Jumaa, K. B.; Donaldson, D. J., Anthracene Photolysis in Aqueous Solution and Ice: Photon Flux Dependence and Comparison of Kinetics in Bulk Ice and at the Air−Ice Interface. *Environ. Sci. Technol.* **2010,** *44* (4), 1302-1306.
28. Malley, P. P. A.; Kahan, T. F., Nonchromophoric Organic Matter Suppresses Polycyclic Aromatic Hydrocarbon Photolysis in Ice and at Ice Surfaces. *J. Phys. Chem. A* **2014,** *118* (9), 1638-1643.
29. Kahan, T. F.; Donaldson, D. J., Heterogeneous Ozonation Kinetics of Phenanthrene at the Air–Ice Interface. *Environ. Res. Lett.* **2008,** *3* (4).
30. Kahan, T. F.; Zhao, R.; Donaldson, D. J., Hydroxyl Radical Reactivity at the Air-Ice Interface. *Atmos. Chem. Phys.* **2010,** *10*, 843-854.
31. Peterson, M. C.; Honrath, R. E., Observations of Rapid Photochemical Destruction of Ozone in Snowpack Interstitial Air. *Geophys. Res. Lett.* **2001,** *28* (3), 511-514.
32. Orlando, F.; Waldner, A.; Bartels-Rausch, T.; Birrer, M.; Kato, S.; Lee, M. T.; Proff, C.; Huthwelker, T.; Kleibert, A.; van Bokhoven, J.; Ammann, M., The Environmental Photochemistry of Oxide Surfaces and the Nature of Frozen Salt Solutions: A New in Situ XPS Approach. *Top. Catal.* **2016,** *59* (5-7), 591-604.
33. Krepelova, A.; Huthwelker, T.; Bluhm, H.; Ammann, M., Surface Chemical Properties of Eutectic and Frozen NaCl Solutions Probed by XPS and NEXAFS. *ChemPhysChem* **2010,** *11* (18), 3859-3866.
34. Blackford, J. R.; Jeffree, C. E.; Noake, D. F. J.; Marmo, B. A., Microstructural Evolution in Sintered Ice Particles Containing NaCl Observed by Low-Temperature Scanning Electron Microscope. *Proc. Inst. Mech. Eng. L J. Mater. Des. Appl.* **2007,** *221* (L3), 151-156.
35. Doppenschmidt, A.; Butt, H. J., Measuring the Thickness of the Liquid-Like Layer on Ice Surfaces with Atomic Force Microscopy. *Langmuir* **2000,** *16* (16), 6709-6714.
36. Tokumasu, K.; Harada, M.; Okada, T., X-ray Fluorescence Imaging of Frozen Aqueous NaCl Solutions. *Langmuir* **2016,** *32* (2), 527-533.

37. Kieber, D. J.; Mopper, K., Photochemical Formation of Glyoxylic and Pyruvic Acids in Seawater. *Mar. Chem.* **1987,** *21* (2), 135-149.
38. Kahan, T. F.; Reid, J. P.; Donaldson, D. J., Spectroscopic Probes of the Quasi-Liquid Layer on Ice. *J. Phys. Chem. A* **2007,** *111* (43), 11006-11012.
39. Chen, N.; Morikawa, J.; Hashimoto, T., Effect of Cryoprotectants on Eutectics of NaCl Center Dot 2H(2)O/Ice and KCl/Ice Studied by Temperature Wave Analysis and Differential Scanning Calorimetry. *Thermochim. Acta* **2005,** *431* (1-2), 106-112.
40. Okotrub, K. A.; Surovtsev, N. V., Raman Scattering Evidence of Hydrohalite Formation on Frozen Yeast Cells. *Cryobiology* **2013,** *66* (1), 47-51.
41. Wei, X.; Miranda, P. B.; Shen, Y. R., Surface Vibrational Spectroscopic Study of Surface Melting of Ice. *Phys. Rev. Lett.* **2001,** *86* (8), 1554-1557.
42. Elbaum, M.; Lipson, S. G.; Dash, J. G., Optical Study of Surface Melting on Ice. *J. Cryst. Growth* **1993,** *129* (3-4), 491-505.
43. Labadia, C. F.; Buttle, J. M., Road Salt Accumulation in Highway Snow Banks and Transport Through the Unsaturated Zone of the Oak Ridges Moraine, Southern Ontario. *Hydrol. Process.* **1996,** *10* (12), 1575-1589.
44. Wang, J.; Hoffmann, A. A.; Park, R. J.; Jacob, D. J.; Martin, S. T., Global Distribution of Solid and Aqueous Sulfate Aerosols: Effect of the Hysteresis of Particle Phase Transitions. *J. Geophys. Res. Atmos.* **2008,** *113* (D11), 11.
45. Colberg, C. A.; Krieger, U. K.; Peter, T., Morphological Investigations of Single Levitated H2SO4/NH3/H2O Aerosol Particles During Deliquescence/Efflorescence Experiments. *J. Phys. Chem. A* **2004,** *108* (14), 2700-2709.
46. Morishige, K.; Kawano, K., Freezing and Melting of Water in a Single Cylindrical Pore: The Pore-Size Dependence of Freezing and Melting Behavior. *J. Chem. Phys* **1999,** *110* (10), 4867-4872.

Appendix

A1. Chapter Three Supplemental Information

Pyrene is a fluorescing polarity probe.[1] Local polarity can be determined from the ratio of intensity at 373 nm 393 nm (the I:III ratio). This ratio increases with increasing polarity. To determine whether FA reduced solution polarity, emission spectra of pyrene in deionized water in the presence and absence of 30 mg/L FA were acquired. As seen in Figure S1, 30 mg/L FA does not change the I:III ratio, which indicates that the polarity is not appreciably lowered.

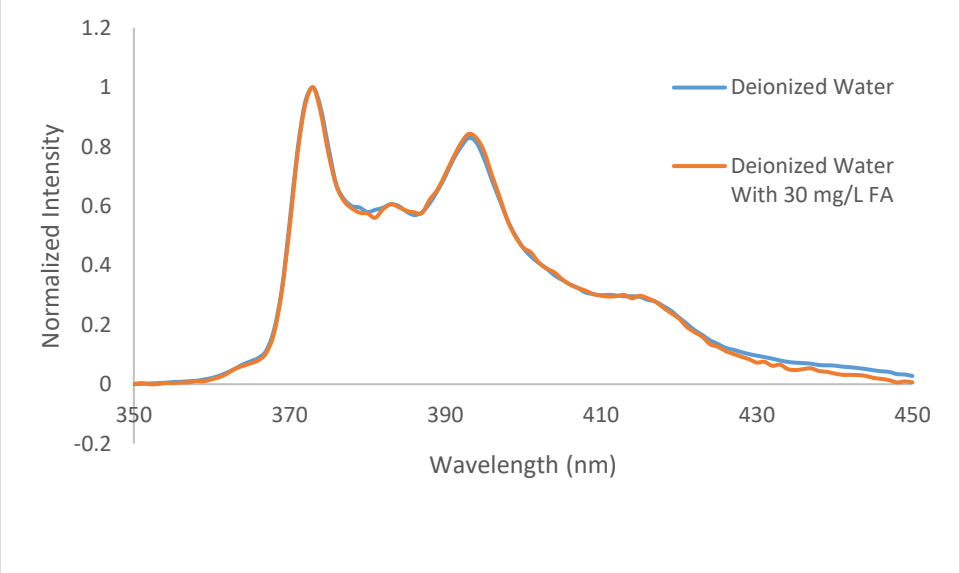

Figure S1. Emission spectra of pyrene in deionized water in the presence (solid black trace) and absence (dashed red trace) of 30 mg/L FA normalized to intensity at 373 nm. Emission from FA has been subtracted.

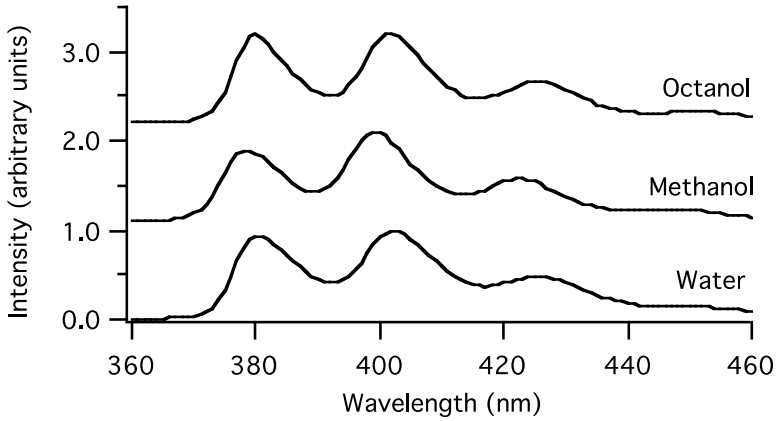

Figure S2. Emission spectra of ~2 × 10^{-7} M anthracene in water, methanol, and octanol. Spectra have been offset for clarity.

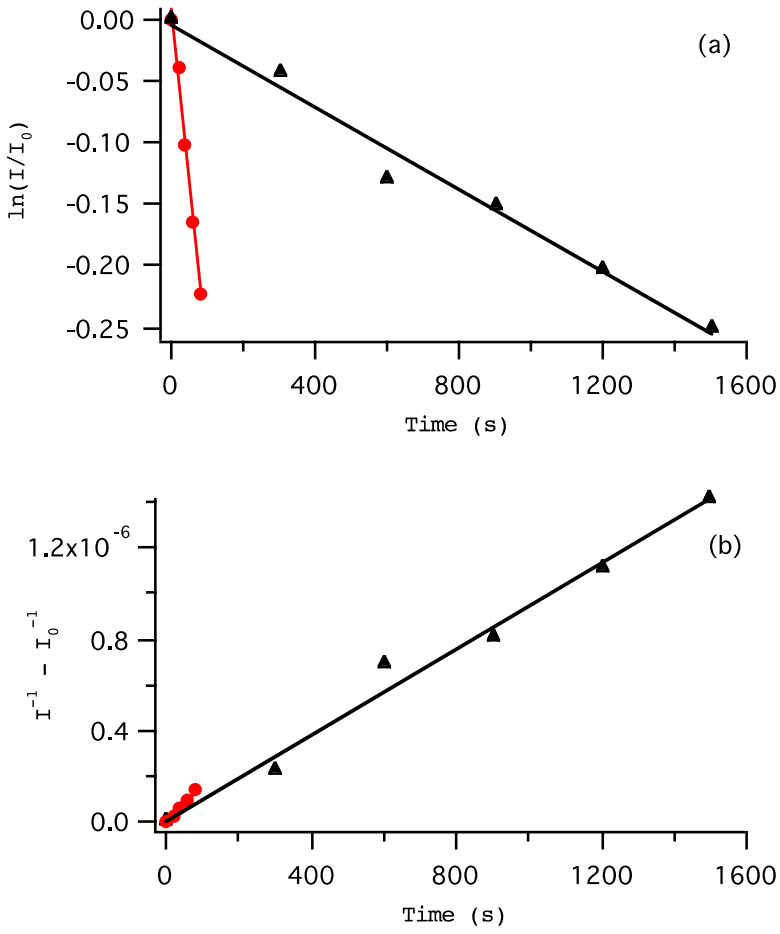

Figure S3. Anthracene fluorescence intensity fit to (a) first order and (b) second-order kinetics for photolysis of samples containing 6.3 × 10^{-8} M anthracene (black triangles) and 3 × 10^{-5} M anthracene (red circles). Fits to first and second order kinetics for the low concentration sample are 0.982 and 0.986, and fits to first and second order kinetics for the high concentration sample are 0.995 and 0.991. The reported fits are representative of the data set.

References:

1. Dong, D. C.; Winnik, M. A., The Py Scale of Solvent Polarities - Solvent Effects on the Vibronic Fine-Structure of Pyrene Fluorescence and Empirical Correlations with Et and Y Values. *Photochem. Photobiol.* **1982,** *35* (1), 17-21.

A2. Chapter Four Supplemental Information

To determine if the laser was having an influence on the surface of the ice, we obtained successive maps of frozen 0.6M NaCl solutions at -15 ºC, -10 ºC, and -5 ºC. If the laser induces melting, we would expect the observed liquid surface coverage to increase with each consecutive map. This was not observed. The measured surface coverage varied by up to 3.6% between consecutive map acquisitions, and by up to 4.5% between maps acquired for any given sample. The measured liquid surface coverage for consecutive maps acquired using 5 μm steps were the same within experimental uncertainty as those acquired using 3 μm steps, which offers further evidence that surface melting by the laser did not introduce artefacts in our experiments.

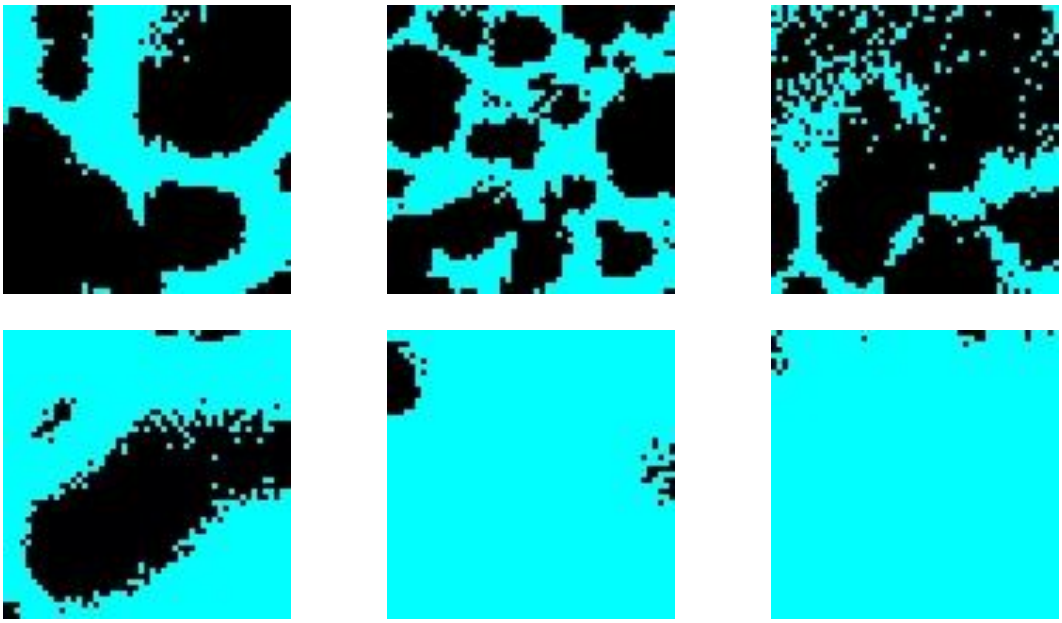

Figure S1. Raman maps of 0.6M NaCl taken above the eutectic temperature. The top row was performed at -15.3°C, -15.4°C, and -15.4°C respectively. The images immediately below the map correspond to the same area warmed to a -5.6°C, -5.4°C, and -5.1°C respectively.

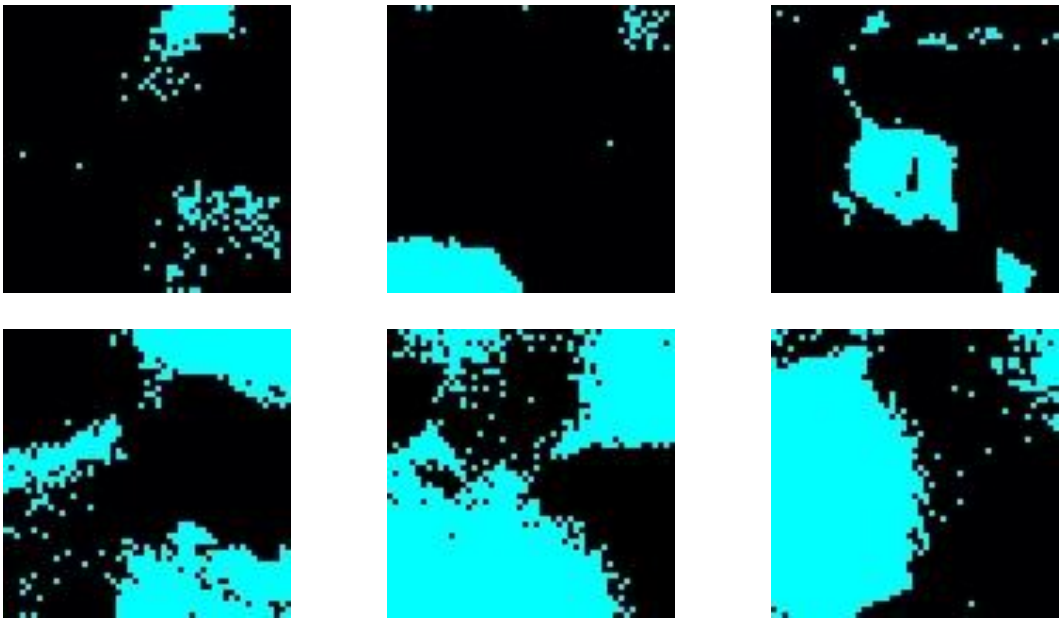

Figure S2. Raman maps of 0.02M NaCl solution maps in the top row were taken at -15.0°C, -15.1°C, and -15.5°C. The bottom row corresponds to the same area in the top row warmed to temperatures of -5.7°C, -4.9°C, and -5.5°C respectively. The amount of solution coverage increase accordingly, but never enough to completely wet the surface.

Figure S3. Raman maps of Sargasso Sea Water obtained at -15.5°C.

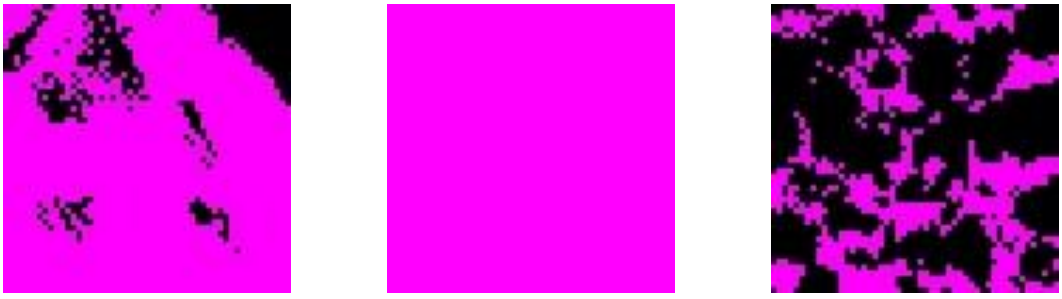

Figure S4. Raman maps of 0.6M NaCl indicating the presence of hydrohalite. Maps were taken at -27.9°C, -31.9°C, and -29.6°C

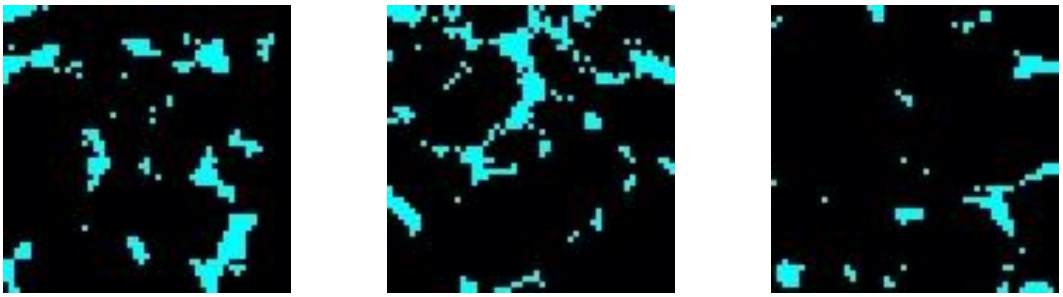

Figure S5. 0.6M NaCl Raman maps taken just above the eutectic temperature. Maps were obtained at temperatures of -20.8°C, -20.6°C, and -20.8°C respectively.

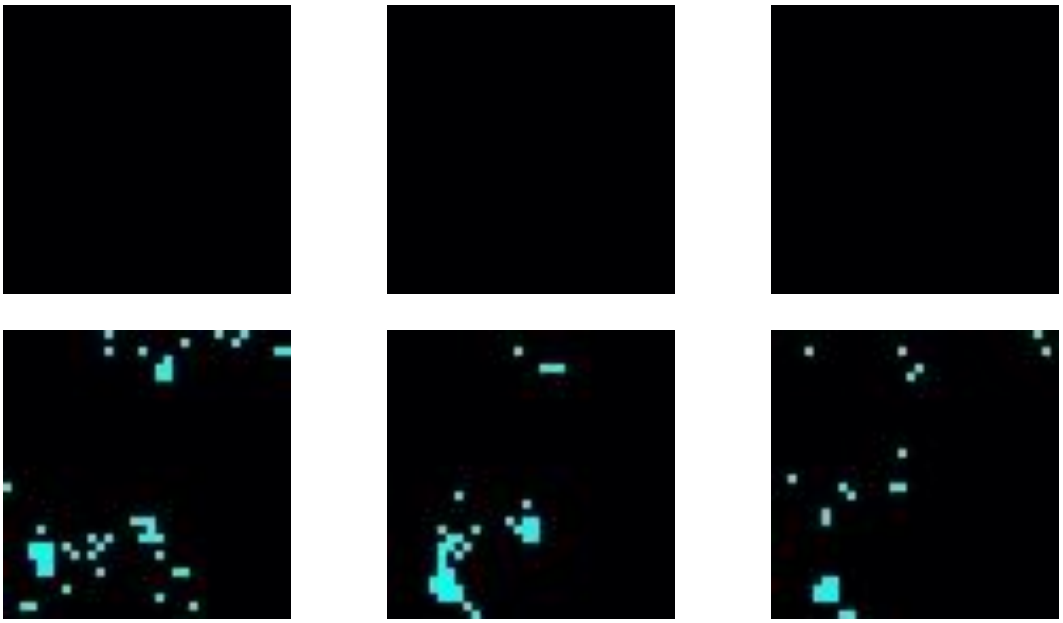

Figure S6. Deionized water maps. The top row represents map's at -15.7°C, -15.5°C, and -15.5°C. The Raman maps in the bottom row were all taken at -4.5°C. The surface coverage by liquid solution came to 1.8±0.7% upon analysis, indicating that even at temperatures closest to water's melting point, the presence of solution at the surface is due primarily to chloride ions.

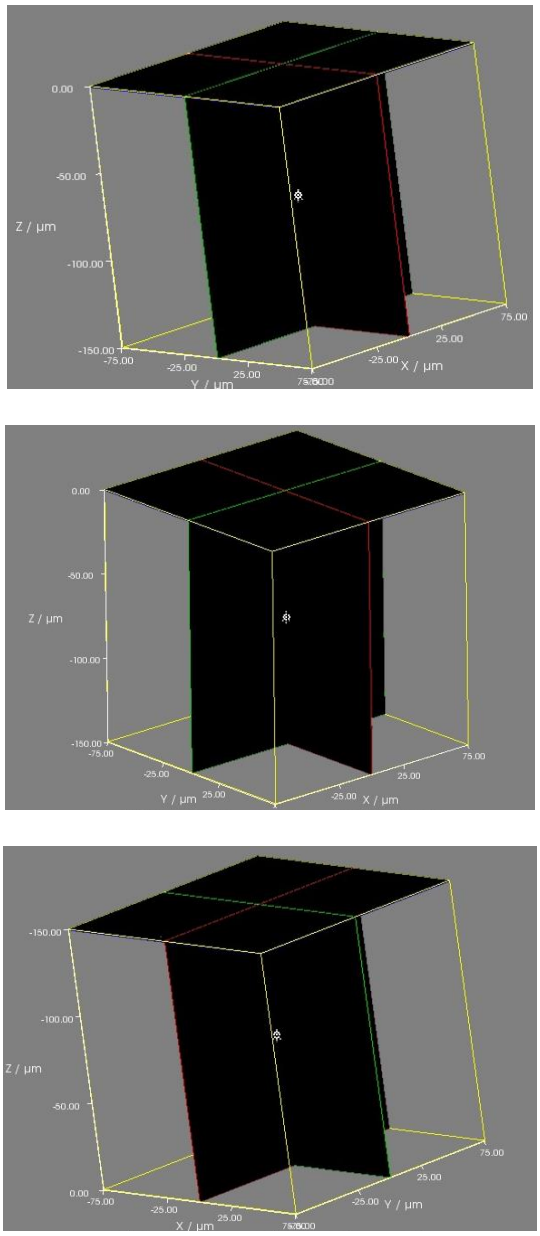

Figure S7. Volume maps of deionized water. All maps were performed at -17.5°C. The lack of liquid water visible indicates that chloride ions are responsible for its presence in salt solutions.

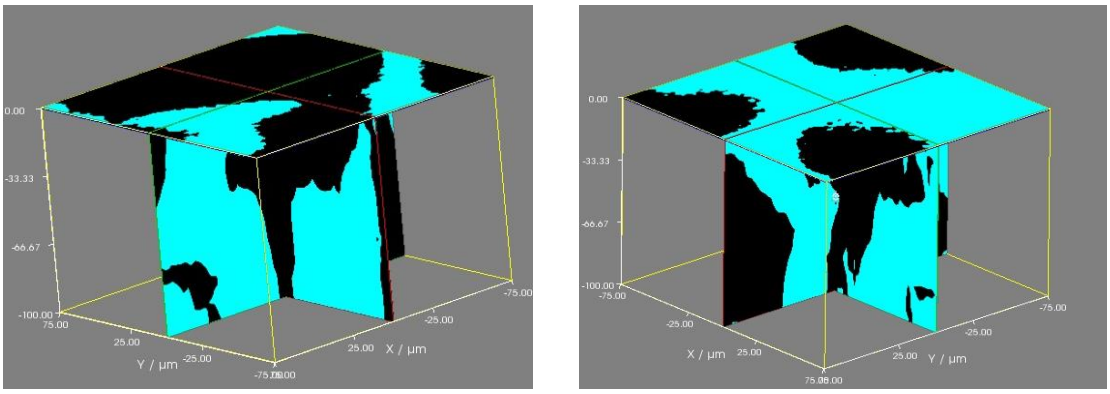

Figure S8. Volume maps of 0.6M NaCl. Both maps were performed at -15.5°C.

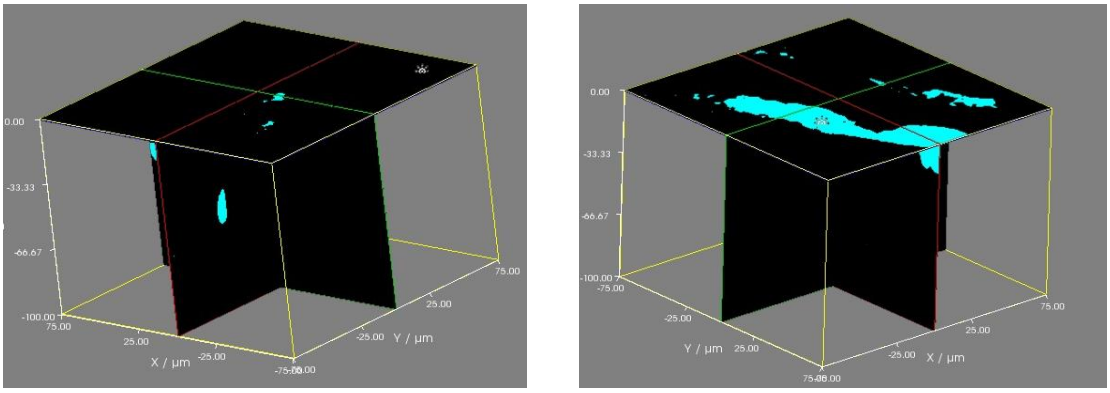

Figure S9. Volume maps of 0.02M NaCl. The map on the left was performed at -15.6°C and the map on the right was performed at -15.2°C.

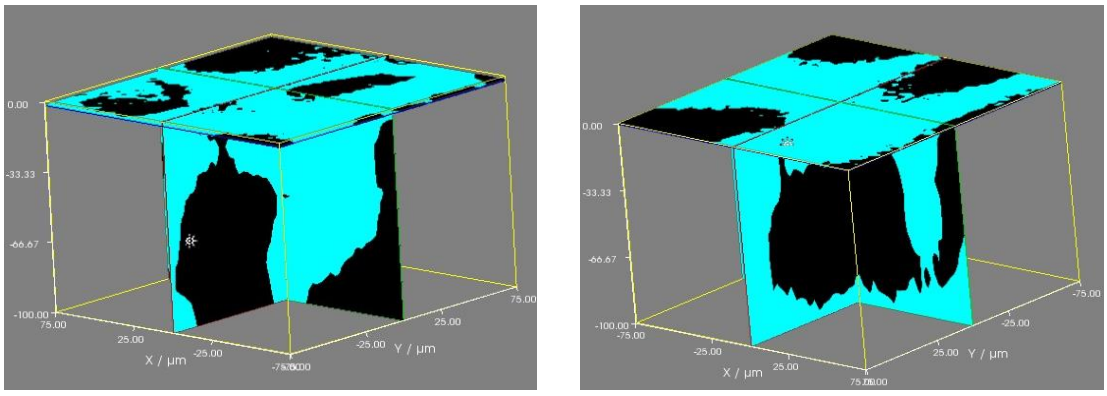

Figure S10. Volume maps of Sargasso Sea Water. The map on the left was performed at -15.2°C and the map on the right was performed at -15.7°C.

Philip P. A. Malley

60 Presidential Court Townhouse 7
Syracuse, NY 13202

Cell: (585)738-1908
Email: ppmalley@syr.edu

Education

Syracuse University Syracuse, NY
Ph.D. candidate, Department of Chemistry, Expected June 2017
Thesis: Investigating the Effects of Environmental Solutes on the Reaction Environment in Ice and Ice Surfaces

University of Scranton Scranton, PA
B. S. Forensic Chemistry, May 2012
B. S. Criminal Justice, May 2012

Awards and Affiliations

American Chemical Society (ACS)
American Geophysical Union (AGU)
The Geological Society of America (GSA)
Graduate Student Organization (GSO) Travel Grant, Fall 2016
ACS Chemistry Award, May 2012, Scranton, PA

Research Experience

Syracuse University
Research Assistant- Fall 2012-present
Advisor: Tara F. Kahan

- Investigated the effects of organic matter on polycyclic aromatic hydrocarbon photolysis in ice and at the ice surface using fluorescence spectroscopy
- Evaluated the effects of salt on the physical properties of ice surfaces using Raman microscopy
- Collaborated with researchers in the department of biomedical and chemical engineering to help characterize their samples based on functional group, curing time, and composition using Raman microscopy
- Presented research at national and regional conferences

University of Scranton
Undergraduate Researcher- February 2012-May 2012
Advisor: David Rusak

- Investigate the chemical composition of prescription drugs, specifically Viagra and Lipitor, against their counterfeits using Laser Induced Breakdown Spectroscopy (LIBS)

Sanofi Pasteur
Summer Intern- May 2011-August 2011
Mentor: Matthew Balmer

- Performed protein assays to identify the p53 gene in thyroid cancer cells, such as Western Blots, Enzyme-linked Immunosorbent Assays (ELISA), and Bicinchoninic Acid Assays (BCA)

Publications

Malley, P.P.A. and Kahan, T.F., 2017. Physical Characterization of Frozen Saltwater Solutions using Raman Microscopy. In Preparation.

Malley, P.P.A., Grossman, J.N., and Kahan, T.F., 2017. Effects of Chromophoric Dissolved Organic Matter on Anthracene Photolysis Kinetics in Aqueous Solution and Ice. Submitted.

Biria, S., **Malley, P.P.A.**, Kahan, T.F. and Hosein, I.D., 2016. Optical Autocatalysis Establishes Novel Spatial Dynamics in Phase Separation of Polymer Blends during Photocuring. *ACS Macro Letters*, *5*(11), pp.1237-1241.

Biria, S., **Malley, P.P.A.**, Kahan, T.F. and Hosein, I.D., 2016. Tunable Nonlinear Optical Pattern Formation and Microstructure in Crosslinking Acrylate Systems during Free-Radical Polymerization. *The Journal of Physical Chemistry C*, *120(*8*)*, pp.4517-4528.

Malley, P.P.A. and Kahan, T.F., 2014. Nonchromophoric Organic Matter Suppresses Polycyclic Aromatic Hydrocarbon Photolysis in Ice and at Ice Surfaces. *The Journal of Physical Chemistry A*, *118*(9), pp.1638-1643.

Presentations

"Effects of Dissolved Organic Matter and Photon Flux on Anthracene Photolysis Kinetics in Ice and at Ice Surfaces." **P.P.A. Malley**, T. F. Kahan. Oral presentation at the 2016 AGU Fall Meeting in San Francisco, CA. December 12, 2016.

"Effects of Organic Matter on Polycyclic Aromatic Hydrocarbon Photolysis Kinetics in Ice and at Ice Surfaces." **P.P.A. Malley**, T. F. Kahan. Poster presentation at the ACS Northeastern Regional Meeting in Ithaca, NY. June 10, 2015.

"Effects of Organic Matter on Polycyclic Aromatic Hydrocarbon Photolysis Kinetics in Ice and at Ice Surfaces." **P.P.A. Malley**, T. F. Kahan. Poster presentation at the 249th ACS National Meeting and Exposition in Denver, CO. March 25, 2015.

Teaching Experience

Syracuse University

- General Chemistry I and II Recitation, Teaching Assistant
  - Taught weekly recitation courses for the general chemistry course. Duties included answering student questions, holding office hours, distributing quizzes, and proctoring exams. (Fall 2013-Spring 2015 Semester)
- General Chemistry Laboratory, Teaching Assistant
  - Instructed and supervised laboratory sections for practical general chemistry application. Duties included teaching, grading, and office hours. (Spring 2013 Semester)
- General Chemistry for Engineers, Teaching Assistant
  - Taught weekly recitation courses for the general chemistry course specifically designed for engineering students. Duties included answering student questions, holding office hours, and proctoring exams. (Fall 2012 Semester)

Skills

Computer: Excel, Sigma Plot, PowerPoint, Word

Lab: Fluorescence spectroscopy, Raman microscopy, High Performance Liquid Chromatography (HPLC), UV-Vis spectroscopy, Laser Induced Breakdown Spectroscopy (LIBS), Western blots, Enzyme-linked Immunosorbent Assay (ELISA), Bicinchoninic Acid Assay (BCA)

Outreach and Volunteer Work

John Katko Reelection Campaign Syracuse, NY

Volunteer for the reelection campaign of Congressman John Katko for the 24th district of New York. Duties included:

- Phone calls to prospective voters and asking for their participation in a short survey about issues effecting central New York
- Door knocking in neighborhoods and providing information about representative John Katko to citizens of the area
- Assisting in outreach at Syracuse University

Honeoye Falls-Lima High School Honeoye Falls, NY

Invited guest speaker for juniors and seniors enrolled in AP Chemistry. Topics covered include:

- The science undergraduate experience
- Graduate school applications
- Graduate school experience
- General questions

Women's Self-Defense Course Syracuse, NY
Assist with the women's self-defense course on campus by posing as an attacker and allowing the women enrolled in the class to practice the techniques they have learned in a more realistic scenario

Extracurricular Activities

- Syracuse University Boxing Club
- Men's club soccer

References

Tara Kahan
Research Advisor
Chemistry Department
Syracuse University
111 College Place, 2-052
Syracuse, NY 13244
tfkahan@syr.edu

Timothy Korter
Ph.D. Committee Member
Chemistry Department
Syracuse University
111 College Place, 1-046
Syracuse, NY 13244
tmkorter@syr.edu

Ian Hosein
Research Collaboration Member
Biomedical and Chemical Engineering Department
Syracuse University
Link Hall, Room 339
Syracuse, NY 13210
idhosein@syr.edu